NONLINEAR VISCOELASTICITY

OF

POLYAMIDE FIBERS

A THESIS

Presented to

The Faculty of the Division of Graduate

Studies and Research

by

Frank Koon-Fun Ko

In Partial Fulfillment

of the Requirements of the Degree

Doctor of Philosophy in the School

of Textile Engineering

Georgia Institute of Technology

September 1976

NONLINEAR VISCOELASTICITY

OF

POLYAMIDE FIBERS

Approved:

John L. Lundberg, Chairman

Denny W. Preston, Jr.

John D. Muzzy

L. Howard Olson

George M. Rentzepis

1/27/1977

Date approved by Chairman

DEDICATION

To My

MOTHER, KING HIN CHANG, who lived without a son

for eight years;

WIFE, CATHERINE, who lived without a husband

for three years; and

DAUGHTER, KARA, who lived without a father

for one year

ACKNOWLEDGEMENTS

I wish to express my sincere appreciation for the following persons who contributed directly and indirectly to this research and to my learning experience:

Professor John L. Lundberg, my thesis advisor, who broadened my research interests and deeply influenced my view toward science,

Professor W. D. Freeston, Jr., Director of the School of Textile Engineering and member of my thesis advisory committee, from whom I learned textile mechanics and who arranged for my continuing financial support,

Professor Hyland Y-L. Chen, friend and member of the faculty of the School of Engineering Science and Mechanics, who taught me the mathematical methods of viscoelasticity, introduced me to new concepts of data acquisition systems, and allowed me unlimited access to equipment in his laboratory,

Professor W. C. Boteler, for his continuous interest in my work and for his patience in reading my thesis,

Professors J. D. Muzzy, L. H. Olson, and G. M. Rentzepis for their patience with my progress and serving as members of my advisory committee and my examining committees,

Professor M. Konopasek, who greatly expanded my computing ability by supplying me with his computer program subroutines and inspired my interest in using the computer as a problem solving aid,

Dr. B. R. Livesay, Senior Research Scientist of the Engineering Experiment Station of the Georgia Institute of Technology, for allowing me full access to his micromechanics laboratory,

Professor Frank L. Scardino, Director of Research of the Philadelphia College of Textiles and Science, who first introduced me to the fascinating field of textile research,

Mr. M. E. Sikorski, who constantly answered my many questions about electronics and transducers and helped me in many other ways,

Professor W. R. Work of the North Carolina State University, who shared with me generously his many years of experience in spider silk research.

Thanks are also due to the Tennessee Eastman Company for awarding me the Tennessee Eastman Fellowship; Dr. James Parker of the American Enka Company for supplying samples and information of drawn and undrawn nylon 6 fibers and The Textile Fiber Division of the E. I. du Pont de Nemous & Company, Inc., for donating the PRD-49 fibers.

Significant assistance was offered by my friends from different laboratories in every phase of my research. Mr. F. D. Smith of our machine shop patiently followed my drawings of apparatus and taught me many machining techniques. Miss Jennifer Buchannan, 1975 NSF research seminar student, helped collect all the spider silk samples and performed tensile tests of the spider silks. Mr. J. M. Smith helped program the data logging system used in these studies. Messrs. Robert

Newsom and Rick Marucci from the Engineering Experiment Station and Steve Lyons from the School of Engineering Science and Mechanics provided expert advice in electronic circuits for the data acquisition systems. Mr. A. Sheppard III helped print the photographs. Mr. John Follin taught me to use computer magnetic tapes. Assistance from the staff members of the Office of Computing Service are also greatly appreciated.

Special thanks goes to Mr. Kenneston Carr, who helped so willingly in every phase of my research.

I also wish to thank Marlene P. Maslin for her expert typing of the entire manuscript.

Last but not least, I would like to thank my parents-in-law for taking care of my family during the last year of my research.

TABLE OF CONTENTS

LIST OF TABLES

LIST OF ILLUSTRATIONS

SUMMARY

Oriented composite structures such as textile fibers have nonlinear stress-strain-time relationships which depend on temperature, humidity and other environmental conditions.

Nonlinear mechanical responses of fibers must be considered in practical design of fibrous structures. In order to characterize the nonlinear behavior of polyamide fibers over wide ranges of stress, strain and time, the nonlinear viscoelastic responses of strong nylon, spider drag line and drawn and undrawn nylon-6 fibers were measured by simple elongation, cyclic loading, stress relaxation, creep, and sinusoidal stretching experiments at various strain rates, strain levels and frequencies. A quasilinear viscoelastic model in terms of continuous relaxation spectra was used to summarize the experimental observations.

Experimental evidence shows that polyamide fibers are no exception to the rule that polymeric materials have nonlinear stress-strain-time relationships which depend on environmental conditions. The quasilinear viscoelastic model gives only a zeroth approximation to the nonlinear viscoelastic behavior of polyamide fibers.

CHAPTER I

INTRODUCTION

Nature of Viscoelasticity

Depending upon the time scale of observation, most materials exhibit properties found in both elastic solids or rubbers and viscous fluids. This combination of elastic and flow properties is called viscoelasticity.

Characteristic viscoelastic behavior manifests itself in: (1) creep; the deformation, casued by a constant load, increases with time; (2) stress relaxation, the stress required to maintain constant deformation of an object decreases with time; (3) hysteresis loss, the dissipation of the strain energy in cyclic loading or extension as shown by a hysteresis loop in the stress-strain plot; (4) stress lagging behind strain such that stress and strain are neither in phase nor 90 degrees out of phase when loaded harmonically.

Linear viscoelastic response requires that elastic and flow contributions be additive. The ratio of stress to strain is a function of time only and can be described by characteristic material functions such as stress relaxation modulus and creep compliance. For nonlinear viscoelastic response, elastic and flow contributions are not simply additive. The ratio of stress to strain is not a function of time only but also a function of stress and/or strain. No characteristic material function can describe nonlinear viscoelastic response.

Often used methods representing viscoelastic responses are by differential operators, integral equations, and complex notations. The accuracy offered by the differential operator representation in describing experimental observations depends on the order of the differential operator used. The integral equation representation depends on selection of the kernel function which can be obtained by fitting experimental data directly. Therefore it is more accurate than the differential operator method in representing experimental observations. Complex notations are used as convenient means to represent dynamic mechanical responses. Models are not necessary to establish quantitative representations of stress-strain-time relationships. However, mechanical models such as combinations of springs and dashpots are used to help discussion and to aid in deducing mathematical relationships of stress, strain, and time. For linear viscoelasticity the above mentioned methods are equivalent and interchangeable.

All materials have nonlinear stress-strain-time relationships. However, if we operate only within the small deformation region, below 0.005 strain for "soft"materials like polyisobutylene and below about 0.001 to 0.002 strain for "hard" materials, linear theory of viscoelasticity gives a good first approximation for many traditional engineering materials and for some "amorphous" polymers. For polymeric fibers, linear viscoelastic theory is inadequate. Useful polymeric fibers have relatively high molecular chain orientation in the fiber direction and are composite structures [108]. These

structural features make fibers highly anisotropic [78], inhomogeneous, and partially irreversible when strained. Therefore, fibers are non-linearly viscoelastic at all strain levels. These structural features give polymeric fibers the combined strength and toughness that no other materials can match.

Studies of Polymer Viscoelasticity

Inspired by the time dependent nature of many properties of matter, many investigators contributed to the development of mathematical theory of linear viscoelasticity over the past century through observations of mechanical, electrical, and magnetic relaxation phenomena [6, 8, 29, 50, 63, 102, 109]. The mathematics for describing linear viscoelastic behavior is the same as that for electrical and magnetic relaxations [4, 43]. One of the best expositions of the mathematical structure of theories of viscoelasticity was written by an electrical engineer, B. Gross [29]. Leaderman [50] gave an excellent account of studies of viscoelasticity prior to 1943.

Of all classes of materials, high polymers have the most spectacular viscoelastic behavior. Since Weber's investigation of the viscoelastic responseof silk fibers [117] and especially after the development of synthetic high polymers in the nineteen forties, viscoelasticity has received increasing attention from investigators. Development of modern phenomenological theory of polymer viscoelasticity is due to the efforts of thoughtful scientists like Alfrey, Eyring, Ferry, Tobolsky, and their students and associates. In three treatises, Alfrey [4], Tobolsky [104], and Ferry [22] recorded their work and

almost all the work on polymer viscoelasticity by other investigators prior to 1970. Works by scientists from other fields, Flugge [24], Reiner [86], and Zener [127], are valuable references. The literature shows that we can describe phenomenologically the mechanical behavior of "amorphous" polymers at small strains. Mechanical response of semi-crystalline polymers, such as fibers, eludes description and understanding. Our lack of understanding of these useful polymeric structures can be attributed to their complex structures and nonlinear mechanical responses. Many experimental studies of the viscoelastic behavior of fibers have been carried out (Table 1). Among these studies, we emphasize the work on simple elongation by Meredith [66], on stress relaxation by Eyring and Tobolsky and coworkers [31, 85, 87, 104], on creep by Leaderman, Catsiff, et al., and Howard and Williams [50], [11], [39], and on dynamic stretching by Dillon, Eyring, Lyons, Dunell, Fujino, and Nielsen [19, 21, 26, 58, 60, 72, 83]. Most of these studies reported only one or two types of the viscoelastic behavior of fibers. Very few examine a wide range of mechanical response. None provide a framework to unify the observed viscoelastic behavior from different experiments such as creep, stress relaxation, sinusoidal loading and elastic response.

Recognizing the nonlinear viscoelastic nature of polymeric materials, a few theories of nonlinear viscoelasticity have been proposed since the nineteen forties; these theories have been reviewed by Schapery [81], Ward [113], and Daniel [18]. Regardless of what these theories are called, whether empirical power law, nonlinear mechanical

TABLE 1. Studies of Viscoelastic Behavior of Fibers

Author(s)	Reference	Fiber(s)	Type of Measurement	Year
Weber	117	raw silk	creep	1835
Hopkinson	38	glass	torsional creep	1878
Shorter	89	wool	cyclic loading	1924
Speakman	92	wool	creep	1926
Peirce	77	cotton, hair, rayon	various rates of loading	1927
Smith and Eisenschitz	90, 91	rayon	creep, stress relaxation	1931
Myer and Lotmar	69	linen, hemp, ramie	dynamic	1936
Steinberger	94, 95, 96, 97, 98, 99, 100, 101	rayons, silk, cotton, wool, ramie	simple elongation hysteresis strain rate, creep torque relaxation	1934 1936
Press	80	acetate & viscose rayon	creep	1943
Mark & Press	61	acetate, viscose rayon	creep	1943
Leaderman	50	nylon, rayon, viscose acetate, and silkworm silk	creep	1943
Halsey, White & Eyring	31	rayon	stress relaxation	1945
Halsey & Eyring	32	wool	stress relaxation	1946
Holland, Halsey & Eyring	34	cotton, viscose rayon	creep	1946

TABLE 1 (continued)

Author(s)	Reference	Fiber(s)	Type of Measurement	Year
Speakman & Saville	93	nylon 66	stress relaxation	1946
Burleigh & Wakeham	9	cotton and rayon	stress relaxation	1947
Burte, Halsey & Dillon	10	wool	cyclic loading	1948
Lyons & Prettyman	58, 59, 60	steel, fiberglas, ramie, rayon, nylon, vinyon & velon	dynamic	1948 1949 1950
Reese & Eyring	85	hair	stress relaxation	1950
Katz & Tobolsky	42	wool	stress relaxation	1950
Abbott	1	nylon	stress relaxation	1951
Dunell & Dillon	19	viscose rayon, acetate rayon, nylon, silk, feather keratin and polyethylene	dynamic	1951
Ree, Chen & Eyring	83, 84	saran, PVC	stress relaxation	1951
de Vries	111	cellulose	dynamic	1951
Kubu	46	wool	stress relaxation	1952
Lincoln	54	wool	flexural fatigue	1952
Catsiff, Alfrey & O'Shaughnessy	11	nylon 66	creep	1953
Lasater	49	cotton	stress relaxation	1953

TABLE 1 (continued)

Author(s)	Reference	Fiber(s)	Type of Measurement	Year
Feughelman	23	wool	creep	1954
Wood	124	human hair	stress relaxation	1954
Fujino	26	rayon, silk, & nylon 66	dynamic	1955
Tipton	103	nylon	dynamic	1955
Lemiszka & Whitwell	52	nylon 66	stress relaxation	1955
Tokita	105	nylon 6	dynamic	1956
Price, McIntyre, Patterson & Dunell	81	nylon 66	stress relaxation	1956
Rigby, Hirai, Spikes & Eyring	87	rat tail tendon	stress relaxation	1959
Dunell, Joanes & Rye	20	nylon 66	stress relaxation	1960
Nagamatsu	70	nylon 66, isotatic polypropylene	torsional stress relaxation	1960
Laible & Morgan	48	polyvinylalcohol	high speed tensile	1961
Meredith & Hsu	67	nylon 66, orlon, polyester & viscose rayon	stress relaxation & dynamic bonding	1962
Howard & William	39	nylon 66	creep	1963
Ward, Hadley, Wolfe & Onat	30, 114, 115	polypropylene	creep	1963, 1965, 1966
Haut & Little	33	collagen	stress relaxation	1972

TABLE 1 (continued)

Author(s)	Reference	Fiber(s)	Type of Measurement	Year
Chapman	12	wool, nylon 66 and polyester	bending stress relaxation	1973
Jenkins & Little	40	elastin	stress relaxation	1974
Lunn, Lee & Yannas	57	polyester & nylon 66	stress relaxation	1974
Woo & Postle	123	cotton, jute, & wool	dynamic	1974
Ko, Chen & Lundberg	44	strong nylon	cyclic extension & stress relaxation	1975
Willet	122	viscose rayon, nylon 66 & polyester	dynamic	1975
Chen, Ko & Lundberg	14	hard elastic polypropylene	cyclic extension & stress relaxation	1976

models, or the multiple integral representation, the common feature among these theories are: (1) the ultimate goal is to fit experimental data, (2) the mathematical tools used are either differential operators or integral equations and, (3) the procedures for establishing the constitutive equations are either through the use of models (combination of springs and dashpots) or based on Boltzmann's superposition integral. None of these theories have been tested over a wide range of responses for fibers.

The Problem

All experimental evidence (Table 1) shows that polymeric fibers have nonlinear stress-strain relationships which depend on previous history (or changing structures), time, temperature, humidity, and other environmental conditions. Fibers and fibrous materials, with their unusual combination of high tensile strength and toughness, are widely used in tensile structures and for reinforcement (e.g. ropes, cords, clothing, fiber reinforced composites, skeletal structures of plants, and skeletal structures of animals). The usefulness and the necessary concomitant, nonlinear mechanical behavior of fibrous materials are consequences of their intrinsic composite structures.

In design and analysis with fibers and fibrous structures, linear elasticity is still widely used, with a few exceptions (e.g. Lee [51], Schapery [88], Turner [82, 107]), despite the fact that this theory assumes small deformations and time independency. This practice is costly and misleading.

In order to make realistic analysis and effective design with fibrous materials, we need constitutive equations of fibers that take time and finite deformation into consideration.

Deriving constitutive equations requires a procedure to unify observed responses from different experiments in such a form that responses can be embedded in the constitutive equations.

To examine the usefulness of these equations, we must test them on a wide spectrum of materials over wide ranges of load, extension levels and time.

In this study, I attempt to obtain one dimensional constitutive equations for polyamide fibers including strong nylon, spider silk, and drawn and undrawn nylon 6. The broad range of mechanical responses and the practical significance of this class of fibers make these polyamides a reasonable first study of the nonlinear viscoelastic behavior of polymeric fibers.

The elastic responses of the polyamide fibers were observed by simple elongation experiments. To check the degree of nonlinearity, the slopes of the stress-strain curves of these fibers were plotted as functions of strain and compared with predictions from finite elasticity theory.

Hysteresis loss as a function of strain rates was observed to examine the mechanical reversibility of the fibers and the range of nonlinearity of viscous responses.

Uniaxial stress relaxation, creep and sinusoidal loading experiments were made at different constant extensions, loads, and frequencies over a range of five to six decades in time. Results from these three types of measurements were unified with a relaxation spectrum characterized by the experimentally observed history dependent behavior of each fiber. This relaxation spectrum and the elastic response were then embedded into a quasilinear mathematical model to form approximate constitutive equations for each fiber.

CHAPTER II

EXPERIMENTAL

Introduction

In this chapter, the tensile viscoelastic response of strong nylon, spider drag line and drawn and undrawn nylon 6 fibers measured by simple elongation, cyclic loading, stress relaxation, creep and sinusoidal stretching at various strain rates, strain levels, load levels and frequencies are given. In Table 2 the physical properties of the polyamide fibers are summarized.

Materials

Strong Nylon

Strong nylon fibers, known as Kevlar® 49[1], was obtained from the Textile Fibers Division of E. I. du Pont de Nemours & Company, Inc. Used mainly for reinforcement of composite structures and specialty cables, Kevlar® 49 is an example of the high modulus industrial organic fibers developed recently.

Kevlar® 49 fibers are of the class of para-oriented aromatic polyamides. The exceptional chain stiffness of these fibers is due to the torsional rigidity and planarity of phenyl rings along the skeletal chains and to the relatively large intermolecular interactions associated with the large polarizability of phenyl rings.

---

[1]This fiber was given to us as PRD 49.

TABLE 2. PHYSICAL PROPERTIES OF POLYAMIDE FIBERS

FIBER (SOURCE)	SPECIFIC GRAVITY (GM./C.C)	APPROX. DIA. (MICRONS)	NOMINAL STRENGTH ($DYNE/CM^2 \times 10^{-8}$)	INITIAL MODULUS ($DYNE/CM^2 \times 10^{-10}$)	APPROXIMATE BREAKING ELONGATION %
STRONG NYLON (DU PONT)	1.45	11.94 (1.46 den.)	306	105.6	2.4
SPIDER SILK (DRAG LINE MILKED FROM ARGIOPE AURENTIA)	1.25	3.10 (.085 den.)	137	12.9	35.0
NYLON 6 (DRAWN) (AMERICAN ENKA)	1.14	43.15 (15 den.)	59	2.1	55.0
NYLON 6 (UNDRAWN) (AMERICAN ENKA)	1.14	43.15 (15.den.)	55	1.9	780.

Published results on the mechanical properties of strong nylons are few [2, 45, 78], but these fibers are receiving increasing attention.

With strength about thirty times that of structural steel and initial modulus approximately three times greater than structural steel on weight basis, the mechanical properties of strong nylon form the upper limit of this study.

Spider Drag Line

Of the more than 1,200,000 species of spiders on earth, about 2500 species are silk makers (orb weavers). Properties of spider silks vary by species and by functions. Depending upon the species, an individual spider has more than five different silk glands where silks of different properties are produced before extrusion through three pairs of spinnerets. The drag line originates in the ampullate gland and is extruded through the anterior spinnerets. Spider drag line is the strongest and toughest of the silks a spider makes. Spider drag line is the structural framework of a spider web and the life line of a spider.

Chemically, spider silk is a fibroin composed of twenty-odd alpha amino acids connected by the amide linkage (-CONH-). Alanine, glycine, serine and proline account for eighty percent of the amino acids [126].

Drag lines of Nephila clavipes (golden silk spider) and Argiope aurentia (black and yellow spider) are among the strongest spider silks that we know. The strength of the drag line of Nephila clavipes

obtained by forcible silking was reported to be about 8 grams/denier and the strength of the drag line of Argiope aurentia was approximately 12 grams/denier [126]. In fact the strength and toughness of the silk from Nephila clavipe was recognized for a long time by the South Sea Islanders who use the silk to make various kinds of bags and fish nets [53]. The books by Levi [53], Kaston [41] and Comstock [16] are entertaining and informative. More serious reading on the biochemical and behavioral aspects of the orb weavers can be found in the book by Witt et al. [118]. Results on the fine structure, chemical composition, synthesis and silk spinning have been reported by Friedrick [25], Peakall [76], Lucas [56], Warwicker [116], Zemlin [126], Work [125], Marples [62], and Wilson [119, 120, 121]. Except for some tensile measurements by Lucas [55], Work [125], and Zemlin [126], little work has been done on the mechanical properties of spider silk.

In this study, the drag lines were forcibly silked from an Argiope aurentia spider collected from the bushes near the School of Textile Engineering on the campus of the Georgia Institute of Technology. The spider was anesthetized with carbon dioxide gas before being taped on a platform with the abdomen of the spider facing a microscope. The drag line was picked up from the anterior spinneret and carefully pulled up to a mandrel 7.6 cm above the spinneret of the spider. After the silk was taped on the mandrel, a black cardboard with a 1.3 cm hole at the center was placed behind the silk which was suspended between the mandrel and the spinneret of the spider. A drawing of the cardboard is shown in Figure 1. The cardboard, with

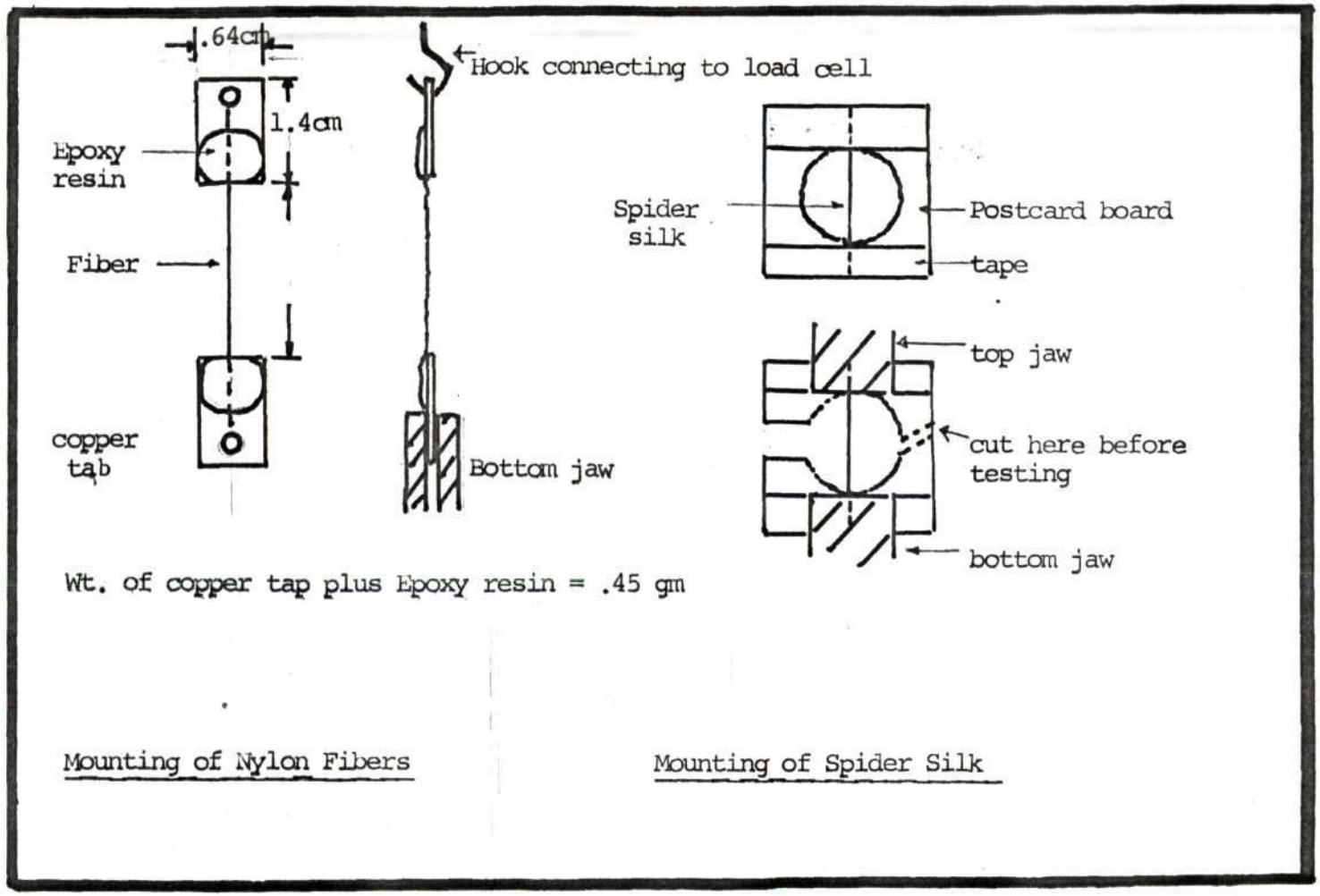

Figure 1. Sample Mounting Methods for Polyamide Fibers

the silk adhering to it, was raised vertically at a rate of 2.54 cm/sec to a position above the mandrel and the silk was taped to the mandrel before collecting another sample. More than 10 yards of silk was obtained from the same spider; this silk was used for all experiments.

Before testing, each specimen was examined under the microscope to insure that only single fibers were used. The diameter of the drag line measured by scanning electron microscopy was 3.1 microns; this corresponds to 0.085 denier assuming 1.25 gm/c.c as the density of the fiber. Scanning electron microscope pictures indicated that the cross-section of the drag line was approximately circular.

Drawn and Undrawn Nylon 6

Fifteen denier nylon 6 (drawn and undrawn) monofilaments were obtained from the American Enka Company. Nylon 6 fibers are used extensively in textile applications. To produce the necessary strength and stiffness, nylon 6 filaments are usually drawn to 3.5 to 4 times their original length. Because of their commercial importance, several studies have been carried out on nylon 6 fibers [7].

Inclusion of drawn and undrawn nylon 6 fibers in this study serves as a cross-check between available information and the results obtained from this study as well as help us to gain some understanding of the effect of drawing on the viscoelastic behavior of nylon 6 fibers.

The high breaking elongation, close to 800%, and the low initial modulus make the undrawn nylon 6 an extreme contrast to strong nylon in mechanical response.

Experiments and Observations

Sample Preparation and Conditioning

Individual strong nylon and drawn and undrawn nylon 6 fibers were attached to clean copper tab surfaces with an epoxy resin cement (a mixture of 60% Epon Resin 820[1] and 40% Versamid Epon curing agent[2]), as shown in Figure 1. A small tension was maintained on the specimen to keep the fiber straight while the cement was applied. A curing time of twenty four hours at room temperature was required before testing. This cement mounting procedure was found to be satisfactory for the different fibers (nylons, polyesters and polypropylenes), for the various kinds of tensile tests over a wide range of temperatures (-75° C to 325° C), humidity (wet and dry) conditions and strain rates (3×10^{-5} to 10^{3} per second).

All the fibers were conditioned at 21° C, 65% RH for more than twenty four hours before testing. Creep of spider silk and sinusoidal stretching experiments were carried out in the micromechanics laboratory of the Engineering Experiment Station at the Georgia Institute of Technology. All tests were performed in laboratories maintained at 21° C $\pm$ 1° C and 65% RH $\pm$ 2% RH.

Data Logging Systems

Depending upon the nature of the tensile experiment, analog data recording devices and a digital data logging system were used.

---

[1] A product of the Shell Chemical Company.

[2] A product of the General Mills Chemicals, Inc.

A. The analog data logging devices include:

1) The Instron tensile testing machines chart recorder -- for recording the cyclic loading hysteresis loops and for recording some of the tensile tests.

2) Mosely 7000A X-Y plotter -- for recording hysteresis loops from low frequency sinusoidal stretching experiments and for recording creep curves.

3) Tektronix® 5103N dual beam oscilloscope (with C-5 oscilloscope camera) -- for monitoring constant load and extension levels in creep and stress relaxation experiments and for recording the stress and strain sinusoids in dynamic stretching experiments.

B. Digital data logging system (Hewlett-Packard Recording System - hereafter called the H-P System)

The data logging system used was one of the earliest programable data logging and processing systems manufactured by the Hewlett-Packard Company. This system includes a digital voltmeter which receives the analog signal from transducers at a programmed rate. The digitized signal is stored in an extended memory through a coupler/controller following program steps from the calculator. When an experiment was completed, data stored in the extended memory were printed out and punched on computer tape by a teleprinter according to the instruction from the calculator. A home-made relay was added to the system for turning the teleprinter on and off for long time experiments. A schematic drawing of the system is shown in Figure 2.

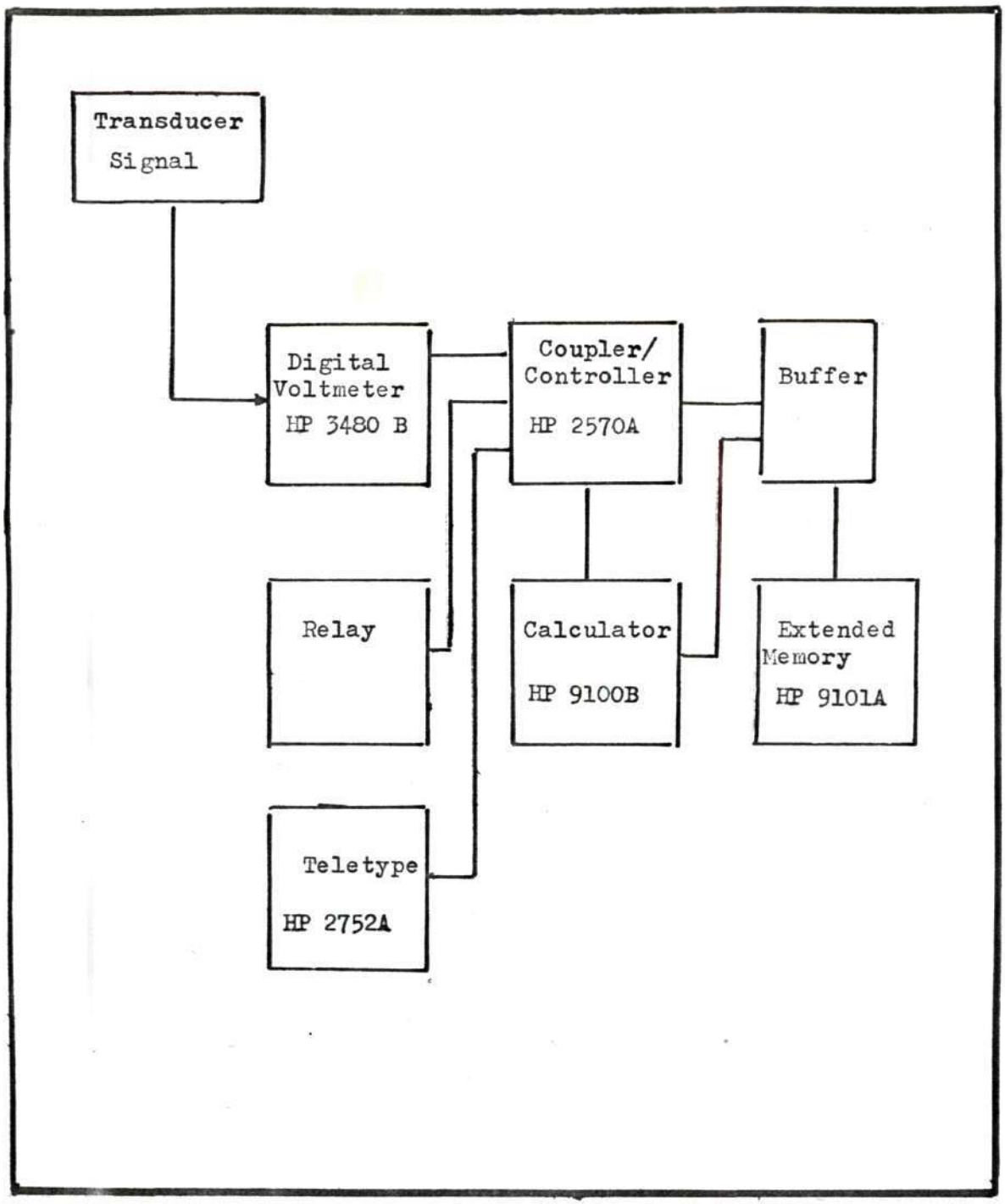

Figure. 2. Schematic Drawing of the Data Logging System

Elastic Response in Simple Elongation

I. Experimental Details:

Apparatus: Instron tensile tester (model TTB)

Force sensor: Instron load cells "A" and "B", Statham UC 4 Silver cell, Sanborn 350-1100AS carrier amplifier

Recorders: Instron chart recorder and H-P system

Testing condition: 21° C, 65% RH

Strain rate: 3.3×10^{-2} per second (100% per minute)

Gage length: strong nylon--12.5 cm, drawn and undrawn nylon 6--2.54 cm, spider silk--1.25 cm

Replication: 10

In simple elongation tests, two types of mountings were used. For strong nylon and drawn and undrawn nylon, the copper tabs with the fiber attached was first hung on the hook attached to the load cell (Figure 1), then the bottom tab was gripped in an Instron pneumatic jaw. The gage length was measured before each test. Due to the fineness of the spider silk, patience and care were necessary to make a successful test. The cardboard with the silk on it was first inserted into the top and bottom grips. The top grip was an Instron plastic grip and the bottom was a pneumatic grip. The connecting part of the cardboard was cut carefully with the top grip fixed by hand (Figure 1).

Tensile testing of soft materials is routine, but when testing stiff materials such as strong nylon, machine compliance must be considered. Machine compliance is caused by deformation of load cell,

jaw, tester frame and slack in the gears. The machine compliance can be determined by measuring the relationship between extension and gage length of a material of known initial modulus under a constant load. The extension extrapolated to zero gage length divided by the constant load is the compliance. The compliance of the testing system was found to be of the order of 10^{-6}cm/gm. This is small compared to the breaking extension of the strong nylon which was on the order of 10^{-2}cm/gm. In addition, the breaking elongation and load are in close agreement with other published data on strong nylon. Therefore the results reported here should be reliable.

II. Observations:

The ratio of fiber length ℓ at any time divided by the gage length ℓ_o is a measure of the strain called the longitudinal stretch ratio $\lambda = \ell / \ell_o$. The strain in tension, ϵ elongation is simply $\epsilon = \lambda - 1 = (\ell - \ell_o)/ \ell_o$. The forces involved are divided by the initial cross sectional area to give the Lagrangian stress or divided by the linear density to give the specific stress, denoted herein by T.

In Figure 3, the average stress strain behavior of the four polyamide fibers are given. The stiff, strong nylon and the soft, undrawn nylon 6 together with spider silk and drawn nylon 6 bracket the material properties of almost all textile fibers.

The stress-strain curves of strong nylon and drawn and undrawn nylon fibers reflect the average stress-strain response with less than 3% error at 95% confidence level. The average deviation from the means are 4.60% for strong nylon, 3.5 % for drawn nylon 6 and 4% for undrawn

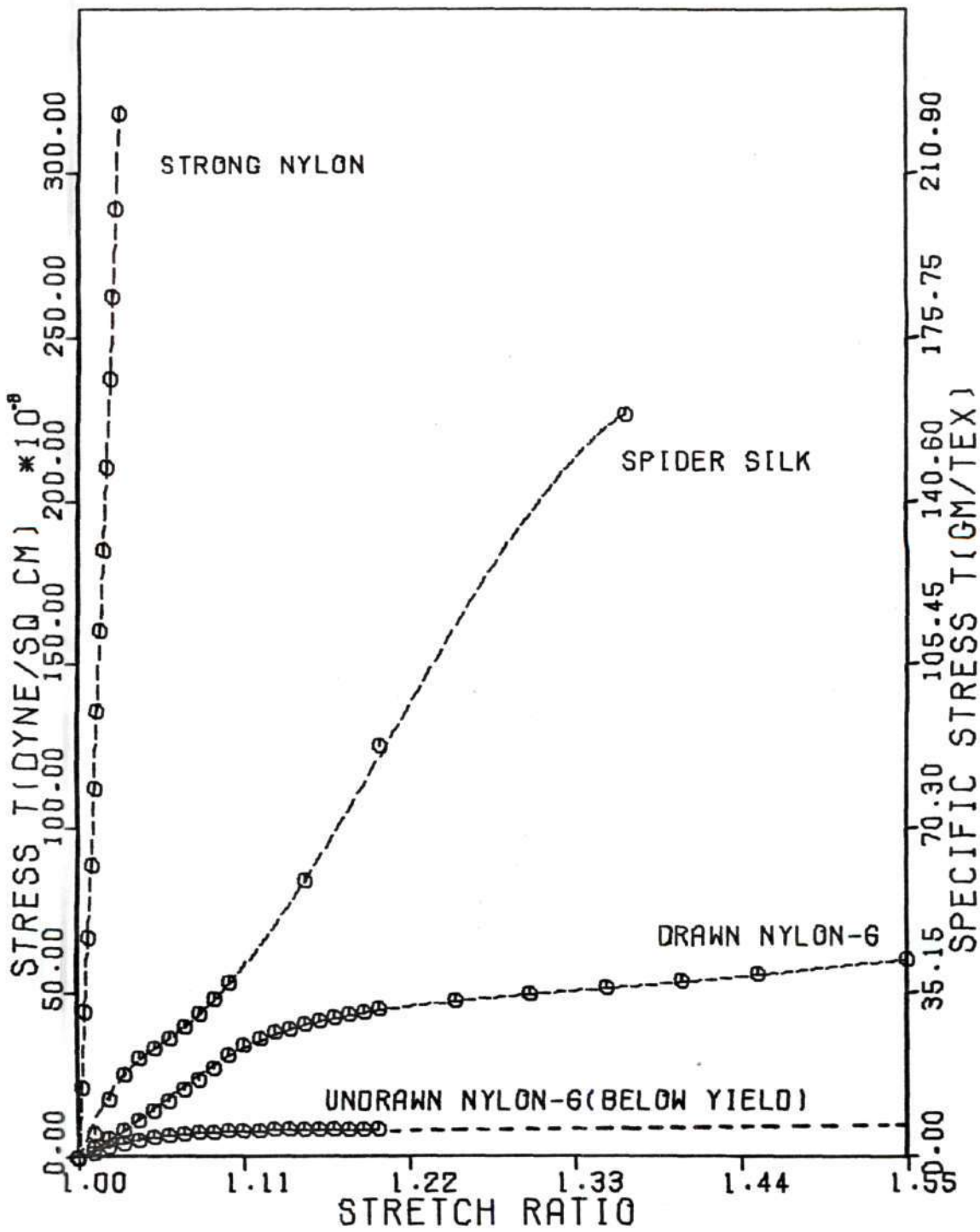

FIGURE 3. STRESS-STRAIN CURVES OF POLYAMIDE FIBERS

nylon 6. The experimental stress-strain data for spider silk are more dispersed. The average deviation from the mean load response at each strain level for spider silk is about 24%. With ten observations, this can be translated into an error of ~ 12% at 95% probability level. The wide dispersion of experimental data of spider silk was also noted by Work [125].

Figures 4 to 7 show the individual stress strain curves and slopes of the stress-strain curves as functions of the stretch ratio for each fiber. The stress-strain curves were fitted with cubic spline functions (Appendix B) and compared to predictions from finite elasticity theorty, e.g. [104], assuming constant volume and using the initial moduli as the material constants.[1]

None of the fibers has a constant "modulus". In no case can finite elasticity theory fit these stress-strain curves.

The strengths of the spider silk (Figure 5) are comparable to those of the high tenacity fibers but with much higher breaking elongations. Such generous combination of strength and toughness is more likely to be found in nature's structural materials than in man-made systems.

Hysteresis by Cyclic Loading

I. Experimental Details:

Apparatus: Instron tensile tester (model TTB)

Force sensor: Instron load cell "A" and "B"

---

[1] $T = \frac{E}{3}\left(\lambda - \frac{1}{\lambda^2}\right)$ where T = stress, E = initial modulus, and λ = stretch ratio

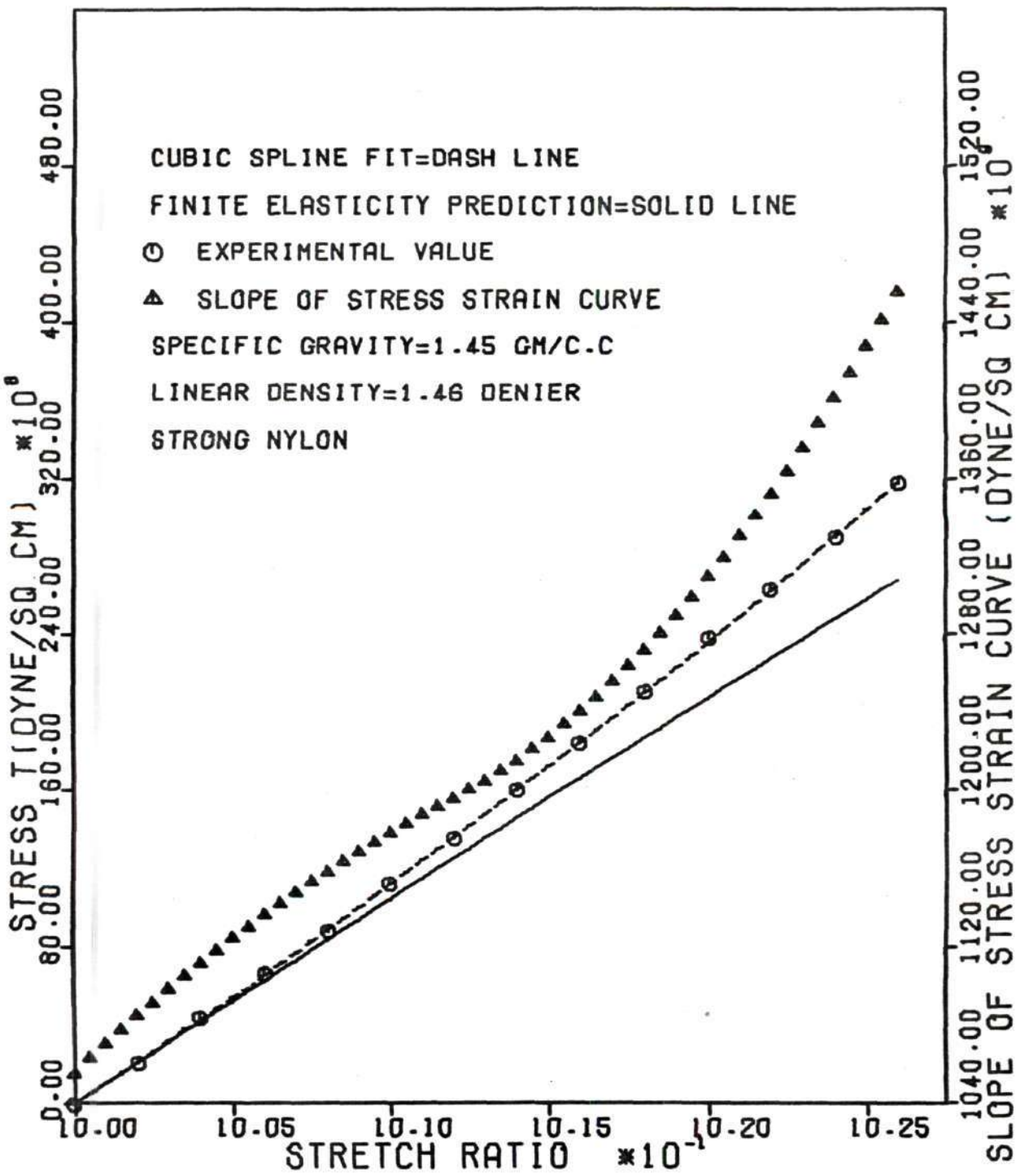

FIGURE 4. STRESS-STRAIN CURVE AND SLOPE OF THE STRESS-STRAIN CURVE OF STRONG NYLON FIBER

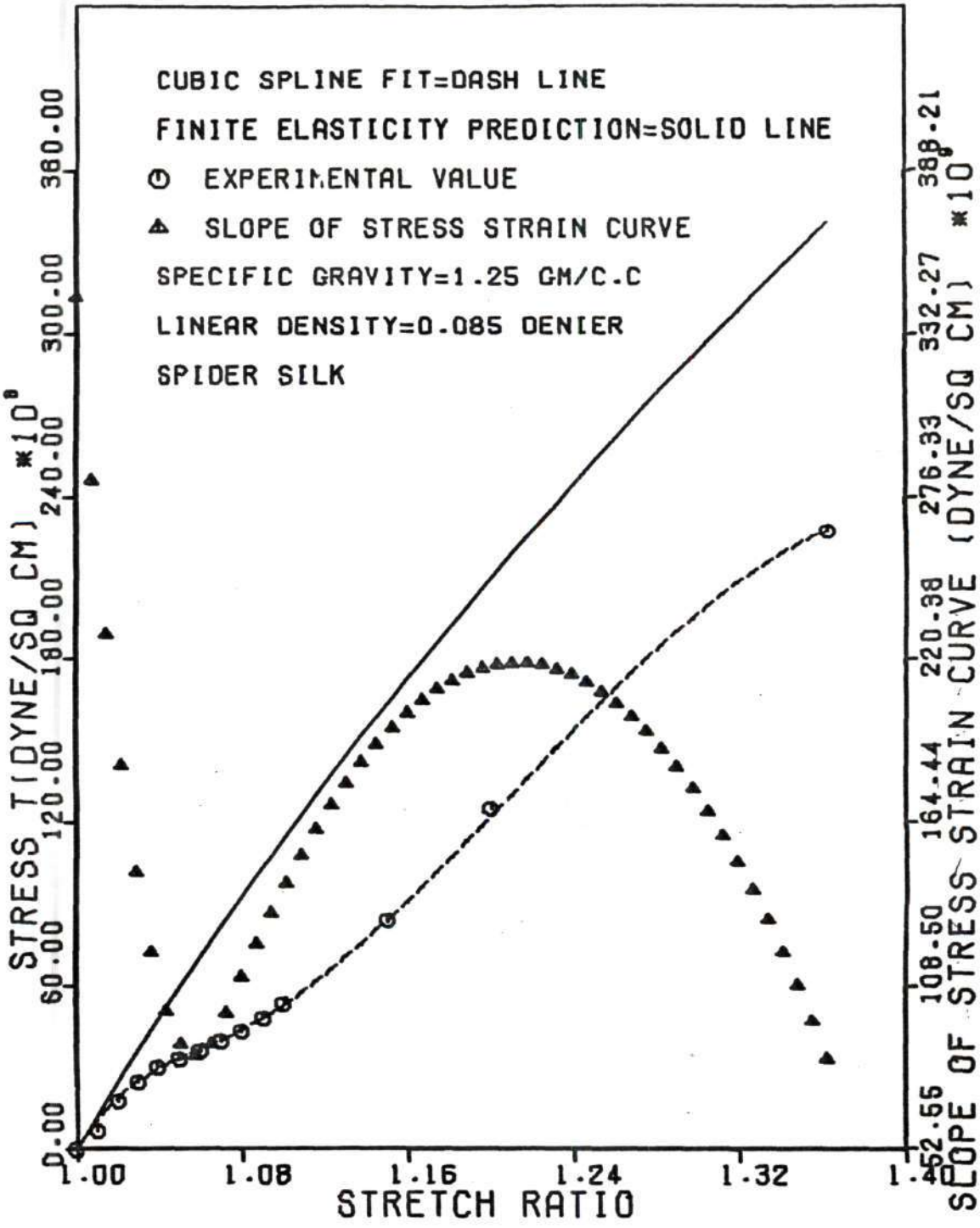

FIGURE 5. STRESS-STRAIN CURVE AND SLOPE OF THE STRESS-STRAIN CURVE OF SPIDER SILK

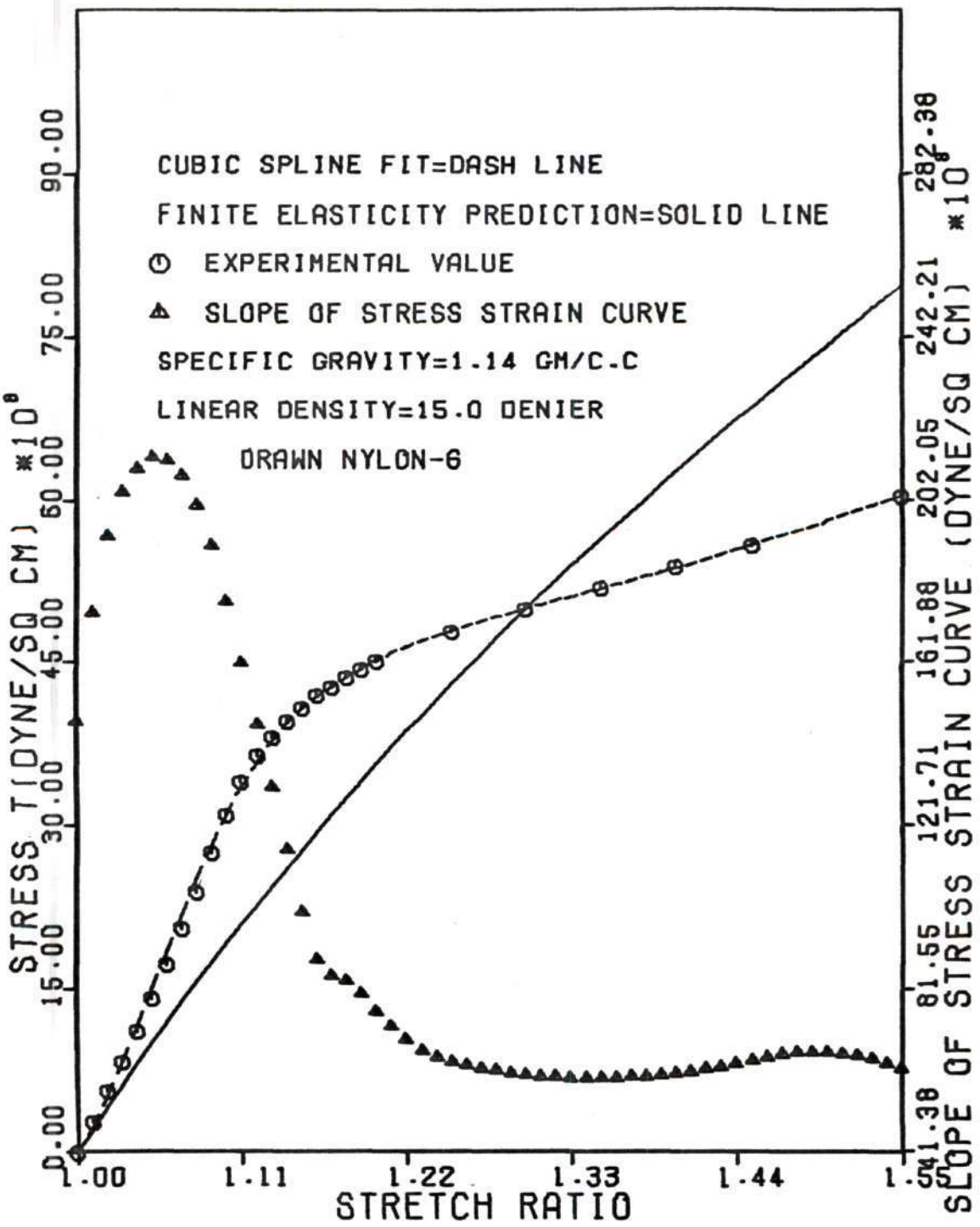

FIGURE 6. STRESS-STRAIN CURVE AND SLOPE OF THE STRESS-STRAIN CURVE OF DRAWN NYLON-6 FIBER

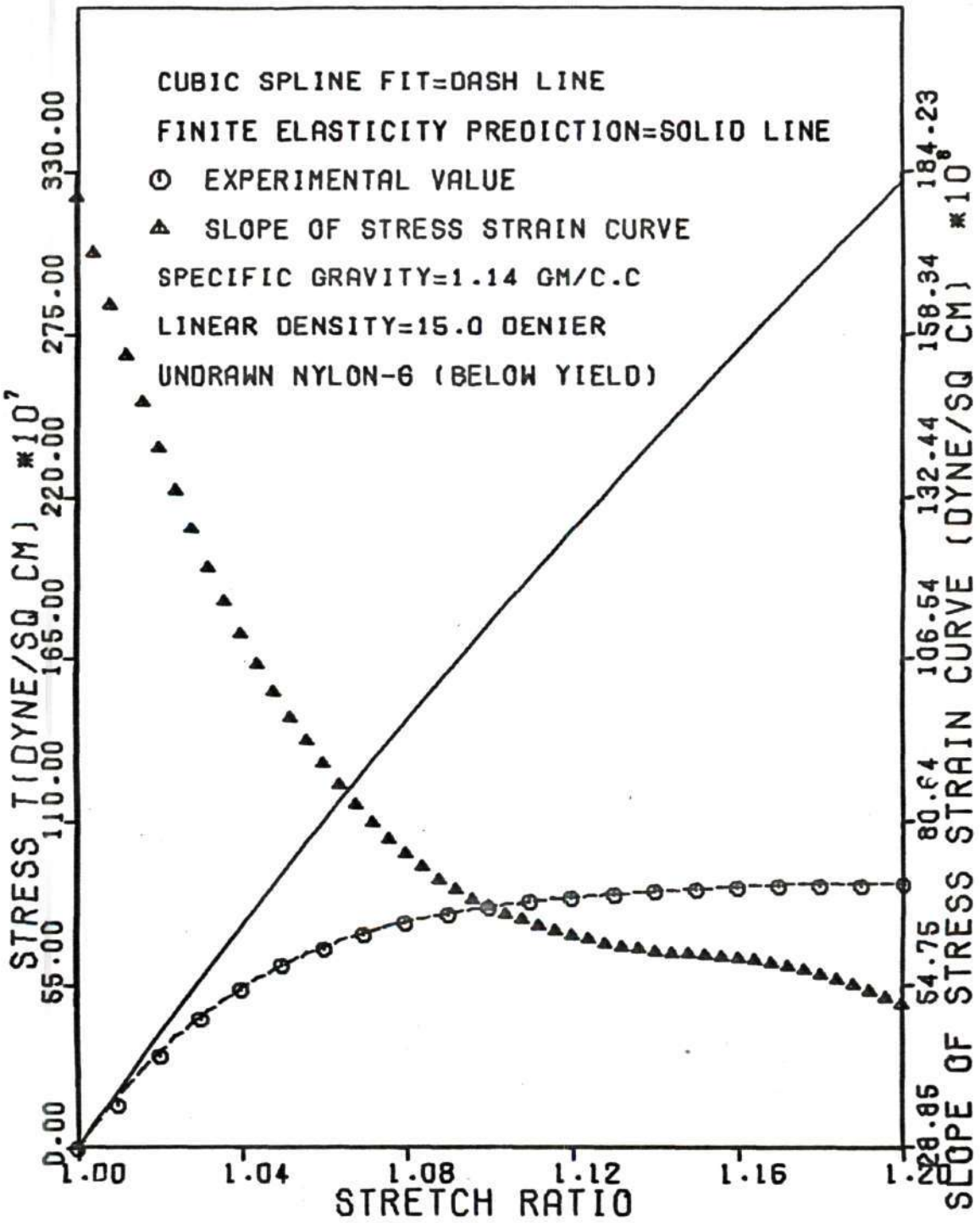

FIGURE 7. STRESS-STRAIN CURVE AND SLOPE OF THE STRESS-STRAIN CURVE OF UNDRAWN NYLON-6 FIBER

Recorder: Instron chart recorder

Testing Condition: 21° C, 65% RH

Strain rates (per second): 3.3×10^{-5}, 6.6×10^{-5}, 3.3×10^{-4}, 1.66×10^{-3}, 8.33×10^{-3}, 1.66×10^{-2}

Load levels: strong nylon--25 gm, spider silk--.5 gm, drawn nylon--20 gm, undrawn nylon--10 gm

Gage length: strong nylon--12.5 cm, spider silk--1.25 cm, drawn and undrawn nylon--2.54 cm

Replication: 10

Cyclic loading experiments were carried out in the same way as in the simple elongation experiments except that the fibers were stretched to predetermined loads then unloaded at the same rate as stretched. The areas within hysteresis loops in cyclic loading measure energy dissipation.

II. Observations:

In general, the difference between the hysteresis loss in the first cycle and the second cycle was the greatest. The difference among subsequent cycles diminished as the number of cycles increased.

Figures 8 to 11 give the typical second cycle hysteresis loops of the polyamide fibers at various strain rates. The energy dissipation of strong nylon was the lowest among the polyamide fibers studied. The energy losses were greater for softer fibers. Hysteresis losses of these fibers tend to be insensitive to strain rates. For example, a ten fold increase in strain rate causes little increase in the hysteresis loss for the strong nylon.

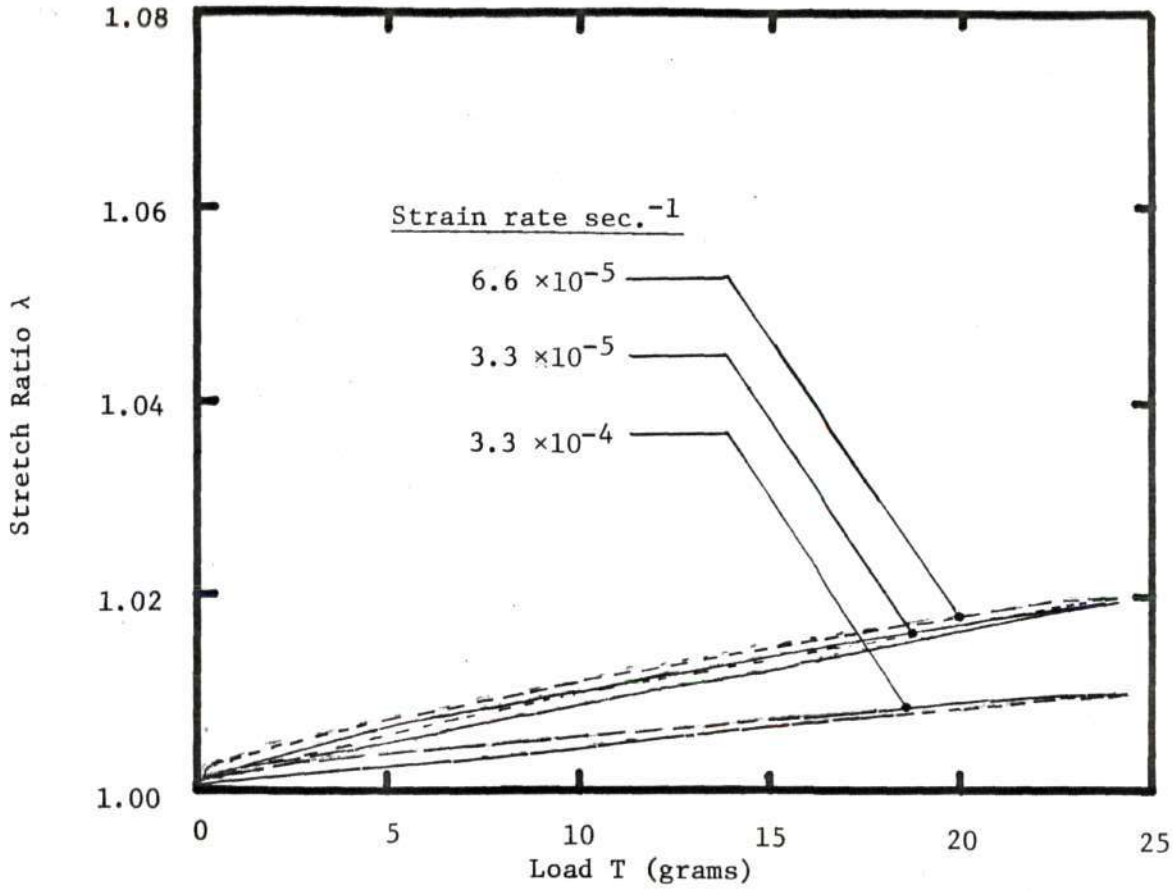

Figure 8. HYSTERESIS LOOPS OF STRONG NYLON FIBERS BY LOAD CYCLIC EXTENSION AT VARIOUS STRAIN RATES

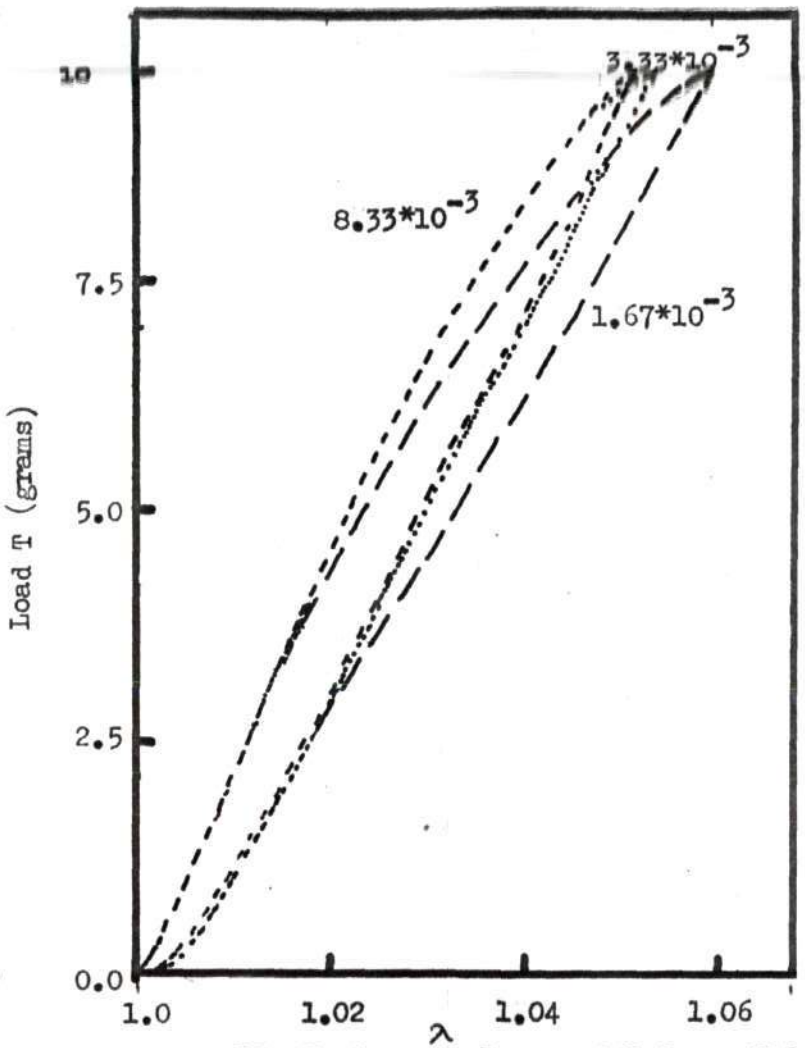

Figure 10. Hysteresis Loops of Undrawn Nylon Fibers by Load Cyclic Extension at Various Strain Rates

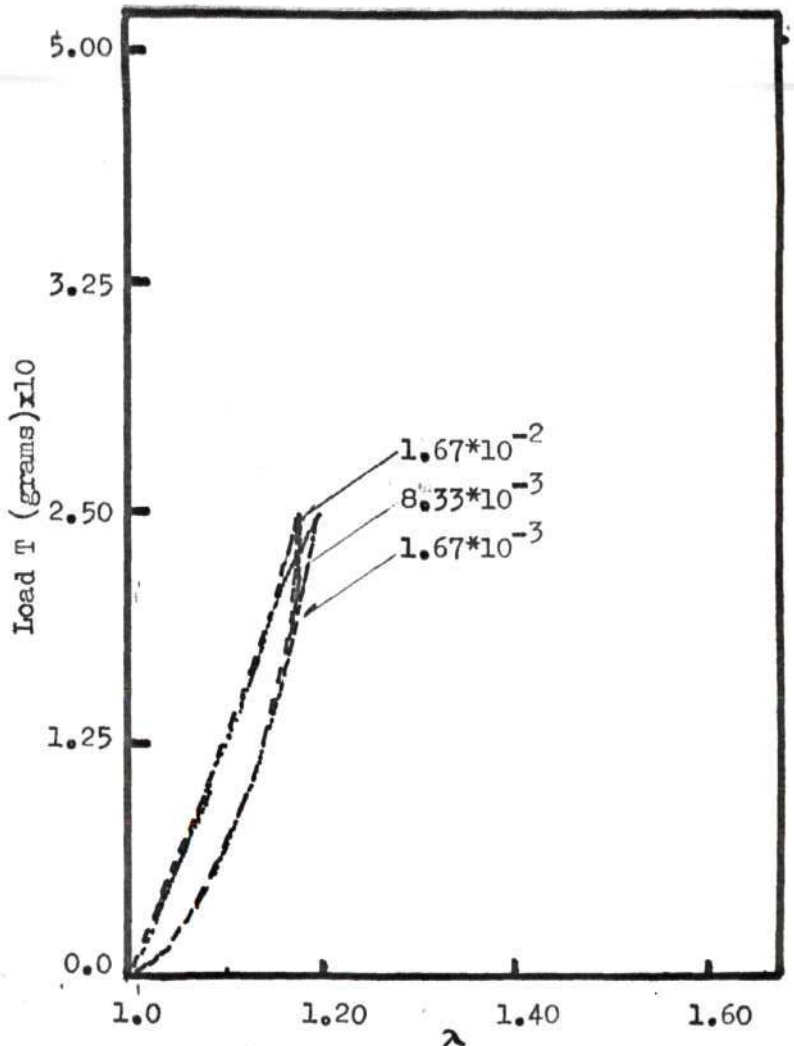

Figure 9. Hysteresis Loops of Spider Silk by Load Cyclic Extension at Various Strain Rates

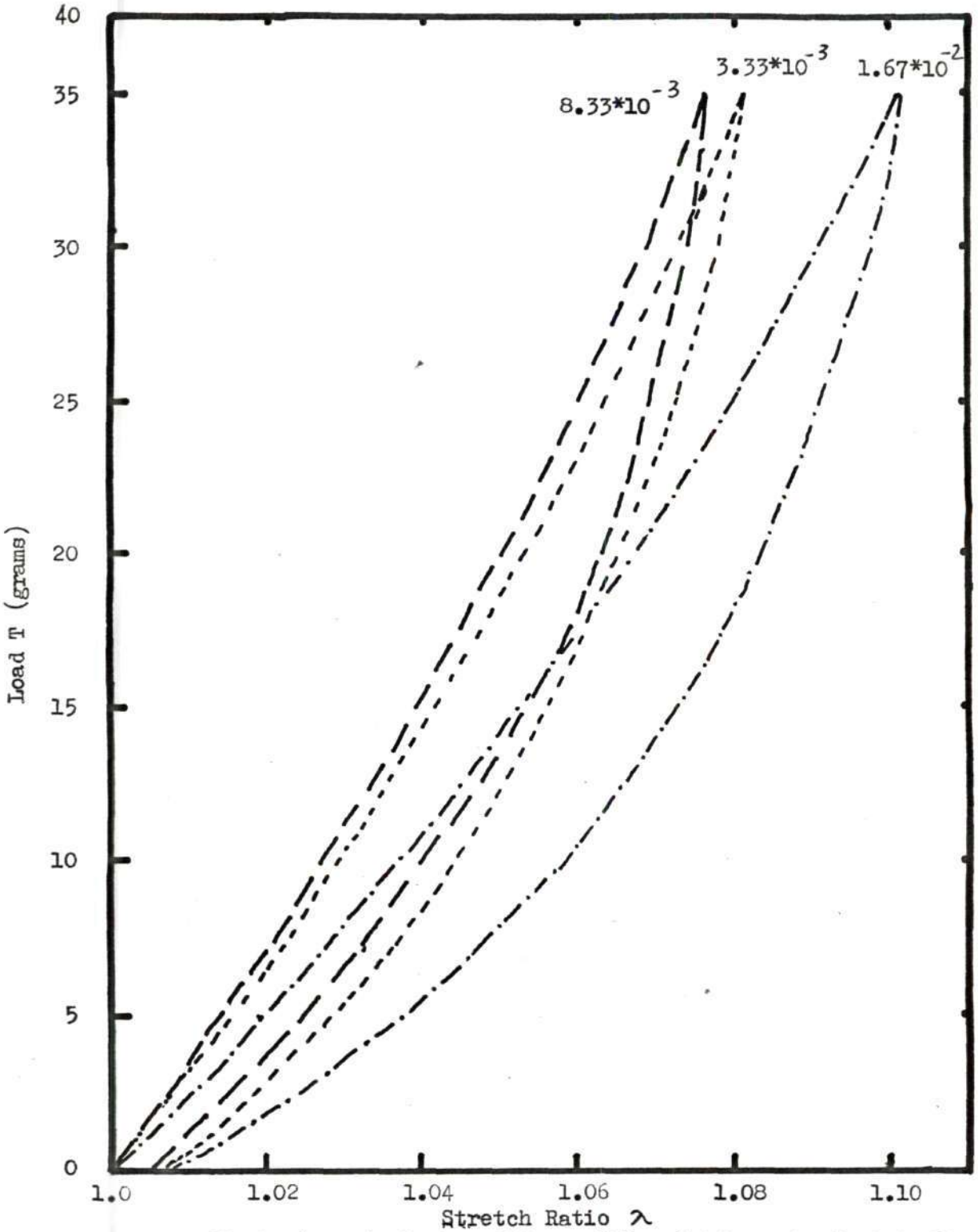

Figure 11. Hysteresis Loops of Drawn Nylon-6 Fibers by Load Cyclic Extension at Various Strain Rates

Stress Relaxation at Constant Strain

I. Experimental Details:

Apparatus: Instron tensile tester

Force sensor: Statham UC4 silver cell, Sanborn 350-1100AS carrier amplifier

Recorder: H-P system

Testing condition: 21°C, 65% RH

Stretch ratios:

strong nylon--1.004 to 1.02,

spider silk --1.01 to 1.15,

drawn nylon--1.02 to 1.20,

undrawn nylon--1.04 to 1.20

Time range: 0 to 10^4 seconds or 10^5 seconds

Gage length: strong nylon--12.5 cm, 2.54 cm for spider silk, and 2.54 cm for drawn and undrawn nylon

Replication: 3 to 5

In a typical relaxation experiment, the fiber was stretched to a predetermined extension level at a strain rate of .017 per second (100% per minute) on the Instron tensile tester. The force decay was recorded with the H-P system.

The cross head did not come to an abrupt stop as it reached the predetermined extension level in the relaxation experiment. Overshoot caused a transient oscillation of the force transducer which can lead to erroneous interpretation of data. To correct for the overshoot, a Schaevitz 3000XS-B linear variable differential transformer(hereafter

called (LVDT))was mounted on the Instron frame with the core and extension rod mounted on the cross head for each experiment. Figure 12 shows the displacement transducer response for various relaxation experiments. On the average, it takes 0.3 seconds for the cross head to reach a steady state. The steady state time was used as the zero time for normalization of data.

II. Observations:

The stress relaxation data obtained at various extension levels which correspond to different maximum loads are shown in Figures 13 to 16. Each datum plotted in the curves is an average value of three or more observations.

The same data shown in Figures 13 to 16 are presented in normalized form in Figure 17. The ordinate G(t) represents the normalized function of time called the reduced relaxation function. This is defined as:

$$G(t) = T(t)/T(t_r) \qquad (II\text{-}1)$$

$$G(0) = 1$$

where T(t) is the tension acting on the fiber at time t corresponding to a stretch imposed at $t - t_r$, and $T(t_r)$ is the tension in the fiber at the instant t_r. The time at which the cross head of the Instron tensile machine reaches a steady state is t_r. The ratio of T(t) and $T(t_r)$ can be interpreted as the Lagrangian stress(tension divided by the initial cross sectional area), the Eulerian stress(tension divided by the cross sectional area of the deformed state), or the specific stress

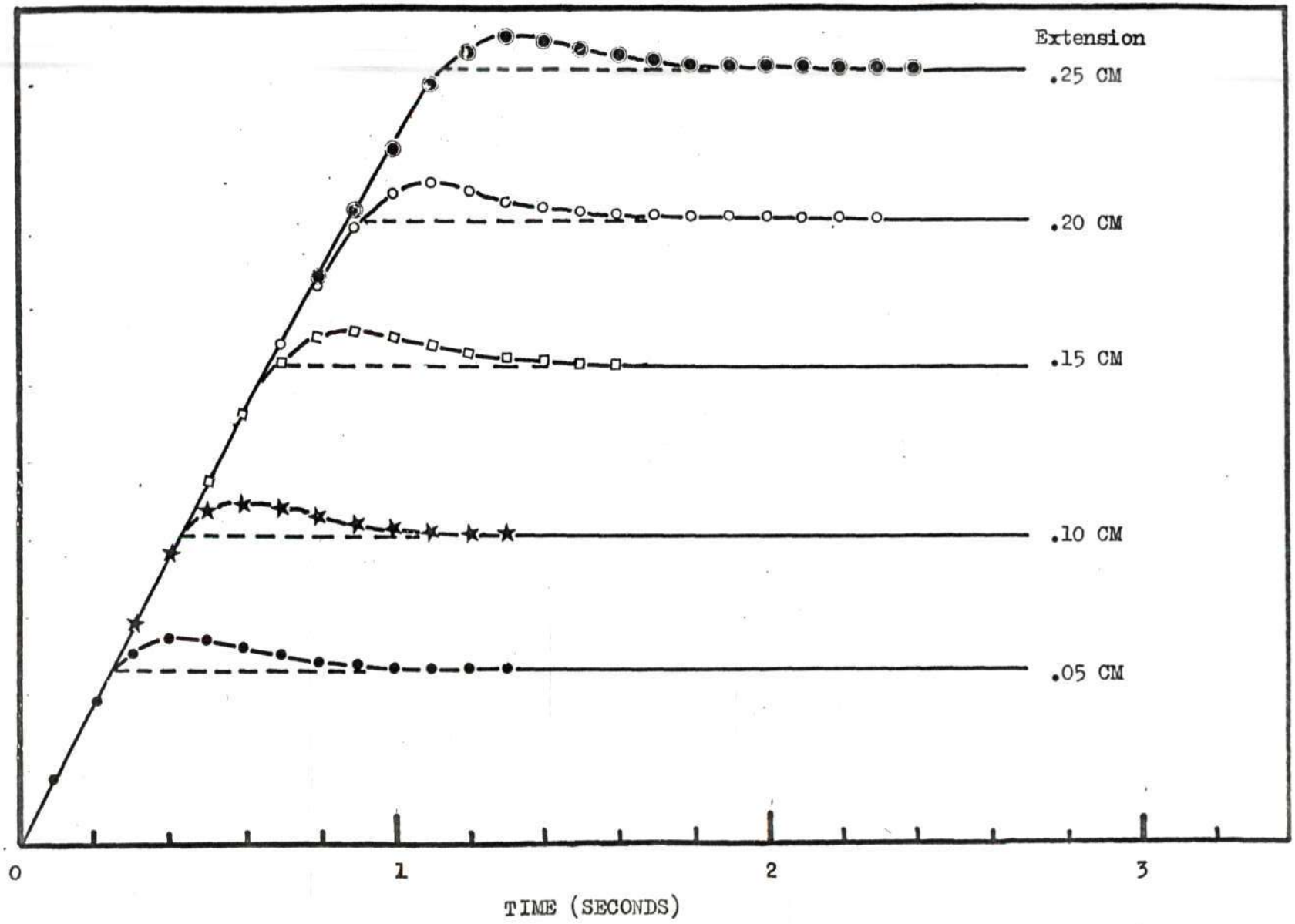

Figure 12. **Displacement Transducer Response in Stress Relaxation Experiments**

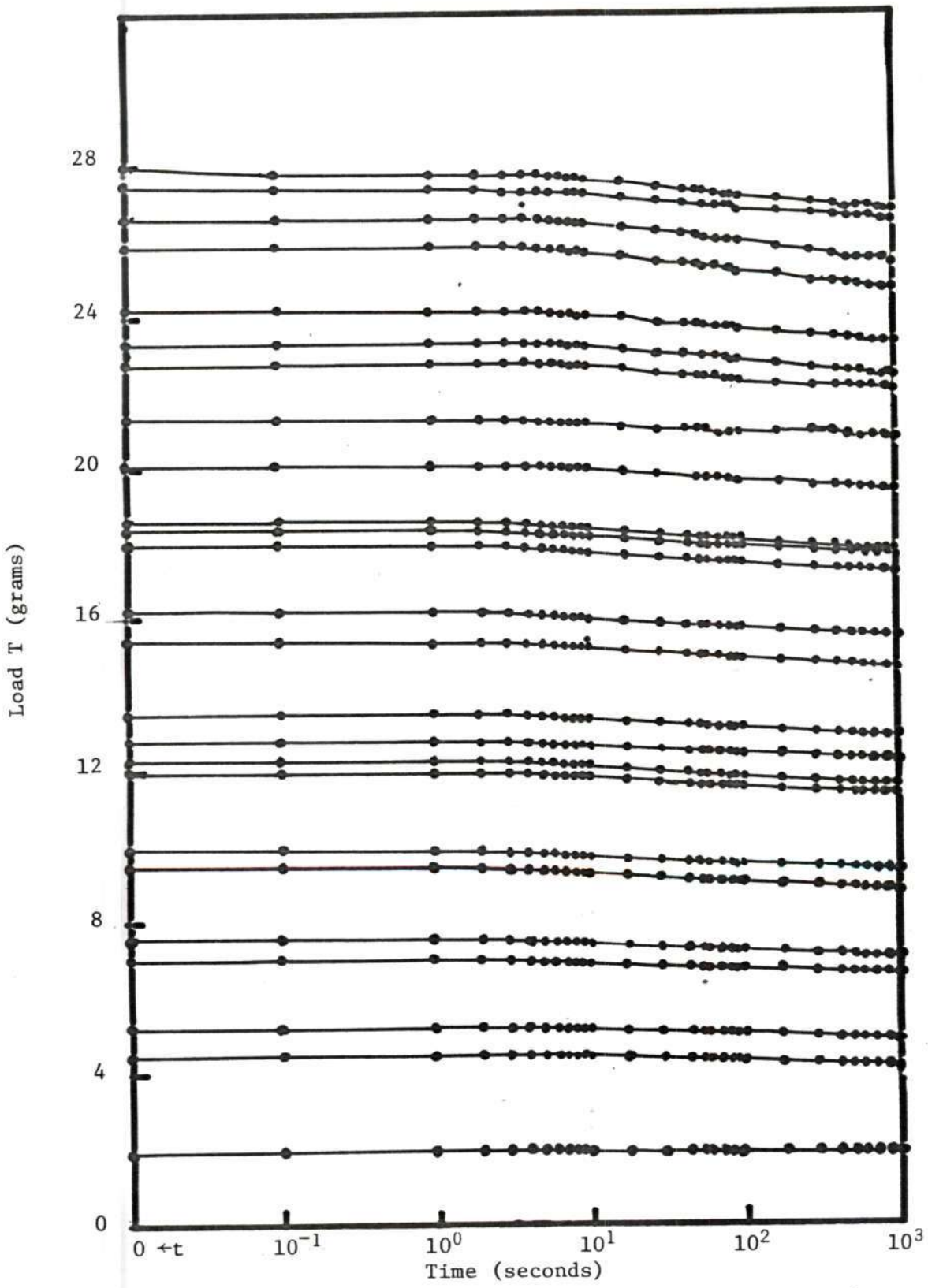

Figure 13. Relaxation Data of Strong Nylon Fibers Obtained At Various Maximum Loads

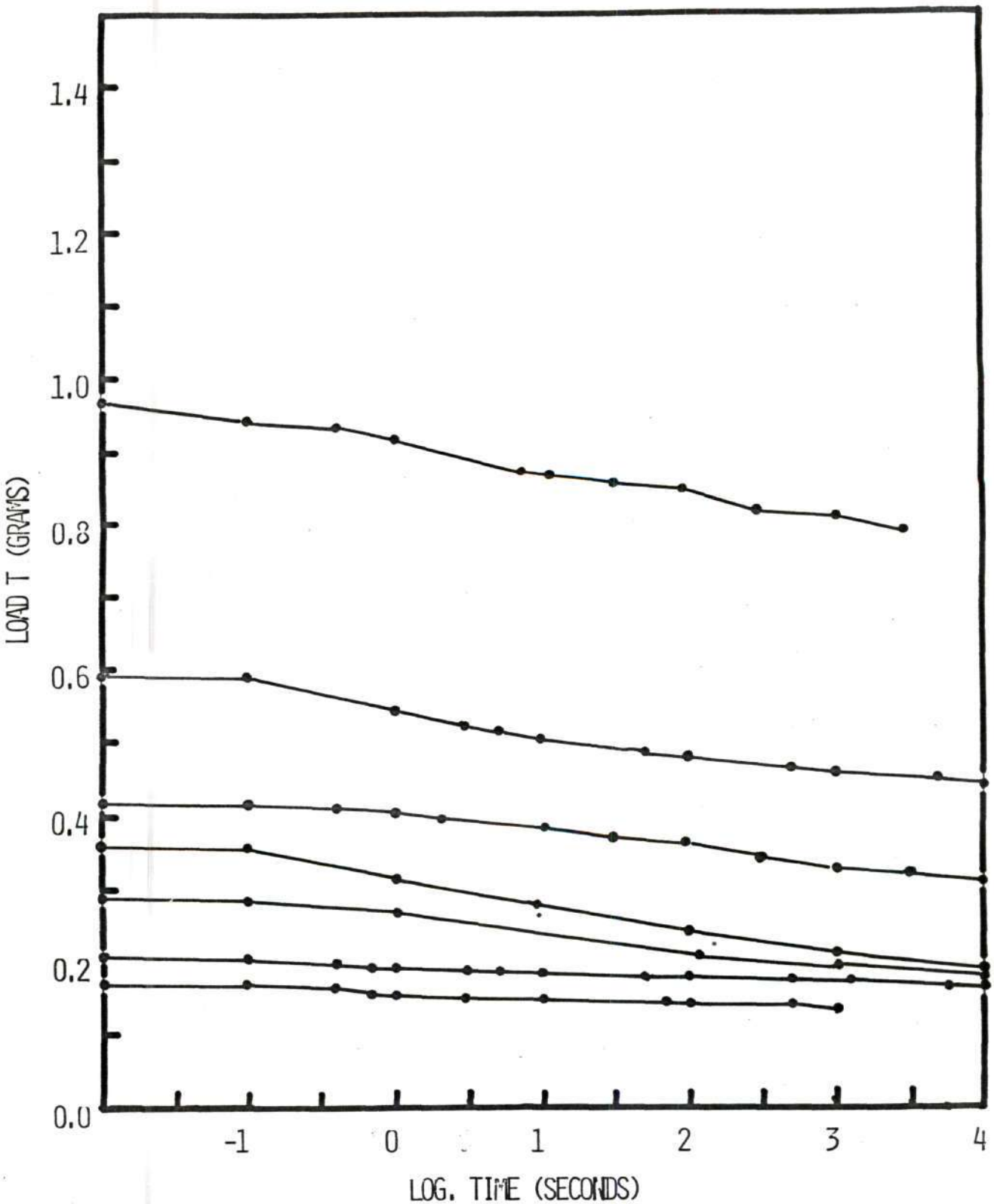

FIGURE 14. STRESS RELAXATION DATA OF SPIDER SILK OBTAINED AT VARIOUS MAXIMUM LOADS

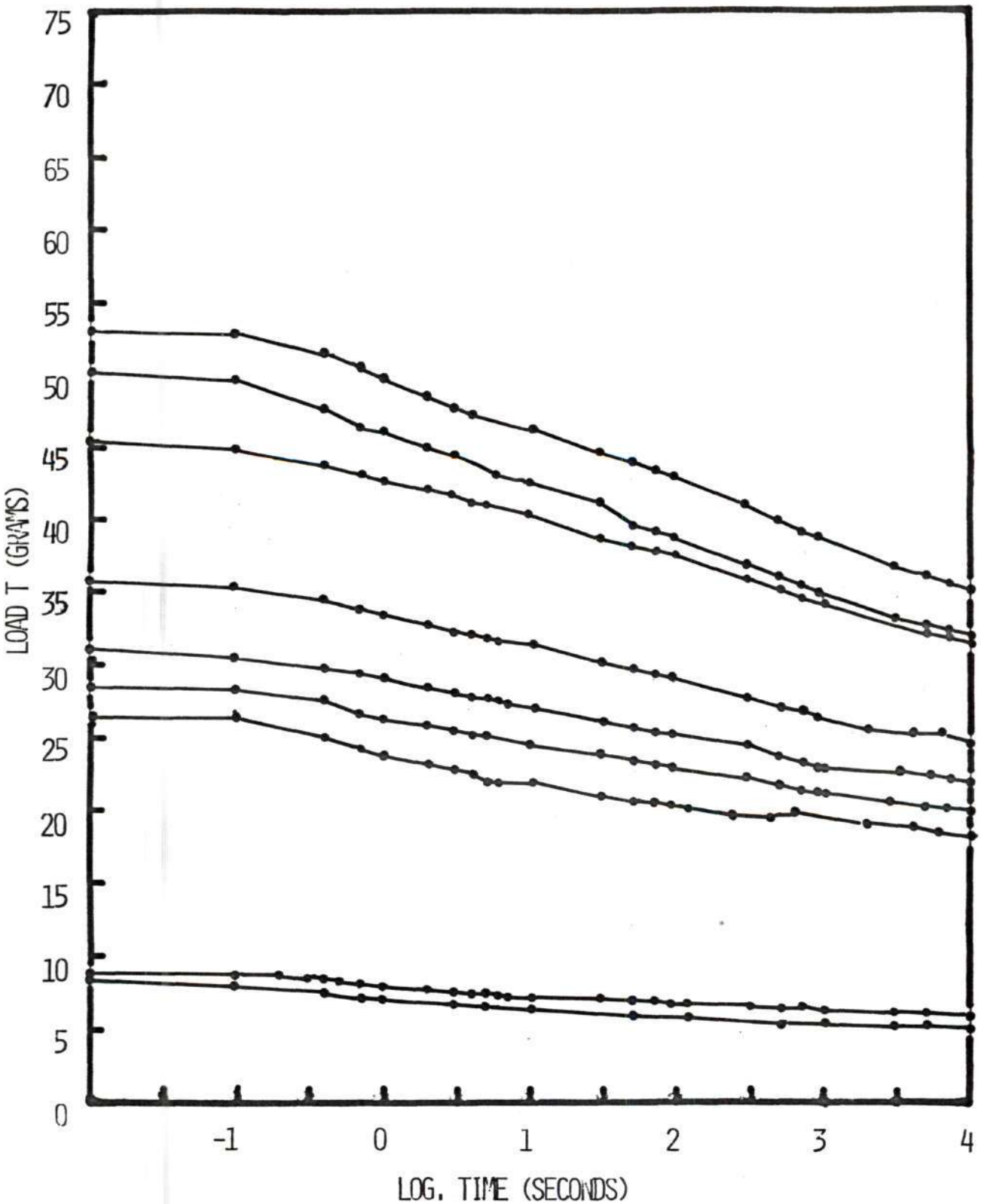

FIGURE 15. STRESS RELAXATION DATA OF DRAWN NYLON-6 FIBERS OBTAINED AT VARIOUS MAXIMUM LOADS

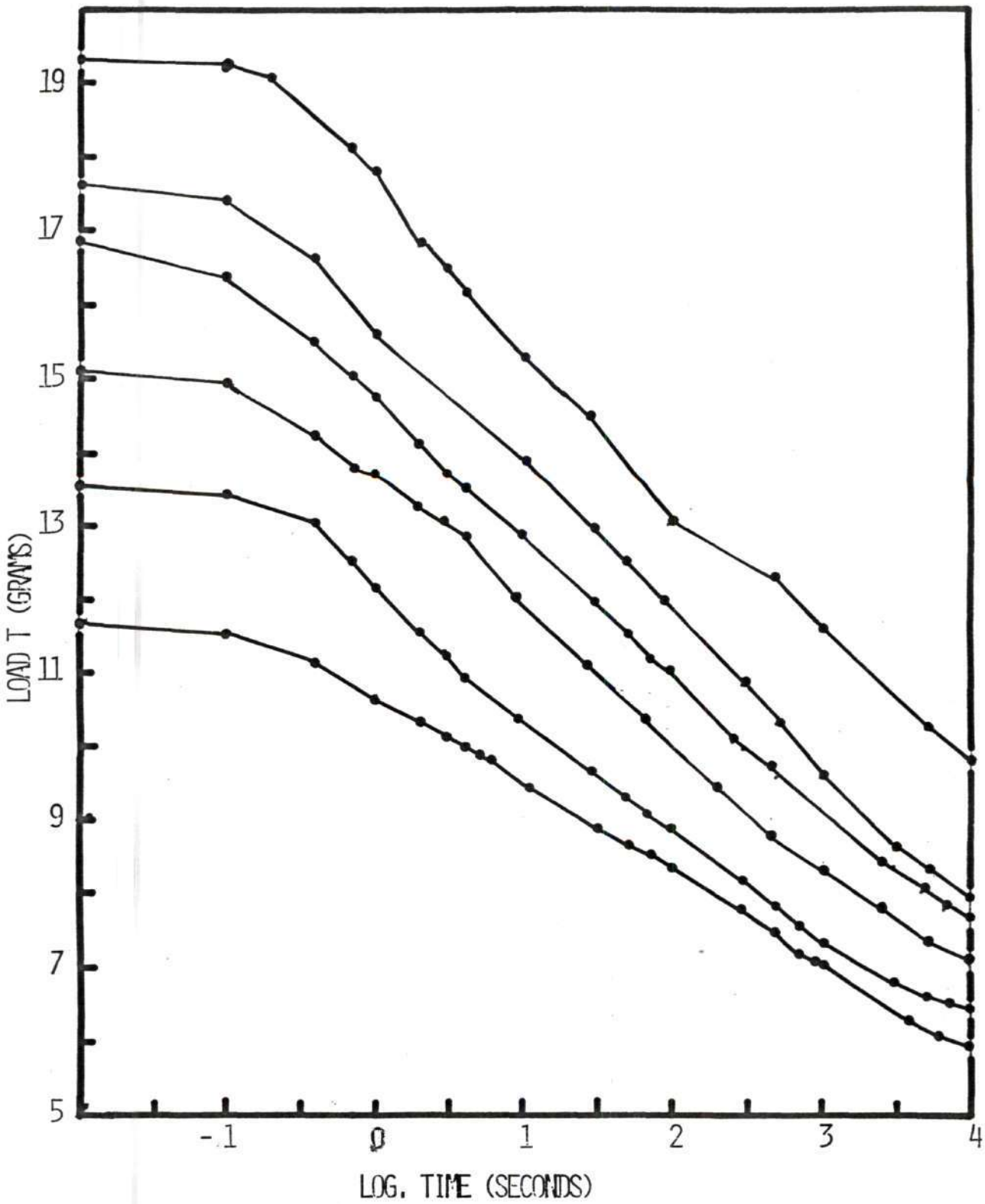

FIGURE 16. STRESS RELAXATION DATA OF UNDRAWN NYLON 6 FIBERS OBTAINED AT VARIOUS MAXIMUM LOADS

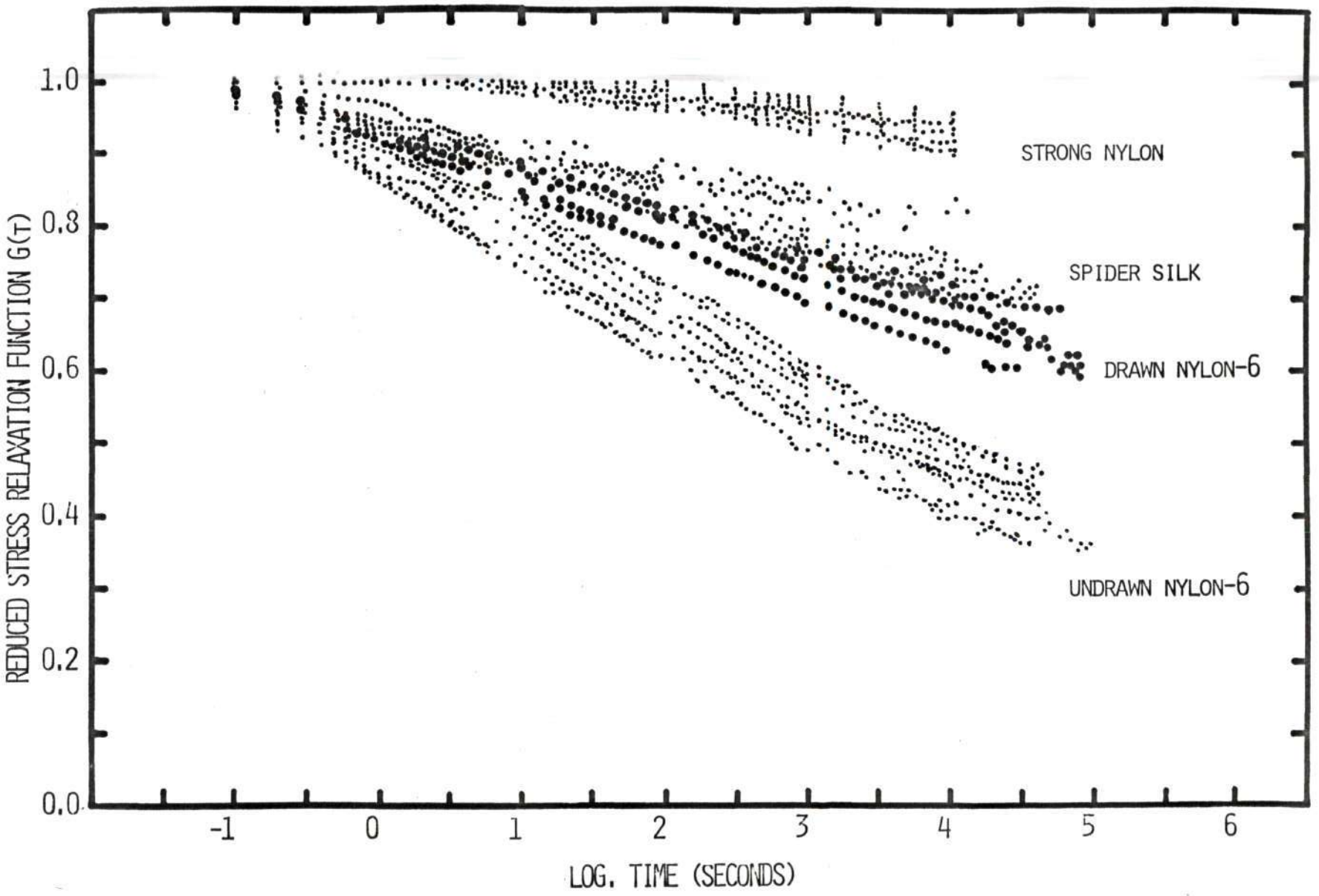

FIGURE 17. REDUCED STRESS RELAXATION FUNCTIONS OBTAINED BY NORMALIZATION OF DATA IN FIGURES 13, 14, 15 & 16.

(tension divided by the initial linear density, expressed as denier or tex).

The normalized experimental data fall into "narrow" bands which decrease monotonically with the logarithm of time. The ability to normalize experimental data into narrow bands indicates the relaxations of the polyamide fibers tend to be somewhat independent of stretch ratio, which is to say that time and strain effects can be separated, to a rough approximation.

Creep at Constant Loads

I. Experimental Details:

Apparatus: Simple creep tester (Figure 18.), microtensile tester (Figure 19 a & b)

Displacement sensor: Schaevitz 500 MHR LVDT, Schaevitz carrier amplifier (Model CAS - 025R)

Recorder: H-P system (Figure 2)

Testing condition: 21° C, 65% RH

Load levels: strong nylon--5 to 25 gm,
spider silk-- .1 to .5 gm,
drawn nylon-- 5 to 45 gm,
undrawn nylon-- 2.5 to 15 gm

Time range: 0 to 10^4 seconds or 10^5 seconds

Gage length: strong nylon - 12.5 cm; 2.54 cm for spider silk, drawn and undrawn nylon

Replication: 3 to 5

Figure 18 gives a schematic diagram of the simple creep tester. In a typical creep test, the fiber mounted on the two copper tabs as shown in Figure 1 was hung between hooks A and B. By adjusting the extension rod, the fiber was kept taut by the weight of the copper tab B. Each fiber was kept in this position for 600 seconds before applying the constant load. During this time, the length of the fiber and the clearance between hook B and the opening on copper tab B were measured. An "instantaneous" load was applied to the fiber when the trigger was released.

The displacement signals sensed by the LVDT were sampled at a programmed rate with the H-P system. The elongation as a function of time under constant load was thus recorded.

Measuring the creep of spider silk was impossible with the simple creep tester used for the other fibers. Spider silk is much too fine for the minimum constant load levels that could be applied. (The breaking load of the spider silk was less than 2 grams; the minimum core weight of the LVDT was more than 2 grams.) A microtensile tester built by Dr. B. R. Livesay of the micromechanics laboratory of the Engineering Experiment Station provided an excellent alternative. With the microtensile tester, the fiber can be tested in a horizontal position avoiding difficulty created by gravitation. Together with a bipolar operational amplifier control and H-P recording system, the microtensile tester proved to be versatile and easily manipulated. Figure 19a gives the schematic diagram of the tester and the control and recording system. A photograph of the same system is shown in Figure 19b.

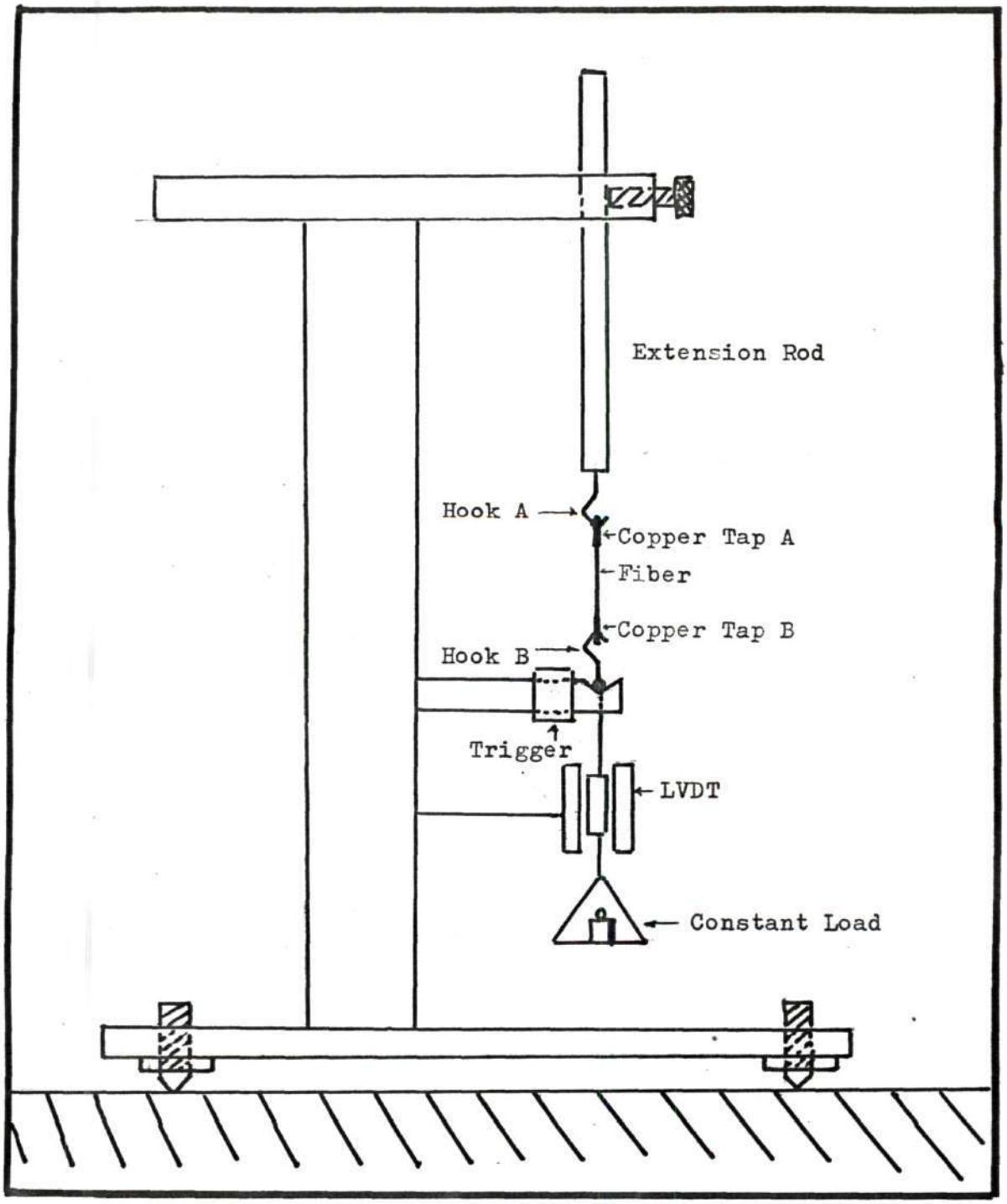

Figure 18. Schematic Drawing of the Simple Creep Tester

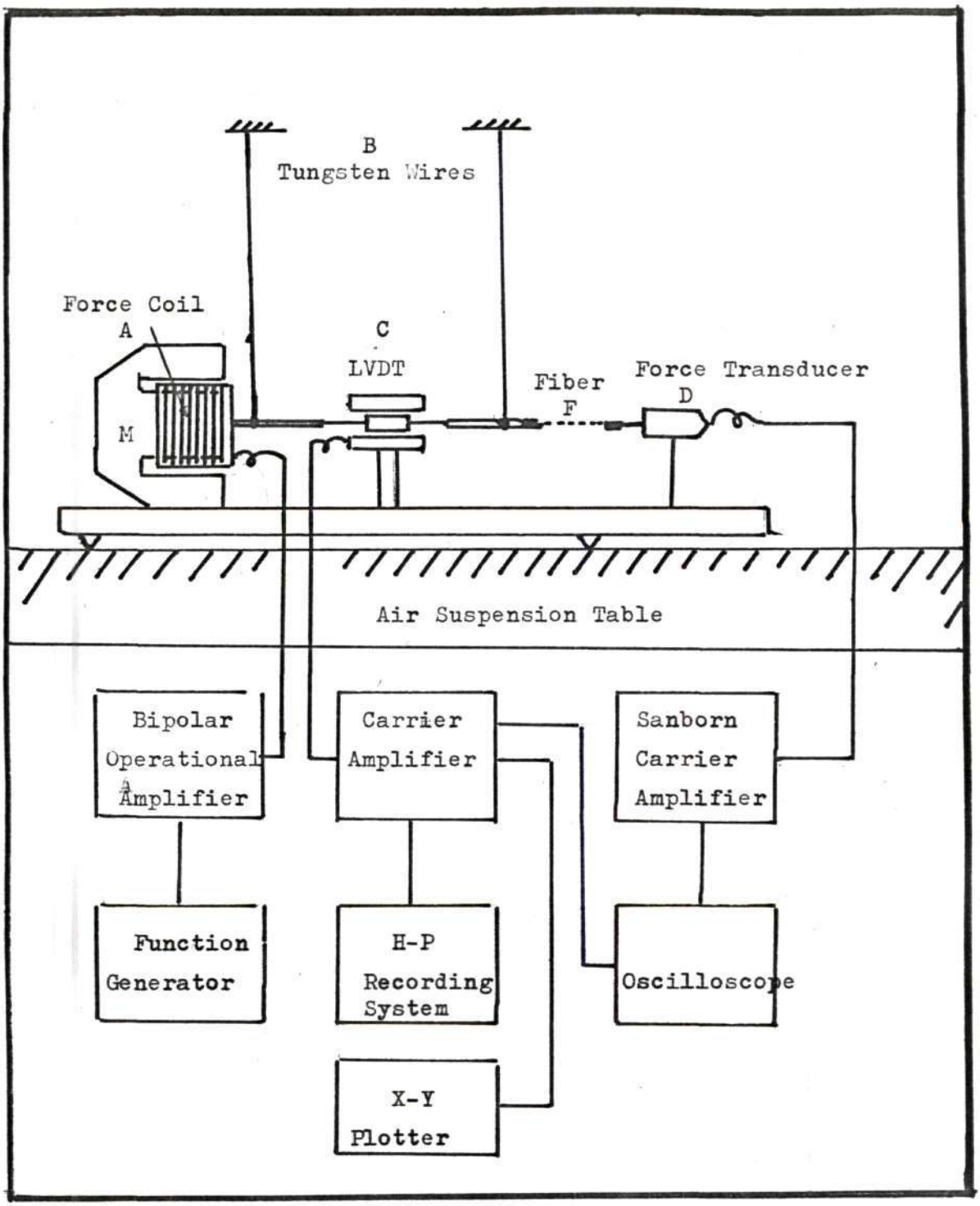

Figure 19a. Schematic Drawing of the Microtensile Tester and Data Logging System

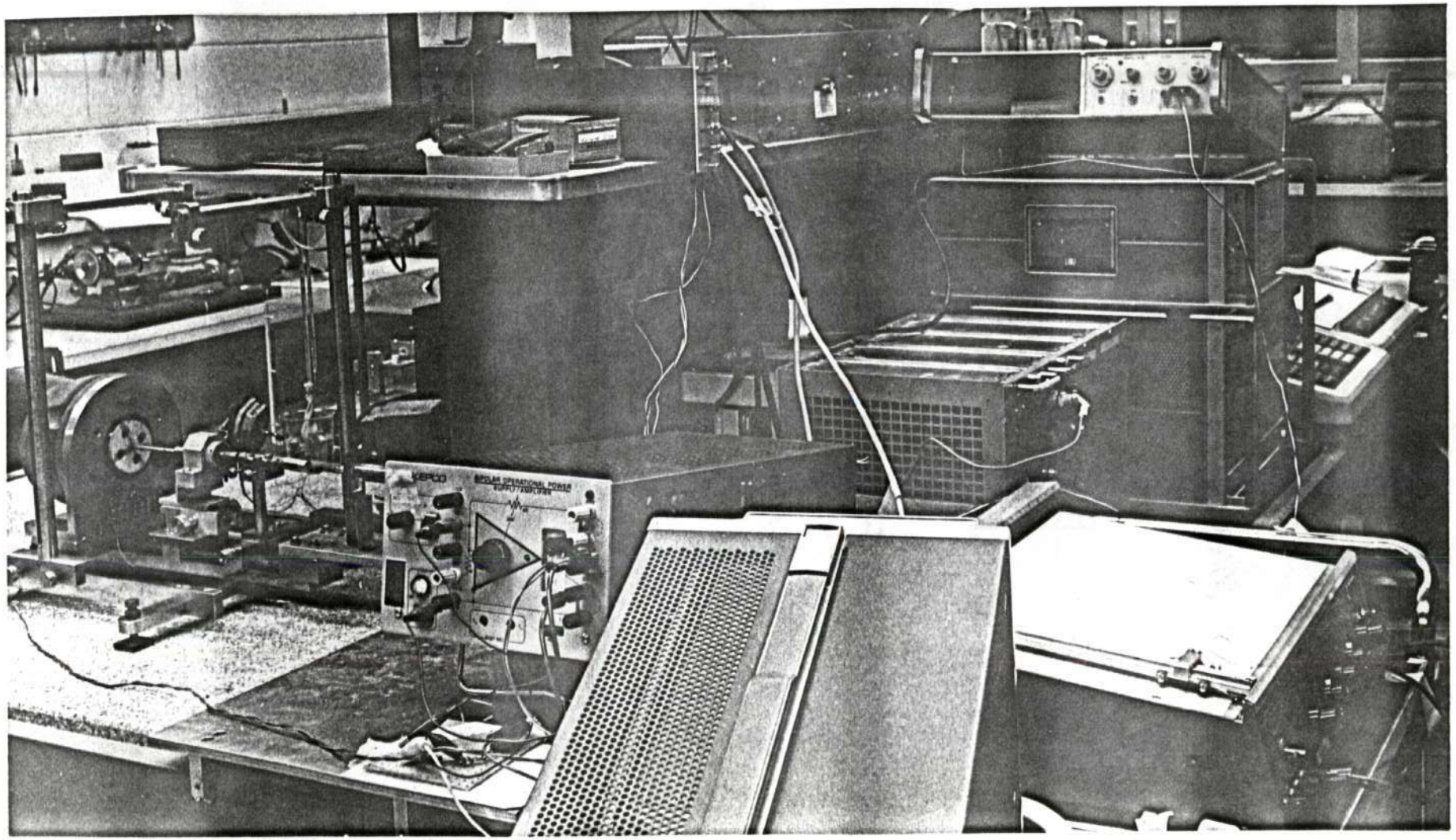

Figure 19b. Photograph of the Microtensile Tester and the Data Logging System

The force coil A and the LVDT core C together with the connecting rods are suspended by four 3.8 micron tungsten wires. By adjusting the lengths of these wires, the clearance between the suspended system and the loudspeaker magnet and the LVDT wall can be maintained.

The microtensile tester is a current driven system. When current is applied to the force coil A, a horizontal force is created in one direction or alternating directions depending upon the nature of current applied. The displacement of the fiber F was measured by the Statham force transducer (Model UC2) D. The microtensile tester was placed on an air suspension table to minimize background vibrations.

A Kepco bipolar operational power supply (model BOP 36-5M) was used as the control device. The bipolar power supply is capable of providing both alternating current (AC) and direct current (DC) outputs simultaneously. For creep tests, only DC output was necessary. By adjusting the DC output level, a constant load was maintained on the fiber. The displacement required for the fiber to maintain force balance was measured by the LVDT and recorded with the H-P system. The extension-time relationship was plotted directly on the Mosely 7000A x-y plotter.

II. Observations:

The creep data, plotting stretch ratio as a function of the logarithm of time, are shown in Figures 20 to 23. Strong nylon creeps slowly. The creep of the undrawn nylon is the greatest. In general, creep rate increases as the load level increases, and this is more

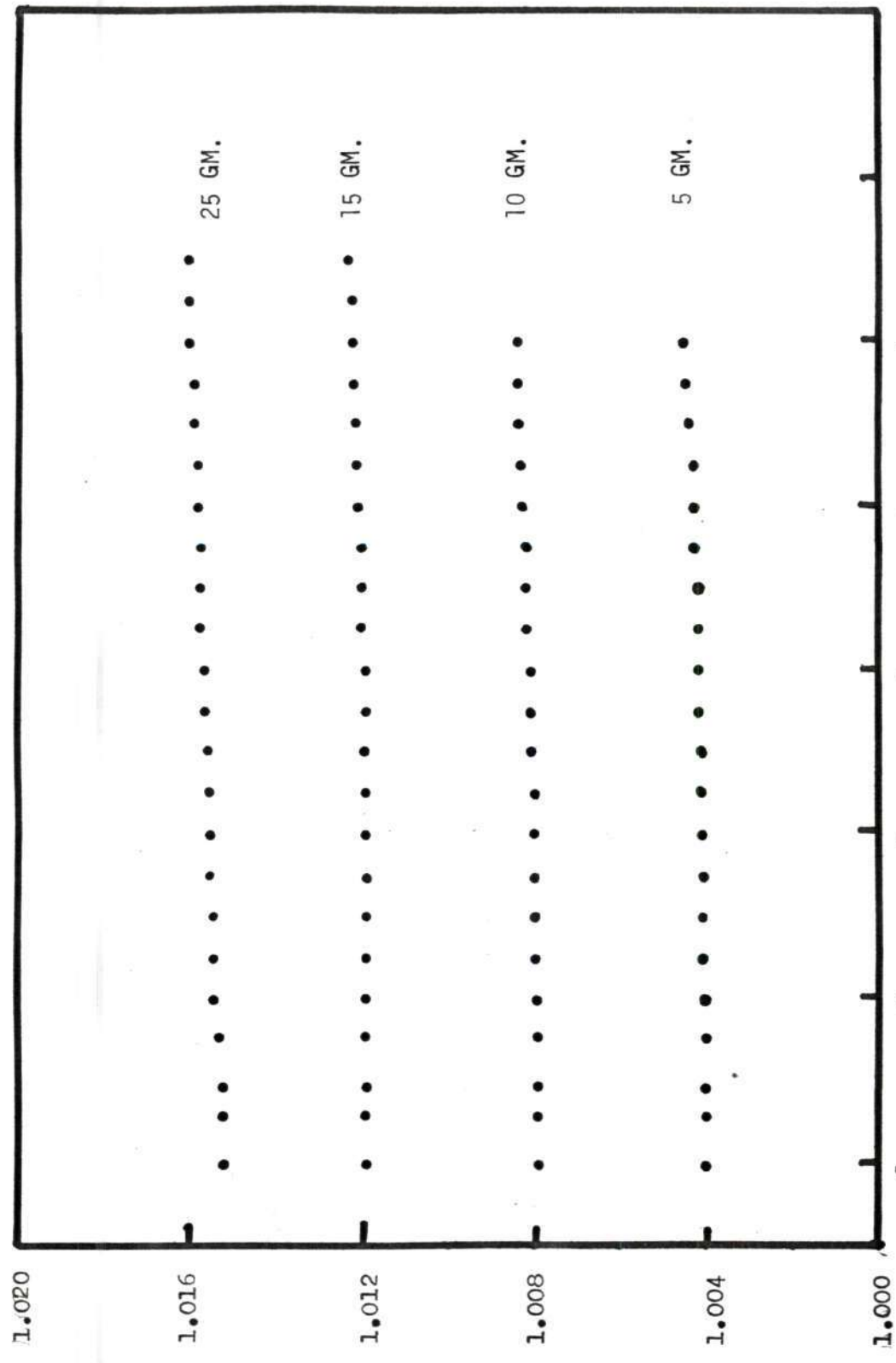

Figure 20. Creep Data of Strong Nylon Fibers Obtained at Various Constant Loads

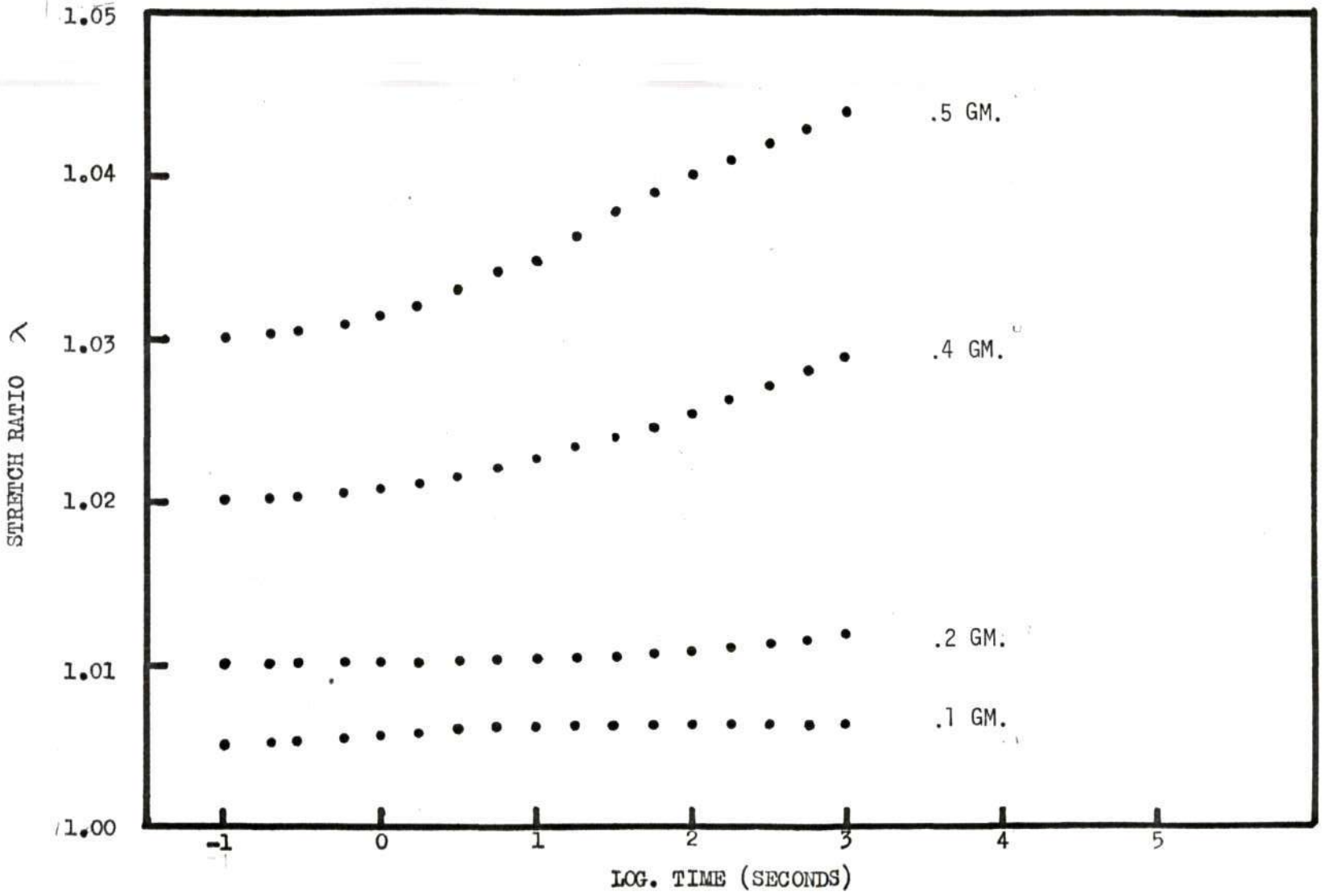

Figure 21. Creep Data of Spider Silk Obtained at **Various** Constant **Loads**

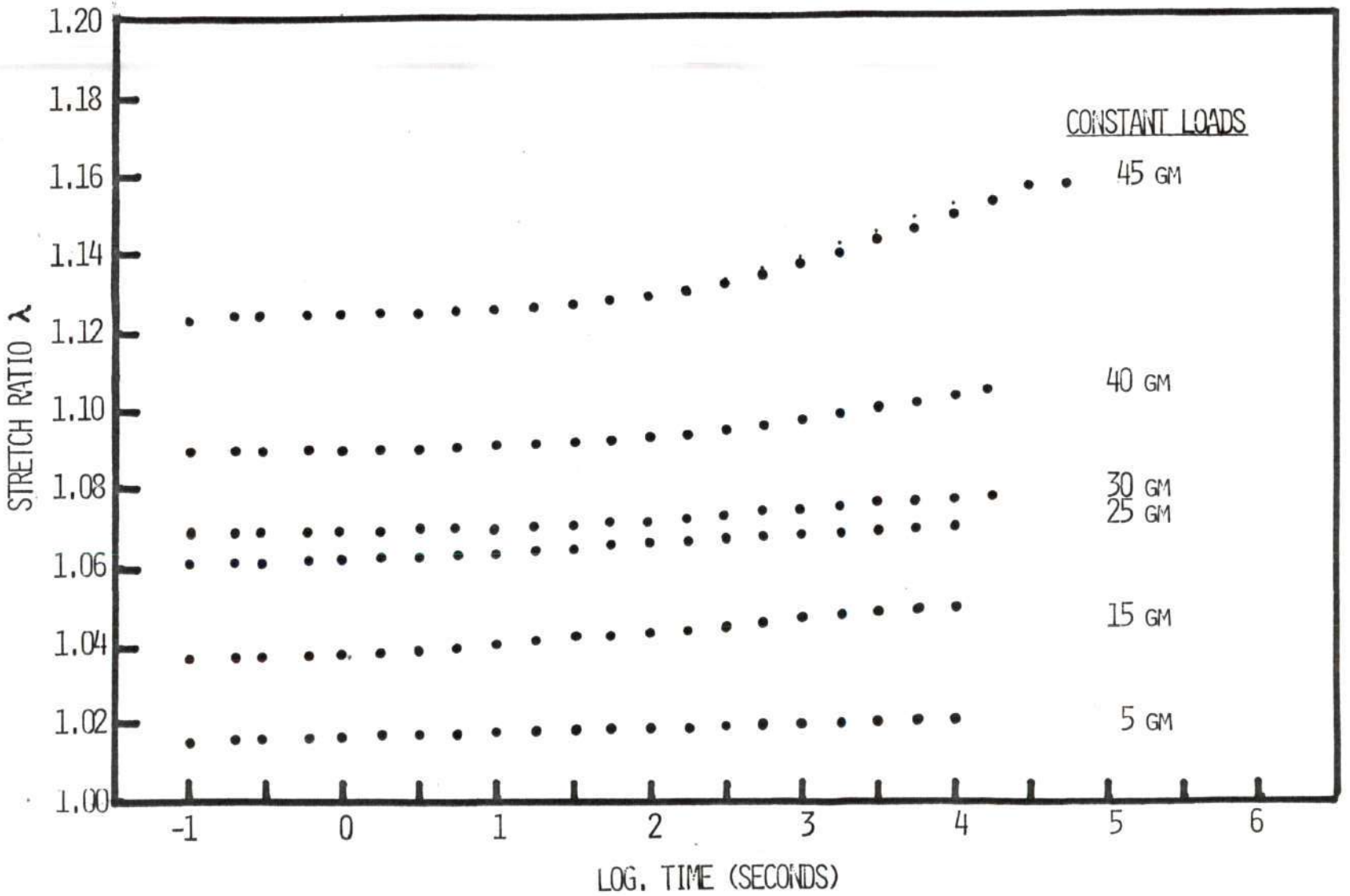

FIGURE 22. CREEP DATA OF DRAWN NYLON-6 FIBERS OBTAINED AT VARIOUS CONTANT LOADS

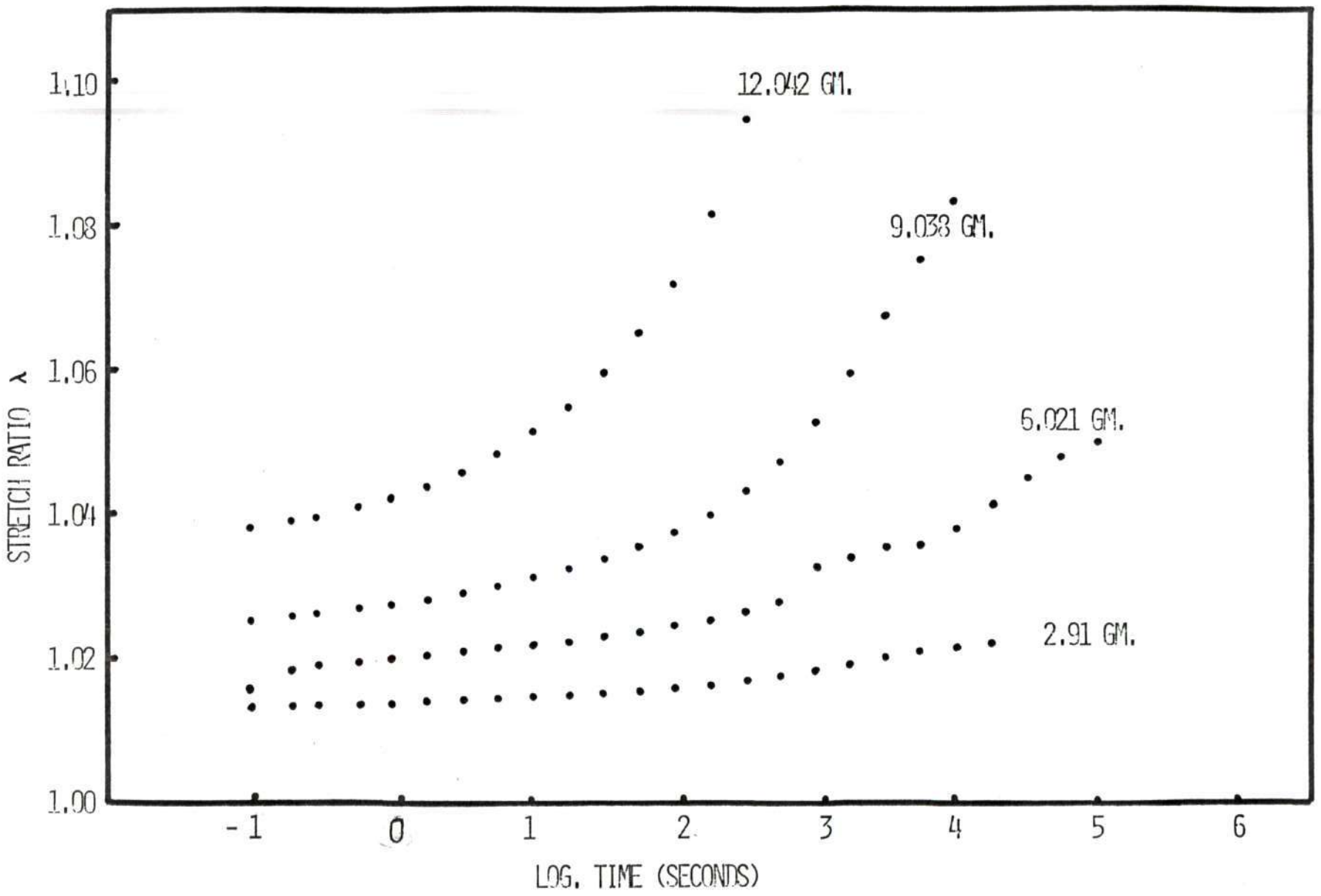

FIGURE 23. CREEP DATA OF UNDRAWN NYLON-6 FIBERS OBTAINED AT VARIOUS CONSTANT LOADS

pronounced for softer fibers. As the load increases the creep response becomes increasingly nonlinear.

Simple elongation experiments show that all the fibers have nonlinear stress-strain relationships (Figures 4 to 7). In order to use linear mathematics in data analyses, the elastic response(or elastic stress) $T^e(\lambda)$ was used instead of the conventionally used strain as a function of time to calculate the reduced creep function $J(t)$.

$J(t)$ is defined as the ratio of the elastic response at time t, $T^e[\lambda(t)]$, to the elastic response at the moment of loading, $T^e[\lambda(t_r)]$, i.e.

$$J(t) = T^e[\lambda(t)]/T^e[\lambda(t_r)] \qquad \text{(II-2)}$$
$$J(0) = 1$$

The data normalized according to this definition are plotted in Figure 31.

Low Frequency Sinusoidal Stretching

I. Experimental Details

Apparatus: Microtensile tester (Figure 19), Hewlett-Packard function generator (Model 202A), bipolar power supply (Model BOP 36-5M)

Force sensor: Statham UC2 green cell, Sanborn 350-1100AS carrier amplifier

Displacement sensor: Schaevitz LVDT (model 500 MHR); Schaevitz carrier amplifier (model CAS-025R)

Recorder: Mosely 7000A X-Y plotter, H-P system, Tektronix dual beam oscilloscope (model 5103N) with a C-5 oscilloscope camera

Testing condition: 21°C, 65% RH

Stretch levels and vibration amplitude:

strong nylon--1.005, 1.01, 1.02

spider silk--1.04, 1.06

drawn nylon--1.005, 1.02, 1.03

undrawn nylon--1.005, 1.01, 1.02

Gage length: 2.54 cm

Replication: 2

In a typical sinusoidal stretching experiment, the fiber is kept taut by stretching it to a predetermined strain. The fiber is vibrated siusoidally at predetermined amplitude. The stress response σ_o to the harmonic strain input ϵ_o can be either harmonic or anharmonic depending upon the material being tested. For viscoelastic materials, there is a phase lag ϕ between strain and stress response.

Symbolically, for an input strain

$$\epsilon = \epsilon_o e^{i\omega t} \qquad \text{(II-3)}$$

where ω = frequency, t = time, the stress response is

$$\sigma = \sigma_o e^{i(\omega t + \phi)} \qquad \text{(II-4)}$$

The resistance to dynamic deformation at steady state, called

dynamic modulus

$$M(\omega) = \frac{\sigma_o}{\epsilon_o} e^{i\phi} \qquad \text{(II-5)}$$

in terms of Euler's equation

$$M(\omega) = \frac{\sigma_o}{\epsilon_o} (\cos\phi + i \sin\phi) . \qquad \text{(II-6)}$$

For a dynamic experiment σ_o, ϵ_o, and ϕ are the measured quantities(Figure 24a).

In this study, the fiber was stretched to a predetermined strain on the microtensile tester using the bipolar power supply. In addition the bipolar power supply amplified a sinusoidal input signal from a function generator and superimposed it on the DC bias (Figure 24b). Thus, one end of the fiber was vibrated at a predetermined frequency and amplitude. The experimental set-up is shown in Figures 19a & b.

To avoid transients and to achieve approximately a steady state condition, each fiber was vibrated for 1000 seconds before recording.

The frequency response of the force transducer used was reported to be 50 Hz. Therefore, only the data obtained below this frequency were reliable even though some measurements were made at 60 and 90 Hz.

For slow response, 0.01 to 1 Hz, data were recorded with the X-Y plotter and the H-P system shown in Figure 2. For fast response, 1 to 90 Hz, data were recorded with the Tektronix C-5 oscilloscope camera by taking pictures of the traces of stress and strain response shown

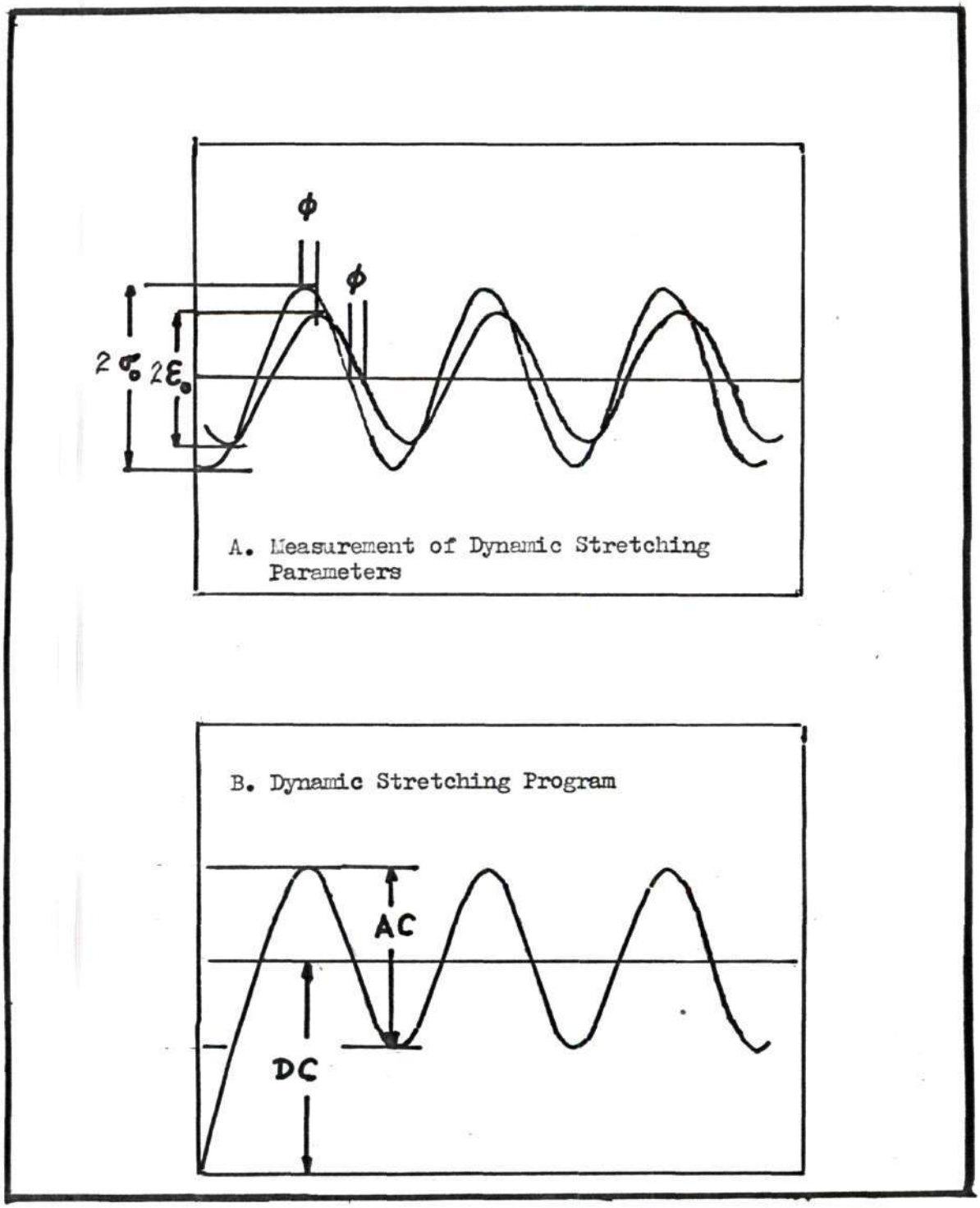

Figure 24. Dynamic Stretching Program and Measurement of Dynamic Stretching Parameters

on the screen of the oscilloscope.

II. Observations:

The frequency responses of polyamide fibers are shown in Figure 25 plotting dynamic modulus or storage modulus (the real part of the complex modulus) versus frequency in log-log scale. The storage moduli of the polyamide fibers are approximately independent of frequency. The dynamic strain amplitude does not affect the frequency response significantly. The dynamic modulus of strong nylon is about ten times greater than the static modulus while the dynamic moduli of drawn and undrawn nylon 6 are about three times greater than the static moduli. In spite of the fact that spider silk had a higher quasi-static initial modulus than nylon 6 in static tensile testing, the dynamic storage modulus of the spider silk was lower. This is reasonable since the static strain level is in the region where the slope of the stress-strain curve are approaching a minimum (Figure 5). When dealing with nonlinear mechanical properties such reversal is not unusual.

Strong nylon has the highest storage modulus among the polyamide fibers tested. No significant difference in the storage modulus between drawn and undrawn nylon was observed.

Figure 26 shows the typical traces of the sinusoidal stress and strain response of the polyamide fibers. Stresses lag strains at phase angles between 10 and 30 degrees. This is typical of viscoelastic materials.

Figure 27 shows the frequency dependence of damping or loss

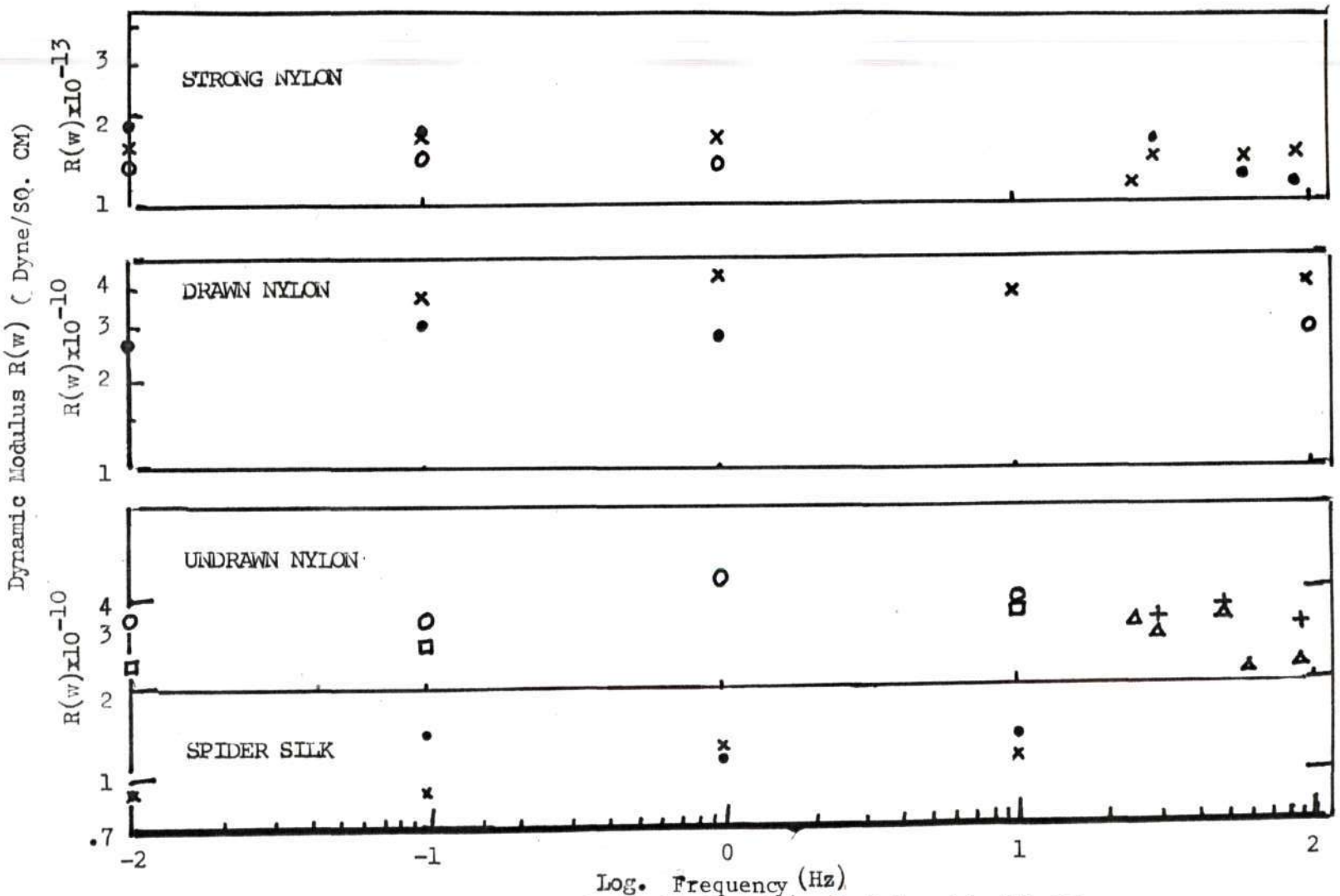

Figure 25. Frequency Dependence of Dynamic Modulus of Polyamide Fibers

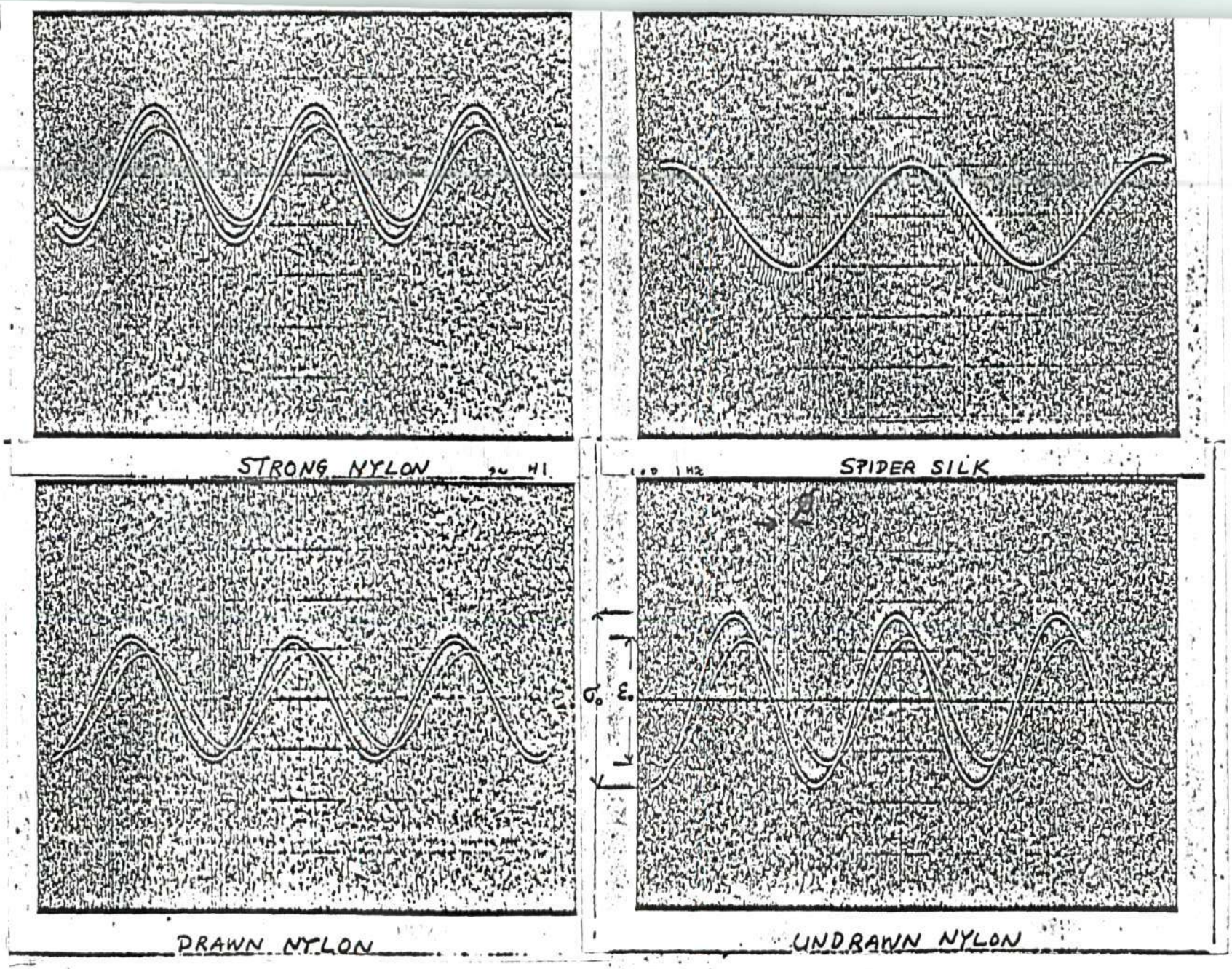

Figure 26. Typical Trace of Simuscidal Stress and Strain Response of Polyamide Fibers

modulus (imaginary part of the complex modulus)of the polyamide fibers. Undrawn nylon has the largest loss; the loss for strong nylon is the least. Dampings of these polyamide fibers are insensitive to frequency within the test range (0.01 to 100 Hz).

Environmental Effects on Stress Relaxation

I. Experimental Details:

Apparatus: Instron tensile tester (model TTB), Instron Environmental Chamber, control console (Figure 24)

Force sensor: Statham silver cell (Model UC 4), Sanborn 350-1100AS carrier amplifier

Recorder: H-P system (Figure 2)

Testing conditions: 1) 112.5° C, 65% RH

2) 112.5° C, 12% RH

Stretch ratios: strong nylon--1.005, 1.012, 1.02

spider silk--1.05, 1.1, 1.15

drawn nylon--1.02, 1.06, 1.10

undrawn nylon--1.04, 1.12, 1.20

Time range: 0 to 1000 seconds

Gage length: strong nylon--12.5 cm, 2.54 cm for spider silk and drawn and undrawn nylon

Replication: 2

The stress relaxation behavior of polyamide fibers under normal conditions(21°C, 65% RH) have been reported in pages 33 to 41. In order to investigate the effect of temperature and humidity on the stress

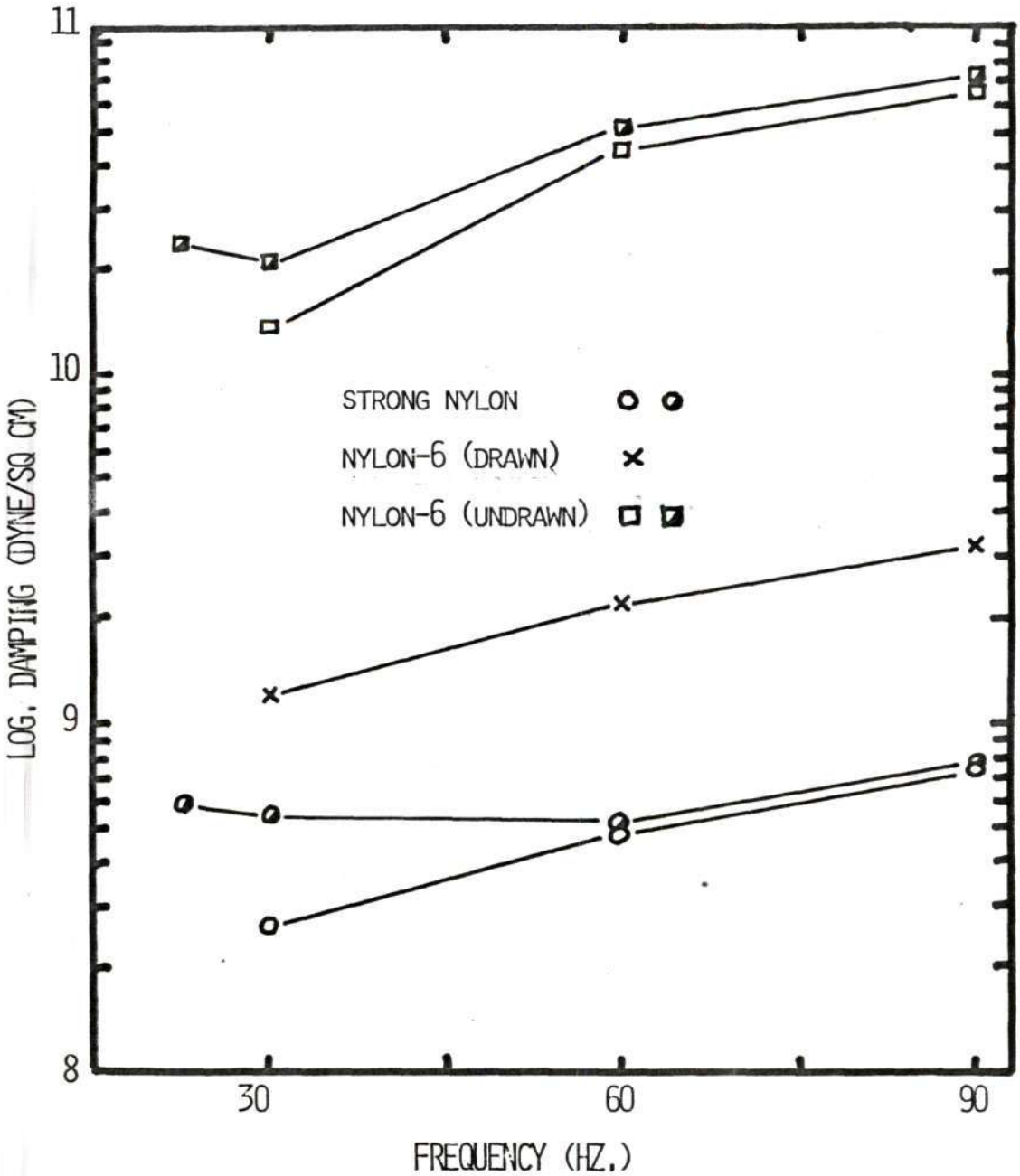

FIGURE 27 FREQUENCY DEPENDENCE OF DAMPING (IMAGINARY PART OF THE COMPLEX MODULUS) OF POLYAMIDE FIBERS

relaxation behavior of the polyamide fibers, two additional sets of experiments were carried out under different conditions.

The effect of temperature was studied by testing the fibers under the 65% RH ± 5% and 112.5° C ± .5° C condition in the Instron environmental chamber. According to the definition of relative humidity (the ratio of the vapor pressure of water vapor in the chamber to the saturated vapor pressure at the same temperature), the 65% RH - 112.5° C condition was achieved by boiling water inside the Instron environmental chamber at 112.5° C. (The vapor pressure of water vapor is 760 mm while the vapor pressure of water at 112.5° C is 1169.23 mm.

The effect of humidity was investigated by raising the environmental chamber temperature to 112.5° C from ambient condition. Wet bulb and dry bulb measurement indicated the relative humidity in the chamber was approximately 12%.

The time for the chamber to reach temperature equilibrium with air inside the chamber was found to be 13 minutes while the time for the fiber to reach temperature equilibrium with the environment was estimated to be less than 25 seconds.[1] A waiting time of 15 minutes was selected before starting an experiment. The relaxation under each set of conditions was carried out the same way as was described in pages 33 to 41. A photograph of the experimental set up is shown in Figure 28.

---

[1]Instron Manual No. 10-74-1 (c) Environmental Chamber System

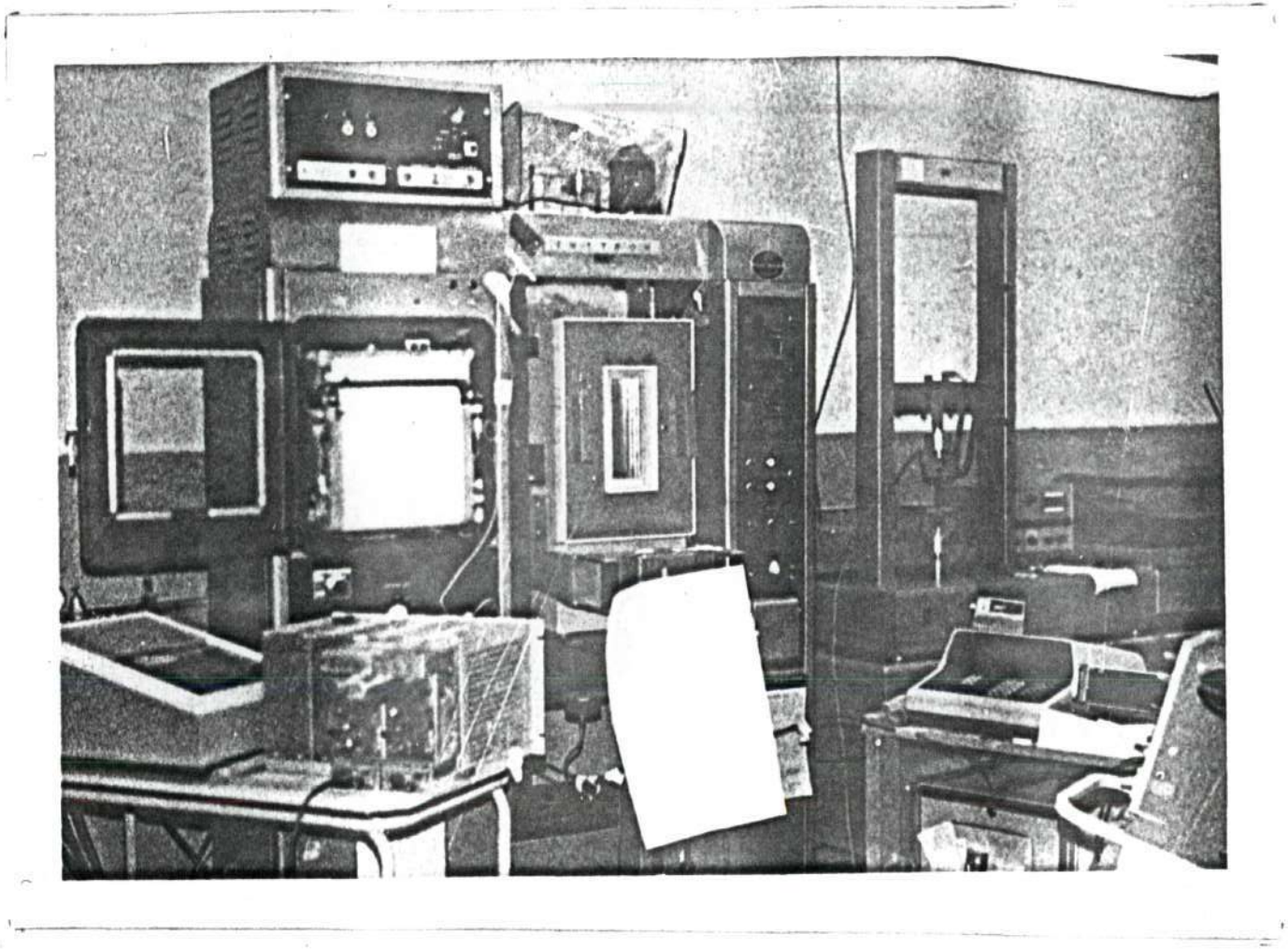

Figure 28. Photograph of Apparatus for Studies of Environmental Effect

In a separate study, the effect of temperature on the elastic properties of strong nylon were measured over a wide temperature range (-75° C to 325° C) and at various strain rates. Both the cooling and heating unit of the Instron environment chamber were used.

II. Observations:

Figures 34 to 37 show the normalized relaxation data of the polyamide fibers under different temperature and humidity conditions.

The effect of temperature on the tensile strength and the initial modulus of strong nylon at various strain rates are shown in Figures 28 a and b. Tensile strength of a fiber reflects the ability of the fiber to carry dead load while the initial modulus of a fiber indicate the ability of the fiber to resist deformation. As temperature increases the tensile strength and the initial modulus of strong nylon fiber decrease . The rate of decay of the initial modulus is about four times faster than the rate of strength decay. Depending upon the strain rate, the extrapolated zero strength temperatures range from 430° C to 650° C and the extrapolated zero resistance to deformation temperatures range from 540° C to 650° C. These extrapolated temperatures agree well with Zimmerman's data on Kevlar® 29 [128], With zero strength temperatures of 430° C to 650° C, according to Zimmerman [129], strong nylon fibers should support a large fraction of their nominal breaking load for more than 100 years.

Except for strong nylon, the increase of temperature and humidity caused an increase in the rate of stress relaxation within the experimental condition range. The spreads of the normalized data were

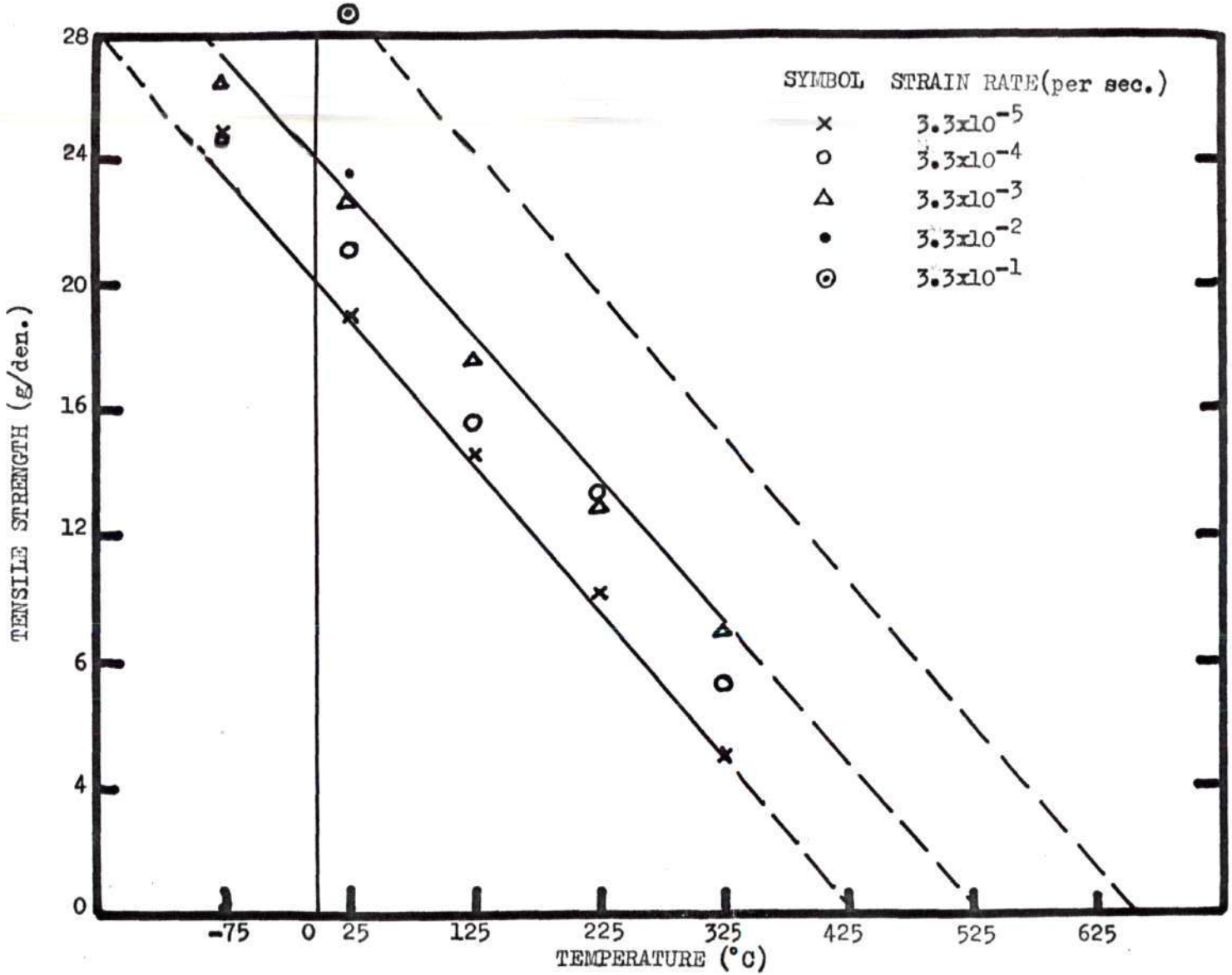

Figure 29a. **Effect of Temperature on the Tensile Strength of Strong Nylon Fibers at Various Strain Rates**

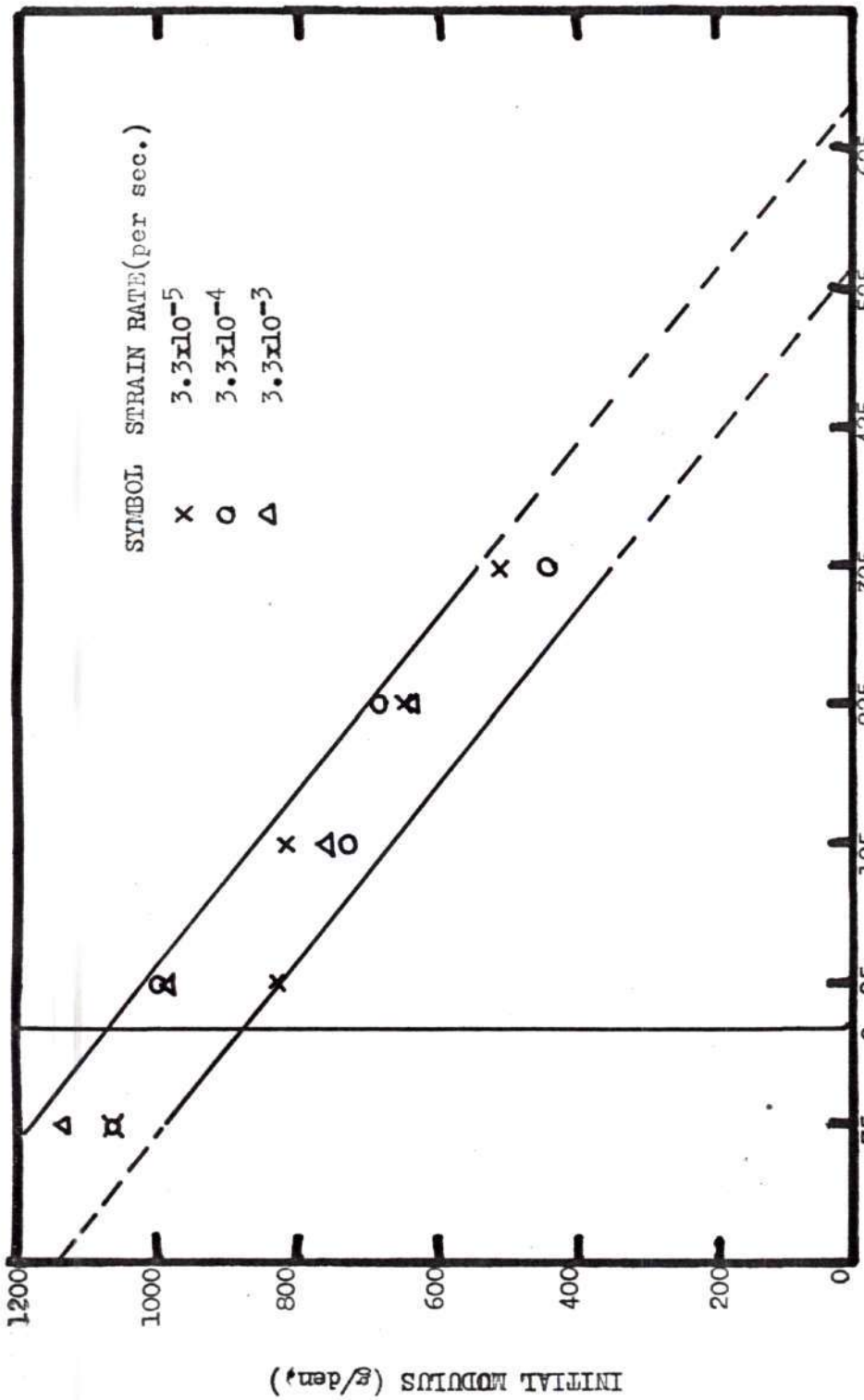

Figure 29b. Effect of Temperature on the Initial Modulus of Strong Nylon Fibers at Various Strain Rates

greater at higher temperatures and humidities.

In spider silk, stress relaxed faster at lower humidity than at high humidity.

CHAPTER III

ANALYSIS

Introduction

Simple elongation experiments show that the stress on the strong nylon, spider drag line and drawn and undrawn nylon 6 fibers vary non-linearly with the strain history and environmental conditions at all strain levels. Hysteresis losses are not proportional to strain rates. In sinusoidal stretching experiments, dynamic stiffness and damping are rather insensitive to frequency within the experimental range.

To account for this complex nonlinear mechanical behavior, we need a finite nonlinear viscoelastic model. Textile fibers are oriented, anisotropic, composite structures; they do not conform to the usual requirements of homogeneity and isotropy of continuum mechanics. This causes mathematical difficulty and experimental complications. For the simplest case of finite linear viscoelasticity, fifteen independent scalar material functions are needed to describe the behavior of an isotropic material [15].

Because of the lack of sufficient knowledge of the morphological structure of polymers, formal step by step development of a constitutive equation is impractical.

As a first approximation, I consider the fibers as one-dimensional continua, and use a quasilinear viscoelastic model proposed by Fung [28] to represent my experimental observations. Like many

models such as those of Leaderman [50], Volterra [110], and those reviewed by Ward [113], the quasilinear viscoelastic model is based on an extension of the Boltzmann superposition principle [8]. In view of the lack of precision of our experimental apparatus, such as the problem of backlash and overshoot of the tensile tester and the slow sampling rate (less than ten readings per second) of the data acquisition system, and our demand for practicality in data reduction, the quasilinear viscoelastic model probably is a fair compromise between the experimentally more involved multiple integral representation, which requires information from multiple-step loading or stretching programs, and the inadequate Boltzmann superposition principle, which assumes linearity in both elastic and history dependent response. The quasilinear viscoelastic model has been used to represent the viscoelastic behavior of biopolymeric materials such as the rabbit mesentery [13] [27] and to represent the relaxation behavior of hard elastic polypropylene fibers [14].

The Quasilinear Viscoelastic Model

The history of stress response, $K(t)$, for a suddenly applied strain history, $\lambda(t)$, in real materials, is a nonlinear function of the stretch magnitude, λ, temperature θ, humidity, h, and the time, t:

$$K = K(\lambda, \theta, h, \ldots, t) \qquad \text{(III-1)}$$

For constant temperature and humidity, the stress relaxation results

shown in Figure 30 suggests that K can be written approximately as

$$K(\lambda, t)_{\theta,h} = T^e(\lambda)G(t) \qquad \text{(III-2)}$$

where G(t) is a normalized function of time and is defined such as G(0) = 1. $T^e(\lambda)$ is the elastic response or the stress as a function of the stretch.

Assume the stress T(t) at any time is linearly related to the elastic response $T^e(\lambda)$ for an arbitrary stretch. The one dimensional constitutive equation can be expressed by the convolution integral[28]

$$T(t) = T^e[\lambda(t)] + \int_0^t T^e[\lambda(t - \tau)]\,\dot{G}(\tau)\,d\tau \qquad \text{(III-3)}$$

the first term on the right hand side of equation (III-3) accounts for the elastic response which is reflected in the stress-strain curve while the second term accounts for the history dependent response which is reflected in hysteresis, stress relaxation, creep and sinusoidal stretching response.

Since $T^e(\lambda)$ is a nonlinear function of λ as indicated in the experimental results (Figures 3 to 7), this model is called quasilinear despite the fact that equation (III-3) is a linear integral equation.

The Elastic Response in Simple Elongation

$T^e(\lambda)$ is defined as the tensile stress generated instantly in the fiber when a step stretch $1 + (\lambda - 1)H(t)$ is imposed on the specimen. Measurements of $T^e(\lambda)$ according to this definition are

impossible to obtain. However, by making use of the fact that the stress response observed is relatively insensitive to strain rates, we may approximate $T^e(\lambda)$ by the tensile stress response in a rapid loading experiment.

Experiment shows that the elastic responses of polyamide fibers in this study are strongly nonlinear (Figures 3 to 7). Quantitative representation of these stress-strain curves with a single function is not possible. One way to obtain an approximate function and to smooth data is to fit the stress strain curve piece by piece. This can be done with a cubic spline interpolation technique (Appendix B). The generalized form of the stress-strain relationships is shown as follows:

$$T_i^e(\lambda) = \sum_{j=0}^{3} C_{ij} \lambda^j \qquad \text{(III-4)}$$

$$C_{oo} = 0$$

$$i = 1, 2, 3, \ldots, n-1$$

where C_{ij} are the interpolation coefficients.

As shown in Figures 3 to 7, equation (III-4) does represent the stress-strain curves well. With these functions, the slopes of the stress-strain curves can be calculated conveniently.

The History Dependent Response

In equation (III-3) the history dependent responses are summarized by the reduced relaxation function G(t). G(t) should be evaluated in such a way that it is consistent with hysteresis, creep,

and sinusoidal stretching experiments.

Cyclic loading experiments showed that the hysteresis loss of the polyamide fibers were somewhat insensitive to strain rates. In sinusoidal stretching experiments, the dynamic modulus and loss modulus were quite insensitive to frequency. Such frequency insensitivity has been found in a wide variety of textile fibers [19, 21, 26], as well as in biopolymeric materials [27, 28].

Energy dissipations characteristic of ordered polymeric materials appear quite insensitive to frequency.

The Continuous Relaxation Spectrum

To account for the frequency insensitive characteristics of the fibers, we need a continuous distribution of relaxation times or a continuous relaxation spectrum $S(\tau)$.

For a system that has a continuous relaxation spectrum $S(\tau)$, we can obtain the generalized reduced relaxation function, $G(t)$, reduced creep function, $J(t)$, and complex modulus as follows: (Appendix C)

$$G(t) = [1 + \int_0^\infty S(\tau)\, \exp(-t/\tau)\, d\tau]/[1 + \int_0^\infty S(\tau) d\tau] \qquad (III\text{-}5)$$

$$J(t) = [1 - \int_0^\infty (S(\tau)/(1 + S(\tau)))\exp\left\{-1/(1 + S(\tau))\right\} d\tau]/$$

$$[1 + \int_0^\infty (S(\tau)/(1 + S(\tau)))\, d\tau] \qquad (III\text{-}6)$$

$$M(\omega) = \left[1 + \int_0^\infty S(\tau)\,(\omega\tau/(\omega\tau + (1/\omega\tau)))\,d\tau + i\int_0^\infty (S(\tau)d\tau/(\omega\tau + (1/\omega\tau)))\right] / \left[1 + \int_0^\infty S(\tau)d\tau\right] \qquad \text{(III-7)}$$

Our task now is to select a spectrum that represents the experimental observations for different loading regimens.

The use of spectra to link various viscoelastic and dielectric phenomena has been reviewed by Gross [29], Ferry [22], and Fung [28]. Techniques for the computation of the relaxation spectra from experimental data were suggested by Hopkins [35, 36, 37] and recently by Meluch [64]. Tobolsky et al. [104] applied relaxation spectra to relate relaxation and dynamic response of textile fibers.

The criteria used in this study for selection of a spectrum is that it will make G(t) and J(t) compatible with experimental observations. In particular, the spectrum of relaxation times should reflect the frequency insensitivity in the dynamic response, that is to say, $S(\tau)$ should be nearly constant over a wide range of frequency.

For this study, a spectrum first introduced by Becker [6] is used

$$S(\tau) = \frac{C}{\tau} \quad \text{for } \tau_1 < \tau < \tau_2 \qquad \text{(III-8)}$$

$$= 0 \quad \text{elsewhere}$$

where C is a constant and (τ) is the relaxation time in the interval $[\tau_1, \tau_2]$.

Computation Methods

By substitution of equation (III-8), equations (III-5), (III-6), and (III-7) can be reduced to the following computational forms:

$$G(t) = [1 + \left\{E_1(t/\tau_2) - E_1(t/\tau_1)\right\}]/[1 + C\left\{\ell n(\tau_2/\tau_1)\right\}] \quad \text{(III-9)}$$

$$J(t) = \frac{[1 - C\left\{E_1(t/(C + \tau_2)) - E_1(t/(C + \tau_1))\right\}]}{1 - C\ell n[(C + \tau_2)/(C + \tau_1)]} \quad \text{(III-10)}$$

$$M(\omega) = [1 + .5C\left\{(1 + \omega^2 \tau_2^2) - \ell n(1 + \omega^2 \tau_1^2)\right\} + i\left\{\tan^{-1}(\omega\tau_2) - \tan^{-1}(\omega\tau_1)\right\}]/[1 + \ell n(\tau_2/\tau_1)] \quad \text{(III-11)}$$

where $E_1(z)$ is the exponential integral

$$E_1(Z) \equiv \int_Z^{\infty} \frac{e^{-t}}{t}\, dt.$$

By an approximation method, [3], equations III-9, III-10, and III-11 can be reduced to forms suitable for evaluation of the relaxation spectrum $S(\tau)$ from stress relaxation and creep data, (Appendix C), for the time interval $[\tau_1, \tau_2]$

$$G(t) = \frac{1 - C\gamma - C\ln(t/\tau_2)}{1 + C\ln(\tau_2/\tau_1)} + o(C) \qquad \text{(III-12)}$$

$$J(t) = \frac{1 + C\gamma + C\ln[t/(C + \tau_2)]}{1 - C\ln[(C + \tau_2)/(C + \tau_1)]} + o(C) \qquad \text{(III-13)}$$

where γ is Euler's constant ($\gamma = 0.5772$) and $o(C)$ is a small residue much smaller than C. The residue varies slowly with time. Neglecting the residue $o(C)$ we have the following relationships:

$$G(t) = \frac{1 - C\gamma - C\ln(t/\tau_2)}{1 + C\ln(\tau_2/\tau_1)} \qquad \text{(III-14)}$$

$$J(t) = \frac{1 + C\gamma + C\ln[t/(C + \tau_2)]}{1 - C\ln[(C + \tau_2)/(C + \tau_1)]} \qquad \text{(III-15)}$$

$$\frac{dG(t)}{d\ln(t)} = -C/[1 + C\ln(\tau_2/\tau_1)] \qquad \text{(III-16)}$$

$$\frac{dJ(t)}{d\ln(t)} = C/[1 - C\ln(\frac{C + \tau_2}{C + \tau_1})] \qquad \text{(III-17)}$$

With stress relaxation and/or creep data, we can calculate C, τ_1, and τ_2 in different ways. Consider these cases separately:

Case 1. Calculation of $S(\tau)$ from relaxation data:

From experimental data expressed in the form of a reduced relaxation function defined by equation (II-1), we obtain the slope

S_R of the middle portion of the relaxation function plotted against the logarithm of time, a typical point $[G(t_o), t_o]$ in the middle portion of the reduced relaxation function, and the value $G(\infty)$, when relaxation approaches a steady state. We can deduce the following equations from equations (III-14), (III-16), and (III-9):

$$G(t_o) = [1 - C\gamma - C\ln(t_o) + C\ln(\tau_2)]/[1 + C\ln(\tau_2) - C\ln(\tau_1)] \qquad \text{(III-18)}$$

$$S_R = -C/[1 + C\ln(\tau_2) - C\ln(\tau_1)] \qquad \text{(III-19)}$$

$$G(\infty) = 1/[1 + C\ln(\tau_2) - C\ln(\tau_1)] \qquad \text{(III-20)}$$

Note that obtaining $G(\infty)$ in the true sense is almost impossible. For a rough approximation, we may use an arbitrary value of G(t) beyond the termination time of an experiment. As in most situations, extrapolations outside the experimental range are hazardous.

With the experimental results, we can solve equations (III-18), (III-19) and (III-20) for the parameters C, τ_1, and τ_2 as shown in Table 3.

Case 2. Calculation of $S(\tau)$ from creep data:

From experimental data expressed in the form of a reduced creep function defined by equation (II-2), we can obtain the slope of S_C of the straight portion of the reduced creep function plotted against the logarithm of time, a typical point $[J(t_o), t_o]$ and an arbitrary value

TABLE 3. PARAMETERS CALCULATED FROM STRESS RELAXATION DATA

Fiber	t_o (sec)	$G(t_o)$	S_r	$G(\infty)$	C	τ_1	τ_2
Strong Nylon	320	.973	-.00903	.935	.0097	28.6907	38262.51
Spider Silk	32	.870	-.0192	.750	.0255	.0643	29988.04
Drawn Nylon-6	56	.810	-.0274	.635	.0431	.0962	59796.54
Undrawn Nylon-6	56	.685	-.0474	.395	.1200	.1293	45395.09
Hard Elastic	10	.887	-.0524	.320	.1638	2.0609	886700.

$J(\infty)$ beyond the termination time of an experiment. Substituting this information into equation (II-15), (III-17), and (III-10), we can solve the following equations for the parameters C, τ_1 and τ_2.

$$J(t_o) = [1 + C\gamma + C\ln(\frac{t}{c+\tau_2})]/[1 - C\ln(\frac{c+\tau_2}{c+\tau_1})] \qquad \text{(III-21)}$$

$$S_C = C/[1 - C\ln(\frac{c+\tau_2}{c+\tau_1})] \qquad \text{(III-22)}$$

$$J(\infty) = 1/[1 - C\ln(\frac{c+\tau_2}{c+\tau_1})] \qquad \text{(III-23)}$$

The experimental values and the calculated parameters are summarized in Table 4.

Case 3. Calculation of $S(\tau)$ with combined creep and relaxation data:

With G(t), the slopes of G(t) and the slope of J(t) obtained as described in Case 1 and Case 2, we can evaluate the parameters C, τ_1, and τ_2 by solving equations (III-18), (III-19), and (III-22).

The experimental values and the calculated parameters are summarized in Table 5.

A fourth case, by taking the dynamic stretching data into consideration, may be examined if we have sinusoidal stretching data over the time range that coincides with the time range of creep and stress relaxation experiments. Limited data were available; therefore, no attempt was made to incorporate dynamic data into the computation of

TABLE 4.PARAMETERS CALCULATED FROM CREEP DATA

Fiber	t_o (sec)	$J(t_o)$	S_c	$J(\infty)$	C	τ_1	τ_2
Strong Nylon	1000	1.0409	.0111	1.0595	.01048	44.703	9515.048
Spider Silk	1000	1.1649	.0265	1.3484	.01965	.334	181116.98
Drawn Nylon-6	1000	1.2206	.0360	1.3021	.02765	3.858	17134.39
Undrawn Nylon-6 (3.2 to 55.4 sec)	1000	1.6668	.1400	2.1733	.06442	15.148	66357.459
Undrawn Nylon-6 (180 to 10^4 sec)	10	1.2270	.0507	1.7250	.02939	.173	328492.804

TABLE 5. PARAMETERS CALCULATED FROM COMBINATION OF CREEP AND RELAXATION DATA

Fiber	t_o (sec)	$G(t_o)$	S_r	S_c	C	τ_1	τ_2
Strong Nylon	320	.973	-.009033	.0111	.009965	28.6886	896721.68
Spider Silk	32	.877	-.019200	.0265	.022680	.09411	29988
Drawn Nylon-6	56	.810	-.027360	.0360	.040230	.09610	11515
Undrawn Nylon-6	56	.685	-.047380	.1400	.071940	.12930	45395

the spectrum. However, the frequency insensitive characteristic of the polyamide fibers was the major consideration in the selection of the relaxation spectrum. Therefore, the quasilinear viscoelastic model should reflect at least qualitatively the frequency insensitivity characteristic of polyamide fibers.

Interpretation of Experimental Observation with S (τ)

With the relaxation spectra computed using the different methods, we can ask some questions about the quasilinear viscoelastic model, namely:

1) Can this model summarize experimental data?

2) Can this model unify creep and relaxation data?

3) What is the relationship between creep and relaxation data?

4) Are the predictions of dynamic response reasonable?

By substitution of the parameters C, τ_1 and τ_2 into equations (III-9), (III-10), and (III-11), we can calculate the generalized relaxation function G(t), creep function J(t), and complex modulus. Computation and curve plotting can be done conveniently with a digital computer.

Consider Case 1,i.e. using the relaxation data to calculate the relaxation spectrum. Figure 30 shows the calculated and the experimental relaxation function plotted as functions of the logarithm of time for different fibers. The calculated results, represented by the solid curves fit closely to the average values of the experimental data. The upper and lower symbols that outline the band of the experimental data show the average deviation of the experimental data from the mean. The quasilinear viscoelastic model fits the average

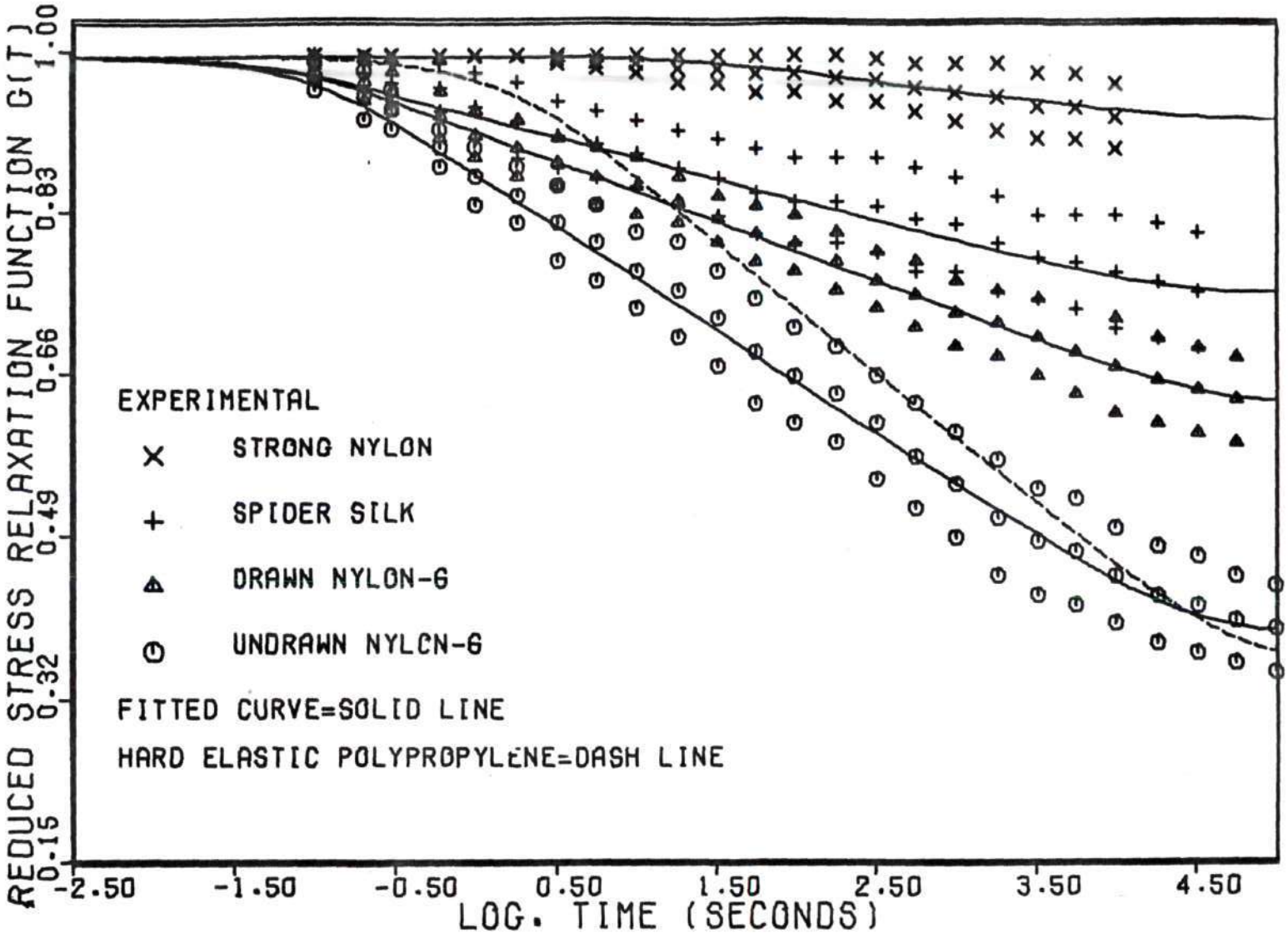

FIGURE 30. COMPARISON OF EXPERIMENTAL AND THEORETICAL REDUCED STRESS RELAXATION FUNCTION G(T)

relaxation data quite well. Table 6 shows the numerical values of the calculated and experimental stress relaxation functions for various polyamide fibers.

For Case 2, i.e. using creep data to calculate the relaxation spectrum. Figure 31 shows the calculated and experimental reduced creep functions of the logarithm of time for the polyamide fibers. This model represents the creep data of strong nylon, spider silk and drawn nylon 6 fairly well. For the undrawn nylon, we need two sets of parameters to fit the creep curve. In Table 7, the numerical values of the calculated and experimental creep functions for various polyamide fibers are given.

Consider Case 3, i.e. using both creep and relaxation data to calculate the relaxation spectrum. The quasilinear viscoelastic model represents the relaxation data fairly well (Table 8a). But for creep response, this model can give only a fair representation for strong nylon. This model tends to overestimate the creep response. The magnitude of overestimate increases rapidly for softer fibers. The calculated results show that this model can unify only approximately the creep and relaxation behavior of the strong nylon fibers (Tables 8a, 8b, and 8c).

Even though the quasilinear viscoelastic model fails to unify the creep and relaxation data for all the fibers, we can make use of the fact that this model fits relaxation and creep data reasonably well with the spectra calculated from creep and relaxation data separately. We can express the relationship between creep and relaxation in terms

TABLE 6. COMPARISON OF THEORETICAL AND EXPERIMENTAL REDUCED STRESS RELAXATION FUNCTION G(t) FOR VARIOUS POLYAMIDE FIBERS

LOG. TIME (SECONDS)	STRONG NYLON		SPIDER SILK		DRAWN NYLON-6		UNDRAWN NYLON-6	
	THEORY	EXPERIMENT	THEORY	EXPERIMENT	THEORY	EXPERIMENT	THEORY	EXPERIMENT
-1.000	1.000	1.000	.979	.985	.978	.980	.969	.975
-.699	1.000	1.000	.967	.980	.963	.970	.948	.955
-.523	1.000	1.000	.959	.970	.953	.960	.931	.940
-.222	1.000	1.000	.946	.965	.934	.935	.900	.900
0.000	1.000	1.000	.936	.945	.920	.915	.876	.870
.255	.999	1.000	.925	.930	.904	.900	.848	.850
.505	.999	.995	.914	.915	.888	.885	.821	.820
.748	.998	.993	.904	.905	.873	.870	.794	.800
1.000	.997	.990	.892	.895	.857	.860	.767	.770
1.255	.995	.985	.881	.880	.841	.845	.739	.750
1.505	.992	.985	.870	.870	.825	.825	.712	.720
1.748	.988	.980	.859	.855	.810	.810	.685	.685
2.000	.983	.980	.848	.845	.794	.800	.658	.660
2.255	.978	.975	.837	.845	.778	.780	.630	.640
2.505	.973	.973	.826	.840	.762	.760	.603	.610
2.748	.968	.965	.816	.825	.747	.745	.576	.575
3.000	.963	.960	.805	.820	.732	.725	.549	.545
3.255	.958	.955	.794	.800	.716	.715	.522	.510
3.505	.953	.945	.784	.785	.701	.700	.497	.485
3.748	.948	.945	.775	.780	.686	.685	.472	.475
4.000	.944	.935	.766	.770	.672	.670	.449	.450

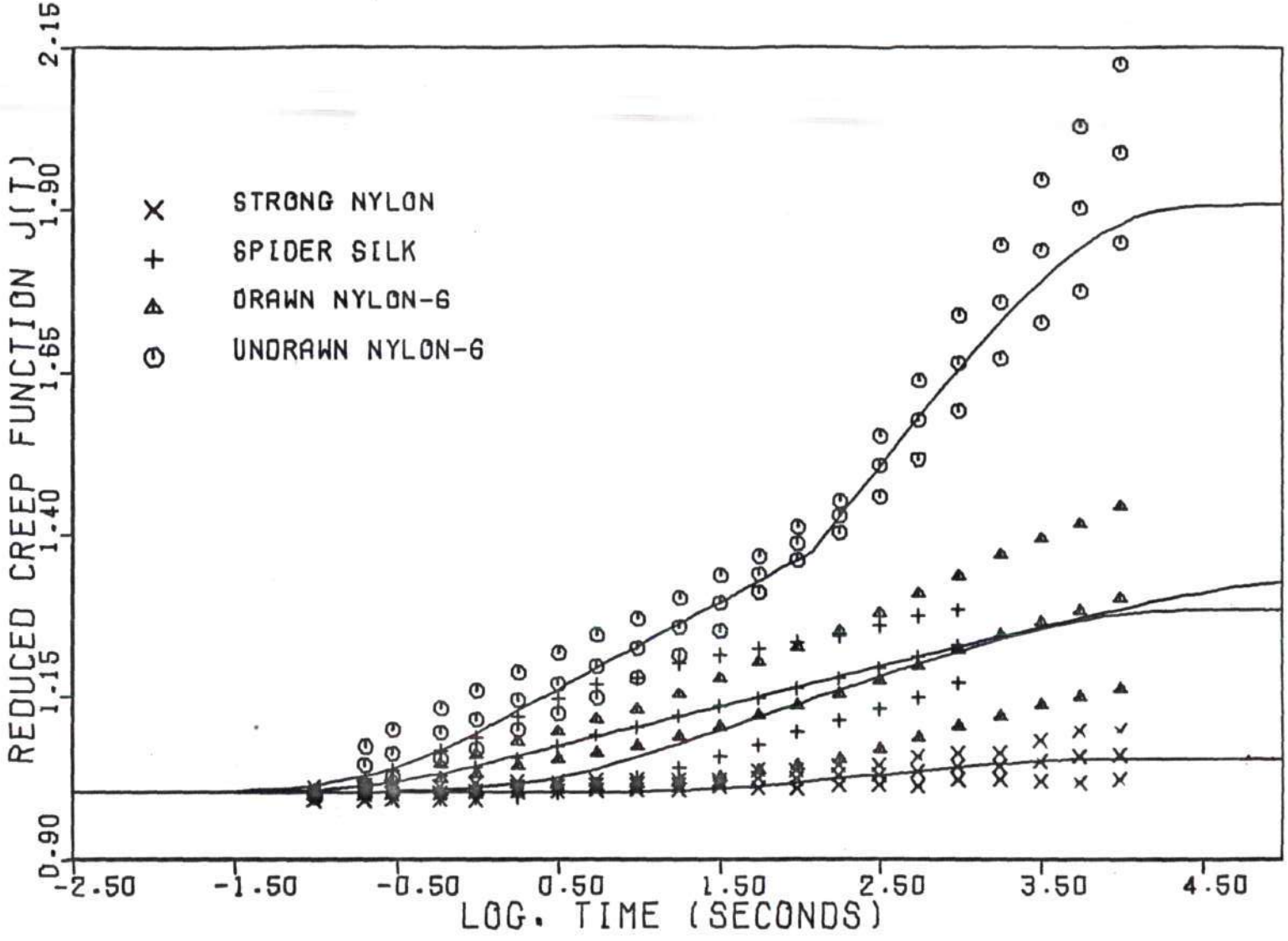

FIGURE 31.COMPARISON OF EXPERIMENTAL AND THEORETICAL REDUCED CREEP FUNCTION J(T)

TABLE 7. COMPARISON OF THEORETICAL AND EXPERIMENTAL REDUCED CREEP FUNCTION J(T) FOR VARIOUS POLYAMIDE FIBERS

LOG. TIME (SECONDS)	STRONG NYLON		SPIDER SILK		DRAWN NYLON-6		UNDRAWN NYLON-6	
	THEORY	EXPERIMENT	THEORY	EXPERIMENT	THEORY	EXPERIMENT	THEORY	EXPERIMENT
-1.000	1.000	1.001	1.007	1.004	1.001	1.002	1.001	1.001
-.699	1.000	1.001	1.013	1.011	1.002	1.009	1.002	1.045
-.523	1.000	1.001	1.018	1.016	1.003	1.014	1.003	1.064
-.222	1.000	1.001	1.031	1.030	1.005	1.025	1.005	1.096
0.000	1.000	1.004	1.043	1.041	1.009	1.032	1.009	1.117
.255	1.000	1.011	1.058	1.057	1.015	1.043	1.016	1.146
.505	1.001	1.011	1.074	1.075	1.024	1.053	1.028	1.173
.748	1.001	1.014	1.088	1.092	1.038	1.065	1.047	1.199
1.000	1.002	1.014	1.104	1.103	1.056	1.074	1.079	1.227
1.255	1.004	1.014	1.119	1.122	1.076	1.088	1.127	1.260
1.505	1.007	1.017	1.135	1.136	1.097	1.103	1.190	1.297
1.748	1.010	1.023	1.149	1.149	1.117	1.120	1.263	1.342
2.000	1.016	1.023	1.165	1.165	1.137	1.136	1.343	1.390
2.255	1.022	1.029	1.180	1.179	1.158	1.153	1.424	1.430
2.505	1.028	1.029	1.196	1.194	1.178	1.174	1.503	1.508
2.748	1.033	1.034	1.210	1.210	1.198	1.197	1.578	1.579
3.000	1.039	1.041	1.226	1.228	1.217	1.221	1.653	1.667
3.255	1.044	1.041	1.241	—	1.235	1.243	1.725	1.760
3.505	1.048	1.050	1.256	—	1.251	1.265	1.788	1.838
3.748	1.051	1.057	1.270	—	1.264	1.282	1.839	1.903
4.000	1.052	1.060	1.284	—	1.274	1.302	1.877	1.988

TABLE 8A. COMPARISON OF THEORETICAL AND EXPERIMENTAL REDUCED STRESS RELAXATION FUNCTION G(T) FOR VARIOUS POLYAMIDE FIBERS

LOG. TIME (SECONDS)	STRONG NYLON		SPIDER SILK		DRAWN NYLON-6		UNDRAWN NYLON-6	
	THEORY	EXPERIMENT	THEORY	EXPERIMENT	THEORY	EXPERIMENT	THEORY	EXPERIMENT
-1.000	1.000	1.000	.979	.985	.978	.980	.976	.975
-.699	1.000	1.000	.967	.980	.963	.970	.959	.955
-.523	1.000	1.000	.959	.970	.953	.960	.946	.940
-.222	1.000	1.000	.946	.965	.934	.935	.921	.900
0.000	1.000	1.000	.936	.945	.920	.915	.902	.870
.255	.999	1.000	.925	.930	.904	.900	.880	.850
.505	.999	.995	.914	.915	.888	.885	.858	.820
.748	.998	.993	.904	.905	.873	.870	.837	.800
1.000	.997	.990	.892	.895	.857	.860	.815	.770
1.255	.995	.985	.881	.880	.841	.845	.793	.750
1.505	.992	.985	.870	.870	.825	.825	.772	.720
1.748	.988	.980	.859	.855	.810	.810	.751	.685
2.000	.983	.980	.848	.845	.794	.800	.729	.660
2.255	.978	.975	.837	.845	.778	.780	.707	.640
2.505	.973	.973	.826	.840	.763	.760	.686	.610
2.748	.968	.965	.816	.825	.748	.745	.665	.575
3.000	.963	.960	.805	.820	.733	.725	.643	.545
3.255	.957	.955	.794	.800	.719	.715	.622	.510
3.505	.952	.945	.784	.785	.706	.700	.602	.485
3.748	.947	.945	.775	.780	.696	.685	.583	.475
4.000	.942	.935	.766	.770	.688	.670	.564	.450

TABLE 88. COMPARISON OF THEORETICAL AND EXPERIMENTAL REDUCED CREEP FUNCTION J(T) FOR VARIOUS POLYAMIDE FIBERS

LOG. TIME (SECONDS)	STRONG NYLON		SPIDER SILK		DRAWN NYLON-6		UNDRAWN NYLON-6	
	THEORY	EXPERIMENT	THEORY	EXPERIMENT	THEORY	EXPERIMENT	THEORY	EXPERIMENT
-1.000	1.000	1.001	1.033	1.004	1.046	1.002	1.280	1.001
-.699	1.000	1.001	1.053	1.011	1.079	1.009	1.504	1.045
-.523	1.000	1.001	1.068	1.016	1.104	1.014	1.685	1.064
-.222	1.000	1.001	1.093	1.030	1.153	1.025	2.069	1.096
0.000	1.000	1.004	1.113	1.041	1.190	1.032	2.386	1.117
.255	1.001	1.011	1.135	1.057	1.234	1.043	2.758	1.146
.505	1.001	1.011	1.157	1.075	1.276	1.053	3.124	1.173
.748	1.002	1.014	1.178	1.092	1.318	1.065	3.479	1.199
1.000	1.004	1.014	1.200	1.103	1.361	1.074	3.848	1.227
1.255	1.006	1.014	1.222	1.122	1.404	1.088	4.221	1.260
1.505	1.010	1.017	1.243	1.136	1.446	1.103	4.586	1.297
1.748	1.014	1.023	1.265	1.149	1.488	1.120	4.941	1.342
2.000	1.020	1.023	1.286	1.165	1.530	1.136	5.309	1.390
2.255	1.027	1.029	1.308	1.179	1.573	1.153	5.681	1.430
2.505	1.033	1.029	1.330	1.194	1.615	1.174	6.045	1.508
2.748	1.039	1.034	1.351	1.210	1.655	1.197	6.397	1.579
3.000	1.046	1.041	1.372	1.228	1.695	1.221	6.760	1.667
3.255	1.052	1.041	1.393	—	1.734	1.243	7.122	1.760
3.505	1.059	1.050	1.413	—	1.768	1.265	7.468	1.838
3.748	1.065	1.057	1.432	—	1.797	1.282	7.792	1.903
4.000	1.071	1.060	1.449	—	1.819	1.302	8.104	1.988

TABLE 8C. COMPARISON OF THEORETICAL AND EXPERIMENTAL RELATIONSHIP BETWEEN REDUCED CREEP AND STRESS RELAXATION FUNCTION G(T)*J(T) FOR VARIOUS POLYAMIDE FIBERS

LOG. TIME (SECONDS)	STRONG NYLON		SPIDER SILK		DRAWN NYLON-6		UNDRAWN NYLON-6	
	THEORY	EXPERIMENT	THEORY	EXPERIMENT	THEORY	EXPERIMENT	THEORY	EXPERIMENT
-1.000	1.000	1.001	1.011	.989	1.022	.982	1.249	.976
-.699	1.000	1.001	1.019	.991	1.039	.979	1.441	.998
-.523	1.000	1.001	1.024	.985	1.052	.974	1.593	1.001
-.222	1.000	1.001	1.035	.994	1.077	.958	1.905	.986
0.000	1.000	1.004	1.042	.984	1.095	.944	2.151	.971
.255	1.000	1.011	1.050	.983	1.115	.939	2.426	.974
.505	1.000	1.006	1.057	.984	1.134	.932	2.680	.961
.748	1.000	1.007	1.064	.988	1.150	.926	2.912	.959
1.000	1.001	1.004	1.071	.987	1.166	.924	3.137	.945
1.255	1.001	.999	1.077	.988	1.181	.919	3.348	.945
1.505	1.002	1.001	1.082	.988	1.194	.910	3.539	.934
1.748	1.003	1.002	1.087	.983	1.205	.907	3.710	.919
2.000	1.003	1.002	1.091	.984	1.216	.908	3.871	.917
2.255	1.004	1.003	1.095	.996	1.225	.900	4.017	.915
2.505	1.005	1.001	1.099	1.003	1.232	.892	4.145	.920
2.748	1.006	.998	1.102	.999	1.238	.892	4.253	.908
3.000	1.007	.999	1.105	1.007	1.243	.885	4.350	.908
3.255	1.008	.994	1.107	—	1.247	.889	4.430	.898
3.505	1.008	.992	1.108	—	1.249	.885	4.493	.891
3.748	1.009	.999	1.109	—	1.250	.878	4.539	.904
4.000	1.009	.991	1.110	—	1.251	.872	4.572	.895

of a product of the creep and relaxation functions. The calculated and experimental relationships between creep and relaxation of the polyamide fibers are shown in Table 9. Value of unity implies exact inversion is possible.

Using the spectra calculated from relaxation data we can make predictions of the response of the fibers to sinusoidal stretching. The predictions of the normalized frequency response of the polyamide fibers are shown in Figures 32 to 33.

Figure 32 shows the prediction of the dynamic moduli. The relative orders of magnitude of the stiffness of the fibers are reasonable. The prediction shows that the resistance to deformation of the fibers increases with frequency at very low frequencies. Strain rate dependence is more significant for softer fibers. This agrees with our experience in "static" tensile testing. At higher frequencies, above 1 Hz, the stiffness of fibers tends to be independent of frequency.

Figure 33 shows the prediction of the normalized damping behavior of the polyamide fibers. The flatness of the curves over a broad range of frequency reflects the frequency insensitivity of the energy dissipative characteristic of the polyamide fibers. The predictions show that damping is higher for less ordered fibers.

In general, the quasilinear viscoelastic model reflects the dynamic mechanical behavior of the polyamide fibers qualitatively.

The foregoing analysis shows that the quasilinear viscoelastic model summarizes the viscoelastic behavior of the polyamide fibers fairly well with one or two sets of parameters.

TABLE 9. COMPARISON OF THEORETICAL AND EXPERIMENTAL RELATIONSHIP BETWEEN REDUCED CREEP AND STRESS RELAXATION FUNCTION G(T)*J(T) FOR VARIOUS POLYAMIDE FIBERS

LOG. TIME (SECONDS)	STRONG NYLON		SPIDER SILK		DRAWN NYLON-6		UNDRAWN NYLON-6	
	THEORY	EXPERIMENT	THEORY	EXPERIMENT	THEORY	EXPERIMENT	THEORY	EXPERIMENT
-1.000	1.000	1.001	.986	.989	.978	.982	.970	.976
-.699	1.000	1.001	.980	.991	.965	.979	.949	.998
-.523	1.000	1.001	.977	.985	.955	.974	.934	1.001
-.222	1.000	1.001	.976	.994	.939	.958	.905	.986
0.000	1.000	1.004	.977	.984	.928	.944	.884	.971
.255	1.000	1.011	.979	.983	.918	.939	.861	.974
.505	1.000	1.006	.982	.984	.910	.932	.844	.961
.748	1.000	1.007	.983	.988	.906	.926	.831	.959
1.000	.999	1.004	.985	.987	.905	.924	.827	.945
1.255	.999	.999	.986	.988	.905	.919	.832	.945
1.505	.999	1.001	.987	.988	.905	.910	.847	.934
1.748	.999	1.002	.988	.983	.904	.907	.865	.919
2.000	.999	1.002	.988	.984	.903	.908	.883	.917
2.255	.999	1.003	.988	.996	.901	.900	.897	.915
2.505	1.000	1.001	.988	1.003	.898	.892	.906	.920
2.748	1.000	.998	.987	.999	.895	.892	.909	.908
3.000	1.000	.999	.987	1.007	.890	.885	.908	.908
3.255	1.000	.994	.986	—	.884	.889	.901	.898
3.505	.999	.992	.985	—	.877	.885	.888	.891
3.748	.996	.999	.984	—	.868	.878	.869	.904
4.000	.993	.991	.984	—	.857	.872	.843	.895

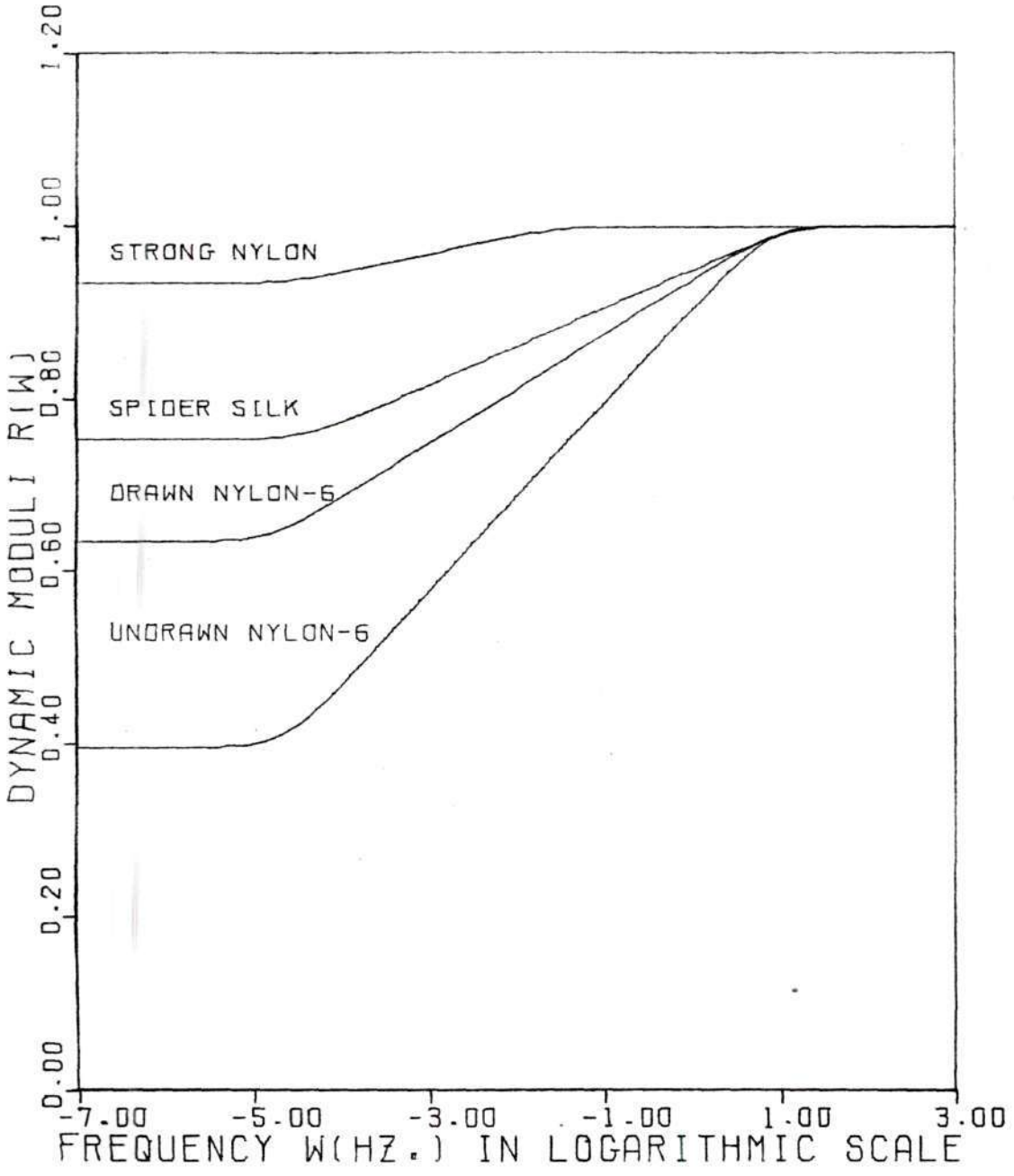

Figure 32. Prediction of Dynamic Stiffness with Parameters Obtained from Stress Relaxation Experiments

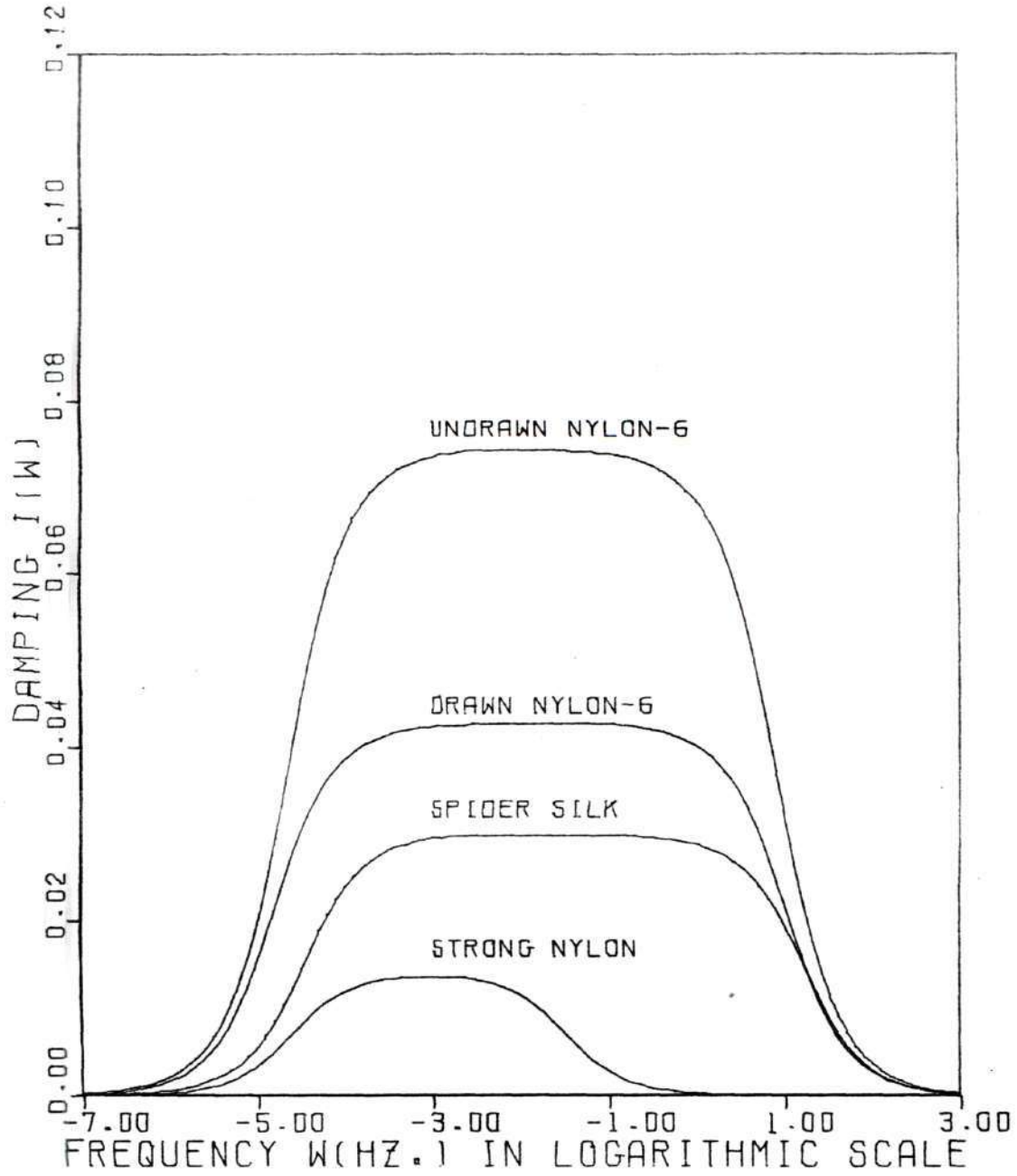

Figure 33. Prediction of Damping with Parameters Obtained from Stress Relaxation Experiments

An examination of the parameters that characterize the spectrum reveals that creep and relaxation are most active within the time interval $[\tau_1, \tau_2]$. This time interval reflects the approximate range of application of the model. The parameter C controls the rate of relaxation and creep. C is associated with the material properties of the fibers: the stiffer the fiber, the lower the value of C (Tables 3 to 4). Values within the interval $.009 < C < .17$ should reflect the viscoelastic behavior of most of the textile fibers at 21° C and 65% RH.

As a check the calculated stress relaxation function for "hard elastic" polypropylene fibers [14] is plotted in Figure 30. The function falls between strong nylon and undrawn nylon, indicating the range of material properties of "springy" polypropylene as reflected by the family of curves. This shows the applicability of the quasilinear viscoelastic model for representing the relaxation behavior of these polypropylene fibers.

Since the relaxation spectrum seems to associate unambiguously with each material, we may apply this model to correlate the viscoelastic properties under different environments. For example, the relaxation data of the polyamide fibers obtained at different temperatures and humidities are summarized using the spectra calculated with relaxation data (Case 1). The calculated spectra are shown in Table 10. Figures 34 to 37 show the effect of temperature on the stress relaxation behavior of the polyamide fibers. At constant humidity, the value of C increases as temperature increases, which means the fibers relax faster at higher temperatures.

TABLE 10. ENVIRONMENTAL EFFECT ON POLYAMIDE FIBERS

Fiber	Parameters	21°C 65% RH	112.5° C 65% RH	112.5° C 12% RH
Strong Nylon	C	.0097	.0097	.0081
	τ_1	28.69	2.036	.07646
	τ_2	38260	339100	64390.
Spider Silk	C	.026	.074	.44
	τ_1	.0643	.1688	.1134
	τ_2	29990.	212700.	162100.
Drawn Nylon-6	C	.043	.23	.15
	τ_1	.0962	.2208	.2748
	τ_2	59790.	1600000.	172300
Undrawn Nylon-6	C	.12	.40	.37
	τ_1	.1293	.2546	.176
	τ_2	45390	146100.	115800

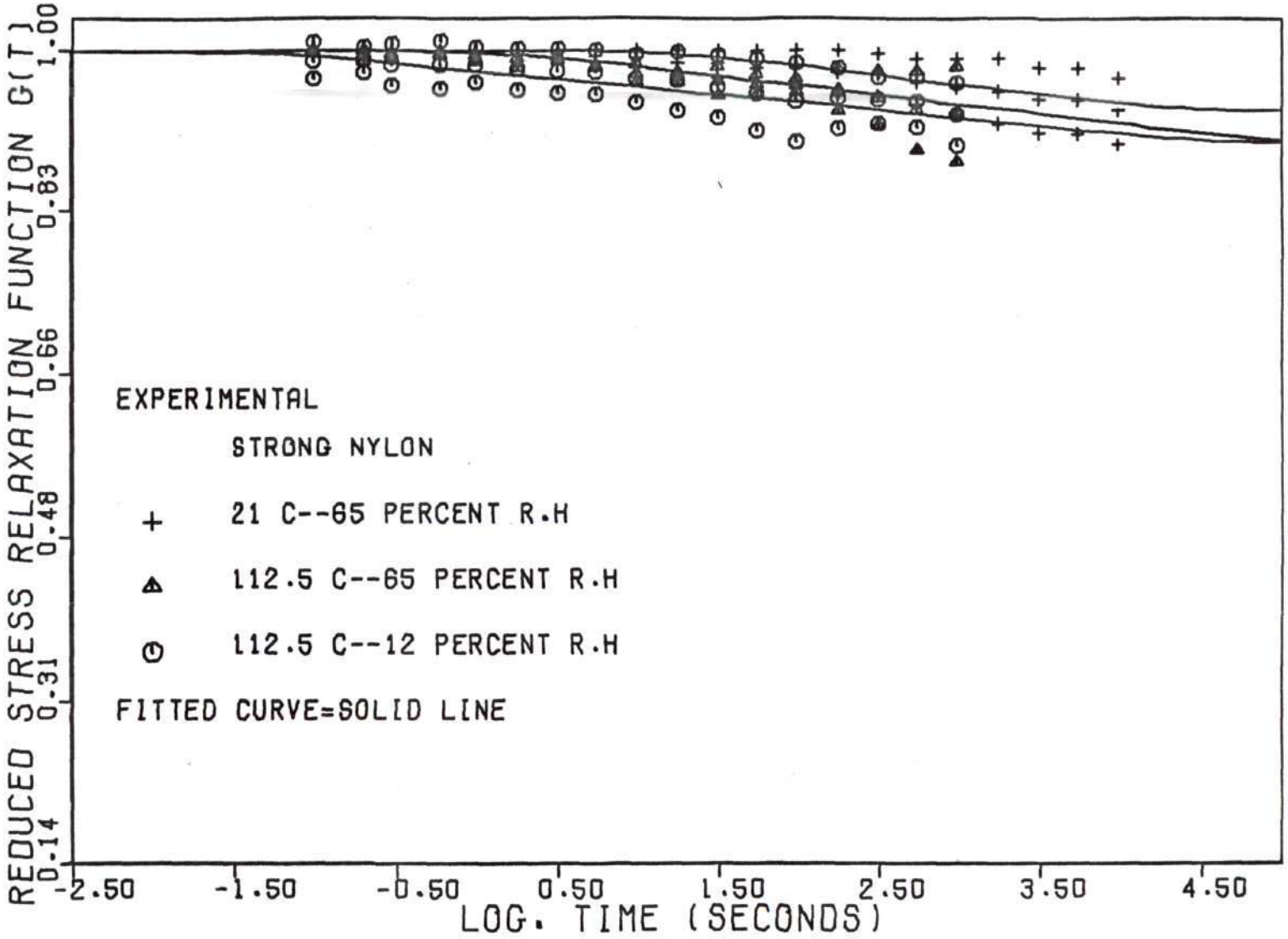

FIGURE 34. ENVIRONMENTAL EFFECT ON THE FRACTIONAL STRESS RELAXATION OF STRONG NYLON FIBER

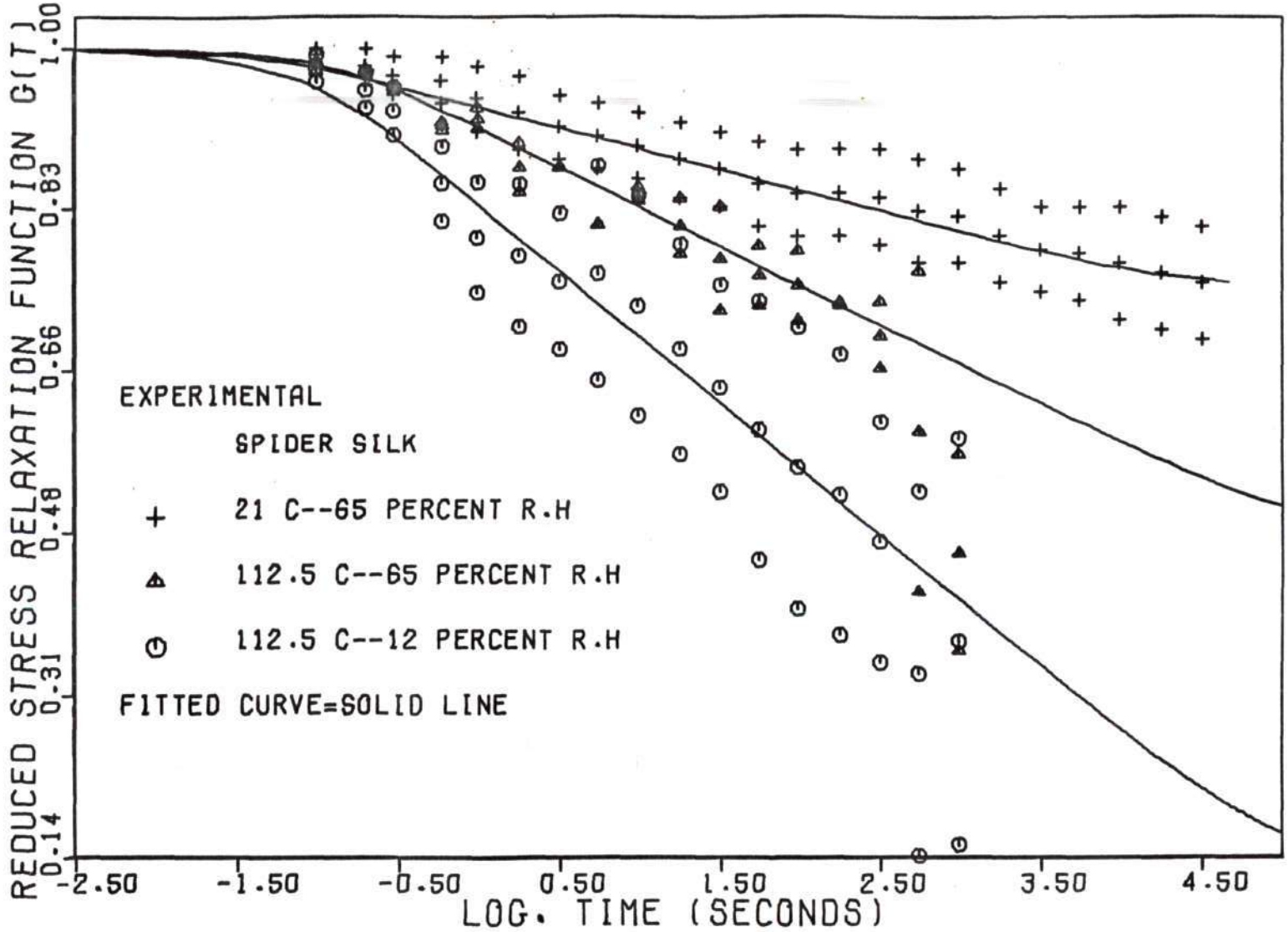

FIGURE 35. ENVIRONMENTAL EFFECT ON THE FRACTIONAL STRESS RELAXATION OF SPIDER SILK

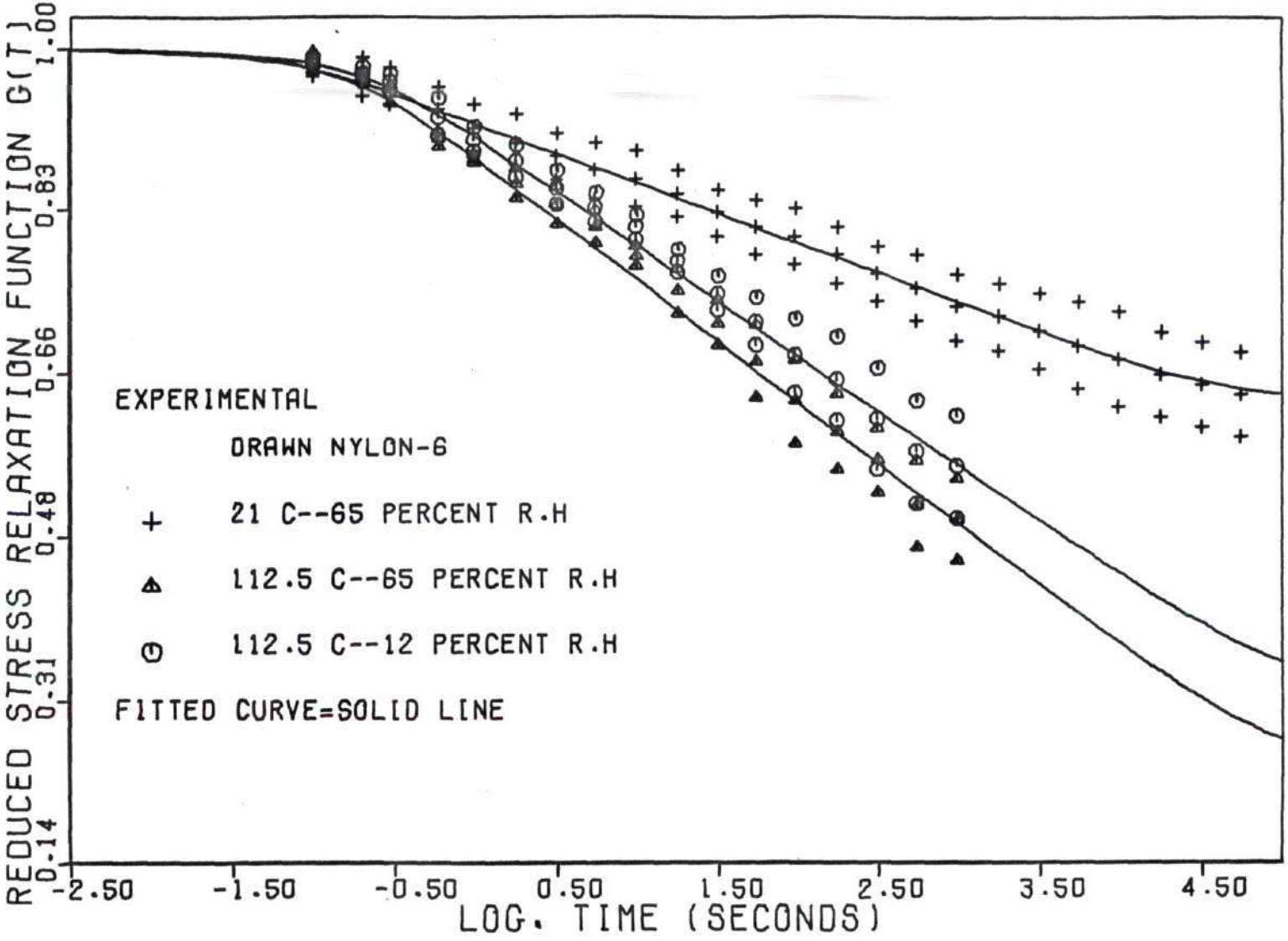

FIGURE 36. ENVIRONMENTAL EFFECT ON THE FRACTIONAL STRESS RELAXATION OF DRAWN NYLON-6 FIBERS

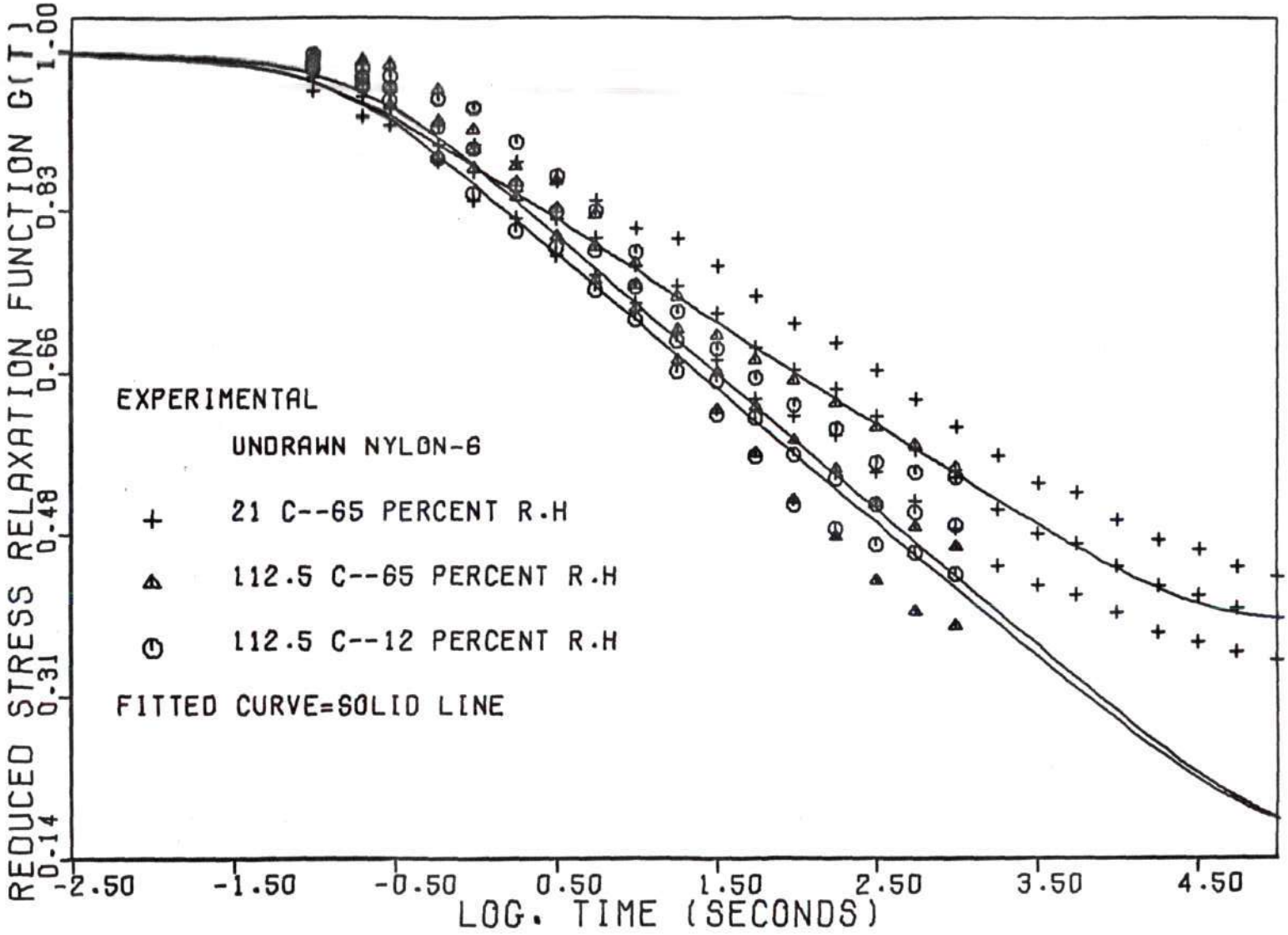

FIGURE 37. ENVIRONMENTAL EFFECT ON THE FRACTIONAL STRESS RELAXATION OF UNDRAWN NYLON-6 FIBER

By observing the values of parameter C (Tables 3 and 4) we can interpret quantitatively the effect of drawing on the viscoelastic behavior of fibers. The relaxation rate of undrawn nylon is about three times greater than that of the drawn nylon. The creep of undrawn nylon is about two times faster than that of drawn nylon. Thus, the parameter C can be associated easily with the draw ratio to provide information for process control as well as for the prediction of fiber properties after drawing.

Isometric Stress-Temperature Relationship

For a reversible process, we can obtain the stress-temperature relationships by combining the first and second laws of thermodynamics, see for example Treloar [106],

$$T = \left(\partial E / \partial \ell \right)_{\theta,v} - \theta \left(\partial S / \partial \ell \right)_{\theta,v} \qquad \text{(III-24)}$$

$$\left(\frac{\partial S}{\partial \ell}\right)_{\theta,v} \simeq -\left(\frac{\partial T}{\partial \theta}\right)_{\lambda,p}$$

where T = stress

p = pressure

θ = absolute temperature

ℓ = length of specimen

λ = stretch ratio

v = volume

S = entropy

E = internal energy

Based on equation (III-24) we can approximate the thermodynamic quantities with the relaxation data obtained at various temperatures. The entropy term can be evaluated from the slopes of the isometric stress-temperature curves and the intercepts are the energy terms.

The isometric stress-temperature curves were obtained by calculating the stress at the 1000th second of the relaxation experiment at different temperatures. For this analysis, the relaxation at constant strains .01 and .02 were considered. Knowing the reduced relaxation function G(1000) and the elastic response corresponding to the two strain levels for each fiber, we can plot the isometric stress-temperature curves as shown in Figure 38. The numerical values of the thermodynamic quantities are shown in Table 11a.

All the polyamide fibers have negative stress-temperature coefficients. The internal energy contribution is much greater than the entropy contribution. This shows that the polyamide fibers are "energy driven" systems. The entropy term in equation (III-24) reflects the degree of structural order of materials. The relative degrees of order of the polyamide fibers with respect to undrawn nylon 6 are shown in Table 11b. Larger values imply higher degree of order. The temperature coefficients become larger as strain levels are increased. For more ordered fibers, such as strong nylon and spider silk, the temperature coefficients become smaller.

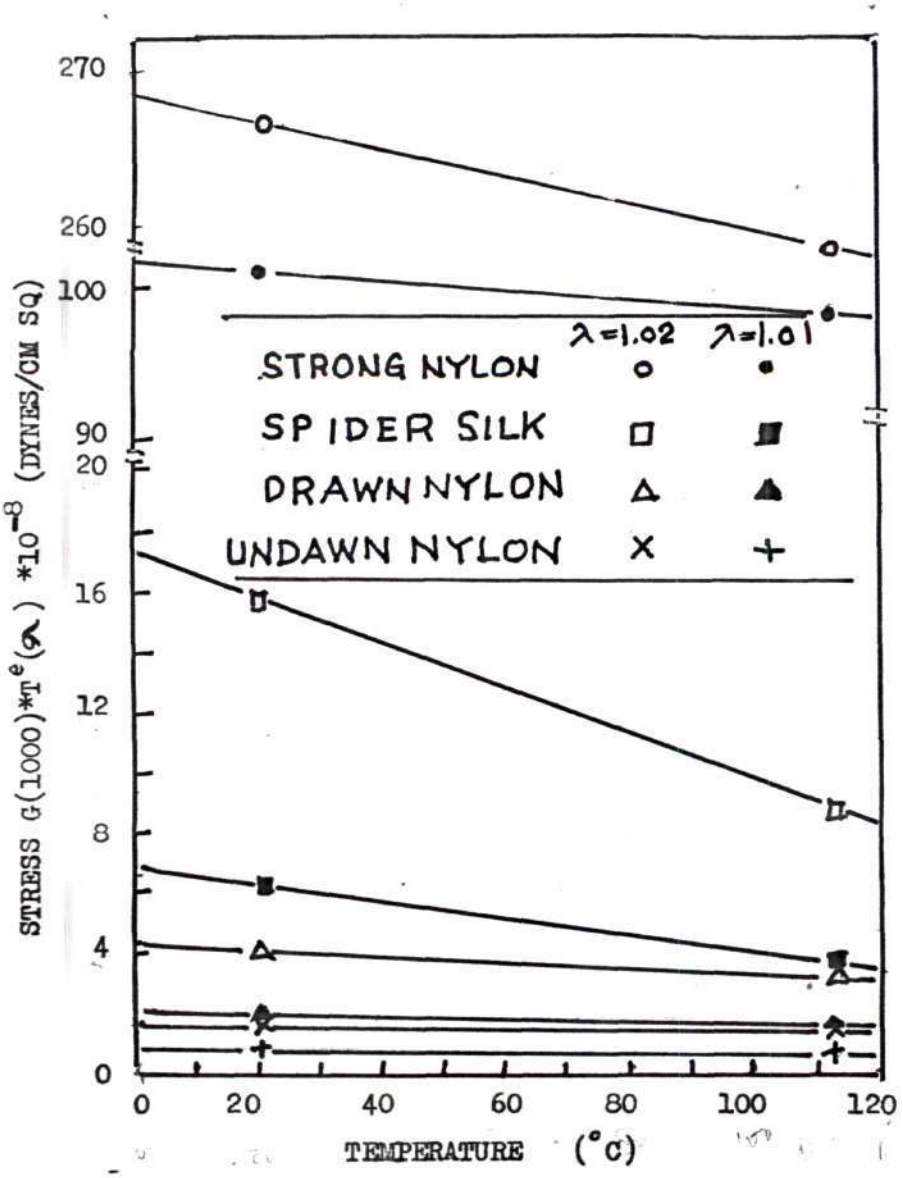

Figure 38. Isometric Stress-Temperature Relationships of Polyamide Fibers

TABLE 11a. ISOMETRIC STRESS-TEMPERATURE RELATIONSHIP OF POLYAMIDE FIBERS

$$T = \left(\partial E/\partial \ell\right)_{\theta,V} - \theta\left(\partial S/\partial \ell\right)_{\theta,V}$$

FIBER	λ = 1.01		λ = 1.02	
	$\left(\partial E/\partial \ell\right) \times 10^{-8}$	$\left(\partial T/\partial \theta\right) \times 10^{-8}$	$\left(\partial E/\partial \ell\right) \times 10^{-8}$	$\left(\partial T/\partial \theta\right) \times 10^{-8}$
STRONG NYLON	102	-0.033	270	-0.87
SPIDER SILK	6.9	-0.030	17	-0.76
NYLON 6 (DRAWN)	2.2	-0.0052	4.3	-0.010
NYLON 6 (UNDRAWN)	.83	-0.0012	1.7	-0.0024

T = Stress at 1000th second of relaxation experiment

θ = Temperature, λ = Stretch Ratio, V = Volume, S = Entropy, E = Internal Energy

TABLE 11b. RELATIVE DEGREE OF STRUCTURAL ORDER OF POLYAMIDE FIBERS

FIBER	$(\partial T/\partial \theta) / (\partial T/\partial \theta)_{\text{undrawn nylon 6}}$	
	$\lambda = 1.01$	$\lambda = 1.02$
Strong nylon	28	32
Spider silk	25	28
Nylon 6 (drawn)	4.3	4.3
Nylon 6 (undrawn)	1.0	1.0

CHAPTER IV

CONCLUSIONS AND CRITQUE

Conclusions

Experimental Observations

Polyamide fibers have nonlinear stress-strain-time relationships which depend on temperature and humidity.

The stress strain relationships of polyamide fibers are nonlinear for all measurable strain levels.

The hysteresis losses are rather insensitive to strain rate. Losses are higher for softer fibers.

Fractional stress relaxations are approximately linear functions of the logarithm of time. Softer fibers have higher rates of stress relaxation.

Fractional creep response increases approximately as a linear function of the logarithm of time. Softer fibers creep faster. Creep responses become increasingly nonlinear as load levels are increased; this nonlinearity is greater for softer fibers.

Except for undrawn nylon 6, dynamic moduli are approximately independent of frequency over the frequency range of .01 to 50 Hz.

Dampings are approximately insensitive to frequency in the range .01 to 30 Hz. Softer fibers have higher dampings.

Rates of stress relaxation of the polyamide fibers increase as the temperature and humidity increase.

All the fibers have negative temperature coefficients in their stress-temperature relationships.

The Quasilinear Viscoelastic Model

The quasilinear viscoelastic model represents the simple elongation, stress relaxation or creep data fairly well when each set of data is fitted individually.

The elastic responses of the polyamide fibers can be represented by the following function:

$$T_i^e(\lambda) = \sum_{j=0}^{3} C_{ij} \lambda^j \qquad \text{(IV-1)}$$

where $i = 1, 2, 3, \ldots, n - 1$; n = number of data points interpolated; and the coefficients C_{ij} for each fiber are listed in Appendix B.

The history dependent responses are represented by the continuous relaxation spectrum model:

$$G(t) = [1 + \int_0^\infty S(\tau)\exp(-t/\tau)d\tau]/[1 + \int_0^\infty S(\tau)d\tau] \qquad \text{(IV-2)}$$

$$J(t) = \frac{1 - \int_0^\infty (S(\tau)/(1 + S(\tau)))\exp\left\{-1/(1 + S(\tau))\right\} d\tau}{1 + \int_0^\infty (S(\tau)/(1 + S(\tau)))d\tau} \qquad \text{(IV-3)}$$

$$M(\omega) = \frac{1 + \int_0^\infty \frac{S(\tau)\, d\tau}{\omega\tau + \frac{1}{\omega\tau}} + i\int_0^\infty \frac{S(\tau)\, d\tau}{\omega\tau + \frac{1}{\omega\tau}}}{1 + \int_0^\infty S(\tau)\, d\tau} \qquad \text{(IV-4)}$$

where the relaxation spectra for the polyamide fibers are:

1) Strong Nylon

$S(\tau) = .0097/\tau$ for $28.69 \leq \tau \leq 3.800 \times 10^4$

$= 0$ elsewhere

2) Spider Drag line

$S(\tau) = .026/\tau$ for $.064 \leq \tau \leq 3.000 \times 10^4$

$= 0$ elsewhere

3) Drawn Nylon 6

$S(\tau) = .043/\tau$ for $.096 \leq \tau \leq 6.000 \times 10^4$

$= 0$ elsewhere

4) Undrawn Nylon 6

$S(\tau) = .12/\tau$ for $.13 \leq \tau \leq 4.500 \times 10^4$

$= 0$ elsewhere

With the exception of strong nylon, this model fails to unify the relaxation and creep response of the polyamide fibers.

The relaxation spectrum is capable of summarizing many relaxation data into three parameters, thus we can correlate conveniently the relaxation behavior of the polyamide fibers with the behavior under different circumstances.

Critique

(1) Experimental

The precision of experimental results was limited by testing instruments and recording systems. Experience gained from this study provides guidance for future development of more precise testing instruments and control and recording systems. For example, an instrument similar to the microtensile tester built by Dr. B. L. Livesay, together with a programmable control and a high speed (faster than 100 samples per second) data logging system is worth considering.

The variation of properties along a filament is well known. In order to obtain good estimates of average fiber properties, many observations are required. This calls for a multichannel testing and recording system.

Only limited dynamic stretching data were obtained; these are exploratory only. In future studies, a force sensor with higher frequency response (higher than 100 Hz) and a broader frequency range should be used. For the study of environmental effects, only two levels of temperature (21° C and 112.5° C) and humidity (12% RH and 65% RH) were considered herein. In future studies, other levels of temperature and humidity should be included to verify the result obtained in this study.

Only tensile viscoelastic properties of the polyamide fibers were measured in this study. Investigation similar to the present study should be carried out for other fibers. Some examples of these fibers are polyester fiber, which is currently the most popular fiber in the industry and is forecast to be the most important fiber in the next decade in terms of consumption; and bicomponent fiber, which is important not only for textile applications but also for serving as a model for our study of the composite nature of polymeric systems. In practice, fibers are subjected to bending and twisting. Studies should be extended to bending and torsional modes.

(2) The Quasilinear Viscoelastic Model

Except for strong nylon, the model fails to unify the history dependent response of the polyamide fibers. We need a nonlinear viscoelastic model that takes nonlinearity in both elastic response and history dependent response into account.

Before a tractable nonlinear model is available, other spectra need be explored. An optimum spectrum may be found to give a first approximation to the nonlinear viscoelastic behavior of the fibers, perhaps by computation.

The quasilinear viscoelastic model is not a unique physical model. The value of this model does not go beyond its ability to summarize experimental observations.

Despite this weakness of the quasilinear viscoelastic model, it can summarize individual sets of data, especially the relaxation data (Figure 30). This provides means to correlate the relaxation behavior of the fibers with particular end use environmental conditions

and processing variables.

Fibers often exist as integral parts of higher order structures such as yarns and planar fibrous assemblies. The information about the fibers summarized by the quasilinear viscoelastic model may be incorporated into the mechanistic analysis and design of fibrous assemblies.

Finally, by observing the viscoelastic response of a broad range of fibers, this study demonstrates that oriented composite structures such as polyamide fibers are no exception to the rule that polymeric materials have nonlinear stress-strain- time relationships which depend on environmental conditions. A simple model such as the quasilinear viscoelastic model gives only a zeroth approximation of the viscoelastic behavior of the polyamide fibers.

APPENDICES

APPENDIX A

NOMENCLATURE

C	=	constant
$E_1(z)$	=	exponential integral
$T(t)$	=	tension in the specimen at time t
$T(t_r)$	=	tension in the specimen at time t_r
$G(t)$	=	reduced relaxation function, defined by equation (II-1)
$G(t_o)$	=	value of reduced relaxation function at t_o
$G(\infty)$	=	value of reduced relaxation function when relaxation approaches equilibrium state
$H(t)$	=	unit step function of time
$J(t)$	=	reduced creep function, defined by equation (II-2)
$K(\lambda, t)$	=	history of stress response, defined by equation (III-2)
ℓ	=	fiber length at any time t
ℓ_o	=	gage length
$M(\omega)$	=	complex modulus, defined by equation (II-5)
S_R	=	slope of the reduced relaxation function, defined by equation (III-19)
$S(\tau)$	=	continuous relaxation spectrum, defined by equation (III-8)
$T(t)$	=	stress at time t
$T^e(\lambda)$	=	elastic response
t	=	time

t_r = reference time corresponding to the maximum load

t_o = time at the middle portion of the reduced relaxation function

γ = Euler's constant

ϵ = strain, $\lambda - 1$

$\lambda(t)$ = strain history

ρ = density, g/c.c

τ = time constant

τ_1, τ_2 = time constants, ($\tau_2 > \tau_1$)

ω = frequency

S_c = slope of the reduced creep

h = relative humidity

θ = temperature

APPENDIX B

Cubic Spline Interpolation

Cubic spline interpolation is a curve fitting method which approximates a general function by a series of cubic polynomials. The theoretical background of spline interpolation functions has been detailed, for example, by Conte and deBoor [17].

Cubic spline interpolation has many applications in engineering and aesthetic design such as for fitting and smoothing stress-strain data and for designing apparel and automobile bodies. The computation aspects of the interpolation method used in this study is demonstrated below.

Assume five data points have been obtained from a tensile test and a function $T(\lambda)$ that smoothes and fits the data is sought.

For five given points, we need four cubic equations to interpolate the intervals between points, namely:

$$T^e_1(\lambda) = C_{10} + C_{11}\lambda + C_{12}\lambda^2 + C_{13}\lambda^3 \qquad (A\text{-}1)$$

$$T^e_2(\lambda) = C_{20} + C_{21}\lambda + C_{22}\lambda^2 + C_{23}\lambda^3 \qquad (A\text{-}2)$$

$$T^e_3(\lambda) = C_{30} + C_{31}\lambda + C_{32}\lambda^2 + C_{33}\lambda^3 \qquad (A\text{-}3)$$

$$T^e_4(\lambda) = C_{40} + C_{41}\lambda + C_{42}\lambda^2 + C_{43}\lambda^3 \qquad (A\text{-}4)$$

To solve these equations for the sixteen coefficients, the following properties of the cubic spline function are used.

1) Continuity of the functions, i.e.

$$T_{12} = T_{21}$$

$$T_{22} = T_{31} \qquad \text{(A-5)}$$

$$T_{32} = T_{41}$$

2) Continuity of the first and second derivatives, i.e.

$$T_{12}' = T_{21}'$$

$$T_{22}' = T_{31}' \qquad \text{(A-6)}$$

$$T_{32}' = T_{41}'$$

$$T_{12}'' = T_{21}''$$

$$T_{22}'' = T_{31}'' \qquad \text{(A-7)}$$

$$T_{32}'' = T_{41}''$$

and make use of the five data points,

$$T_1, T_2, T_3, T_4, T_5 \qquad \text{(A-8)}$$

The remaining two conditions can be satisfied by letting the

second derivatives of the end point of the stress-strain curve equal zero.

$$T''_1 = 0, \quad T''_5 = 0 \qquad \text{(A-9)}$$

With the foregoing eleven conditions and the five given data points, we can now solve equations (A-1) to (A-4) for the sixteen coefficients.

Equations (A-1) to (A-4) can be generalized for n data points.

$$T^e_i(\lambda) = \sum_{j=0}^{3} C_{ij} \lambda^j \qquad \text{(A-10)}$$

$$C_{00} = 0$$

where i = 0, 1, 2, ..., n - 1; j = 0, 1, 2, 3; n = number of interpolation data points; and C_{ij} are the material coefficients.

The calculated material coefficients C_{ij} for the elastic response of the polyamide fibers are tabulated in Table 12.

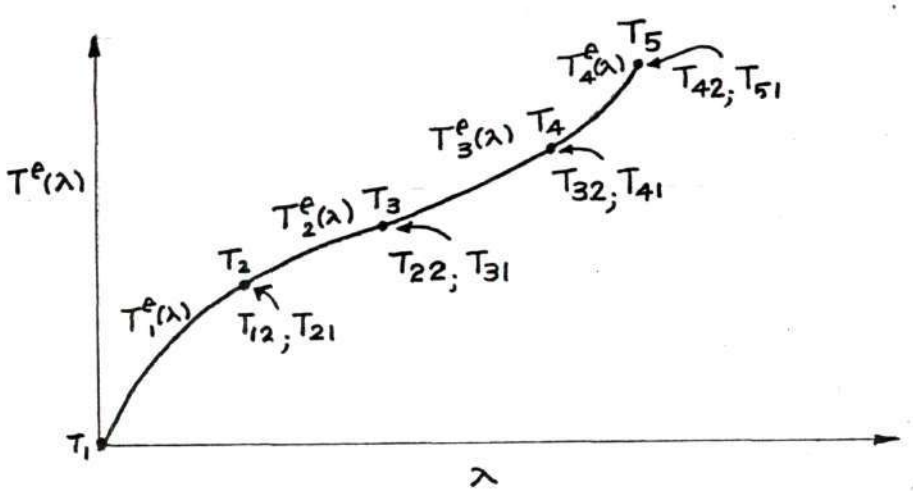

TABLE 12. MATERIAL COEFFICIENTS OBTAINED BY SPLINE FIT OF THE ELASTIC RESPONSE OF THE POLYAMIDE FIBERS

$$T^{0}(\lambda) = C_0 + C_1\lambda + C_2\lambda^2 + C_3\lambda^3$$

Fiber	C_0	C_1	C_2	C_3	Stretch ratio range
Strong Nylon	117282.84	-345623.85	338195.28	-109854.27	$1 \leq \lambda \leq 1.0115$
	-288359.69	856873.77	-850043.47	281528.71	≤ 1.026
Spider Silk	-895.19	2539.74	-2403.50	758.95	$1 \leq \lambda \leq 1.03$
	-841.56	2383.53	-2251.84	709.87	≤ 1.05
	-784.74	2221.20	-2097.24	660.79	≤ 1.07
	93.10	-240.04	202.99	-55.79	≤ 1.362
Drawn Nylon	201031.88	-598491.29	593501.09	-196041.68	$1 \leq \lambda \leq 1.01$
	45413.48	-136258.43	135844.79	-45000.00	≤ 1.02
	-114873.16	335172.88	-326342.76	106041.68	≤ 1.03
	-10836.34	32153.03	-32148.73	10833.26	≤ 1.04
	56889.45	-163209.83	155700.17	-49374.72	≤ 1.05
	-112170.51	319818.61	-304326.92	96665.63	≤ 1.06
	226022.53	-637331.51	598644.89	-187287.47	≤ 1.07
	-263716.88	735769.66	-684627.23	212485.47	≤ 1.08
	158462.47	-436950.76	401225.01	-122654.11	≤ 1.09
	222197.22	-612367.51	562157.81	-171869.03	≤ 1.10
	-33353.80	84589.82	-71439.76	20130.23	≤ 1.11
	88067.38	-243575.54	224204.71	-68651.89	≤ 1.12
	-259659.49	784264.32	-693509.45	204477.32	≤ 1.13
	84882.53	-226024.24	200551.22	-59257.39	≤ 1.14
	-125214.65	326863.06	-284437.64	82552.22	≤ 1.15
	245124.05	-639237.89	555650.15	-150951.49	≤ 1.16
	-367067.50	944016.12	-809224.00	231253.73	≤ 1.17
	218029.22	-556231.87	473039.24	-134063.43	≤ 1.18
	-26886.77	66435.90	-54645.32	15000.00	≤ 1.19
	-278082.36	699702.08	-586801.77	164063.43	≤ 1.20

TABLE 12 (continued)

Fiber	C_0	C_1	C_2	C_3	Stretch ratio range
Undrawn Nylon (up to 9% stretch)	100772.88	-305286.42	307783.60	-103270.06	$1 \leq \lambda \leq 1.01$
	-7343.53	15851.44	-10174.68	1666.67	≤ 1.02
	-118703.22	343379.95	-331281.07	106603.39	≤ 1.03
	115887.38	-339893.66	332091.37	-108080.24	≤ 1.04
	-237092.49	678317.52	-646957.84	205717.58	≤ 1.05
	145511.44	-414836.56	394141.28	-124790.08	≤ 1.06
	-90587.00	253366.57	-236239.03	73442.72	≤ 1.07
	-1865.05	4613.43	-3759.46	1019.18	≤ 1.08
	21488.30	-60256.98	56305.74	-17519.46	≤ 1.09

With the stress-strain curve expressed in terms of known functions, we can conveniently obtain other quantities such as the strain energy and the slopes of the stress-strain curve at various strain levels. The slopes of the stress-strain curves (moduli) plotted as functions of the stretch ratios of the polyamide fibers are shown in Figures 4 to 7. The moduli were obtained by differentiation of equation (A-10) with respect to the stretch ratio:

$$\frac{dT^{e}_{i}(\lambda)}{d\lambda} = \sum_{j=1}^{3} (j)\, C_{ij}\, \lambda^{(j-1)} \qquad \text{(A-11)}$$

Cubic spline interpolation is a powerful tool for fitting experimental data, but we should be aware of the extra sensitivity of the derivatives of the spline function to the density of the interpolation points. When the interpolation points are too close to each other, especially at inflection points, the cubic equations are forced to fluctuate unrealistically between the interpolation points. The amplitude of fluctuation is markedly amplified when we take derivative of the spline function. The deviations between the calculated and the measured moduli in this study are about 10%.

APPENDIX C

DERIVATION OF THE GENERALIZED FUNCTIONS

The reduced relaxation function $G(t)$, creep function $J(t)$, and complex modulus $M(\omega)$ can be derived by generalization of a large number of discrete elements of mechanical responses represented by differential equations.

The starting differential equations relating stress and strain and their time derivatives may be assumed to have the form of differential operators or they can be obtained by consideration of mechanical models.

In this study, the starting differential equation was obtained by consideration of a linear solid model. The response of standard linear solid can be represented by a three element model consisting of a spring connecting in series with a Voigt unit (a dashpot and a spring in parallel). It is important to realize that the use of a model is not necessary and the type of model one uses can be quite arbitrary when a large number of model elements are combined to represent the viscoelastic behavior of materials. This point has been demonstrated by Kuhn [40] and stated best by Treloar:

> any system of springs and dashpots connected into a network of arbitrary structure may always be reduced to one or two basic types of model, provided one is allowed to include one degenerate element of either type (i. e. isolated spring or dashpot). There is therefore no point in exploring more complex types of models [106].

The differential equation for a standard linear solid has the following form[24, 28, 71]:

$$T + \tau_\epsilon \dot{T} = E_R \, (T^e + \tau_\sigma \dot{T}^e) \qquad \text{(A-1)}$$

where τ_ϵ, τ_σ and E_R are coefficients of the differential equation. T is the stress and T^e is the elastic response. $\dot{T} = dT/dt$.

The initial condition for equation (A-1) is

$$\tau_\epsilon T(0) = E_R \, \tau_\sigma \, T^e(0) \qquad \text{(A-2)}$$

and by definition $G(0) = 1$, the parameters τ_σ and τ_ϵ are related by

$$E_R = \tau_\epsilon \, / \, \tau_\sigma$$

We can now describe the stress-strain response of a linear solid for different types of mechanical tests:

1) Stress Relaxation: For a unit step strain input

$$T^e(t) = T^e \, \mathbb{1}(t) \qquad \text{(A-3)}$$

the Laplace Transformation (LPT) for equations (A-1) and (A-3) are

$$\bar{T} + \tau_\epsilon \dot{\bar{T}} = E_R \bar{T}^e + E_R \, \tau_\sigma \dot{\bar{T}}^e \qquad \text{(A-4)}$$

and $\bar{T} = T \, / s$ then

$$\bar{T} = (E_R\, T_o^e / \tau_\epsilon\,)/[(1/\tau_\epsilon\,) + s]s + T_o/[(1/\tau_\epsilon\,) + s] \tag{A-5}$$

the inverse LPT of equation (A-5) is

$$T(t) = E_R\, T_o^e\, [1 - \exp(-t/\tau_\epsilon\,)] + T_o \exp(-t/\tau_\epsilon\,)$$

from assumption, $T_o^e = T_o$ and let $T_o = T(t_r)$

$$T(t) = E_R\, T(t_r)\, (1 - \exp(-t/\tau_\epsilon\,) + T(t_r)\exp(-t/\tau_\epsilon\,) \tag{A-6}$$

by definition $G(t) = T(t)/T(t_r)$, therefore

$$G(t) = E_R[1 - \exp(-t/\tau_\epsilon\,)] + \exp(-t/\tau_\epsilon\,) \tag{A-7}$$

and for $t = 0$, $G(t) = 1$, this agrees with the definition.

2) Creep: For a unit step loading

$$T(t) = T_o\, \mathbb{1}(t) \tag{A-8}$$

the LPT of equation (A-8) is

$$\bar{T} = T_o/s \tag{A-9}$$

from equation (A-4)

$$(T_o/s) = (E_R + E_R\,\tau_\sigma\,s)\overline{T}^e - E_R\,\tau_\sigma\,T_o^e \qquad \text{(A-10)}$$

i. e.

$$\overline{T}^e = [T_o/E_R\,\tau_\sigma\,((1/\tau_\sigma) + s)s] + T_o^e[1/((1/\tau_\sigma) + s)] \qquad \text{(A-11)}$$

the inverse LPT of equation (A-11) is

$$T^e = [1 - \exp(-t/\tau_\sigma)]T_o/E_R + T_o^e\exp(-t/\tau_\sigma) \qquad \text{(A-12)}$$

by definition, $J(t) = T^e(t)/T^e(t_r)$ and by assumption $T_o = T_o^e$, therefore the creep function

$$J(t) = [1 - \exp(-t/\tau_\sigma)]/E_R + \exp(-t/\tau_\sigma) \qquad \text{(A-13)}$$

and for $t = 0$, $J(t) = 1$, this agrees with the definition.

3) Sinusoidal Stretching: The sinusoidal elastic and stress response can be expressed in terms of complex notations as follows

$$T^e(t) = T\exp(i\omega t), \quad T(t) = T\exp(i\omega t)$$

and their derivative with respect to time are

$$\dot{T}^{e}(t) = [T \exp(i\omega t)]i\omega , \quad \dot{T}(t) = i\omega [T \exp(i\omega t)] \tag{A-14}$$

Substituting (A-14) into (A-4)

$$[T_o \exp(i\omega t)] (1+ \tau_\epsilon i\omega) = E_R \exp(i\omega t) + T(1 + i\omega \tau_\sigma) \tag{A-15}$$

and by definition, the complex modulus $M(\omega) = T_o/T_o^{e}$, therefore

$$M(\omega) = [(1 + i\omega \tau_\sigma)/(1 + i\omega \tau_\epsilon)]E_R \tag{A-16}$$

$$= [(1 + \omega^2 \tau_\sigma^2)/(1 + \omega^2 \tau_\epsilon^2)]E_R + i[(\tau_\sigma - \tau_\epsilon)/(1 + \omega^2 \tau_\epsilon^2)]\omega E_R \tag{A-17}$$

Use a different notation, let $E_R = 1/(1 + S)$, and express in terms of τ_ϵ. Equations (A-7), (A-13), and (A-17) can be expressed as follows:

$$G(t) = [1 + S \exp(-t/\tau_\epsilon)]/(1 + S) \tag{A-18}$$

$$J(t) = \frac{1 - \frac{S}{1+S} \exp[-t/(1 + S)\tau_\epsilon]}{1 - [s/(1 + S)]} \tag{A-19}$$

$$M(\omega) = \frac{1}{1+S}\left(1 + S\,\frac{\omega\tau_\epsilon}{\omega\tau_\epsilon + \frac{1}{\omega\tau_\epsilon}} + i\,S\,\frac{1}{\omega\tau_\epsilon + \frac{1}{\omega\tau_\epsilon}}\right) \qquad \text{(A-20)}$$

Replacing τ_ϵ by a continuous variable τ and let $S(\tau)$ be a function of τ, the reduced relaxation function G(t), creep function J(t) and the complex modulus are generalized as follows:

$$G(t) = \frac{1 - \int_0^\infty S(\tau)\,\exp(-t/\tau)\,d\tau}{1 + \int_0^\infty S(\tau)\,d\tau} \qquad \text{(A-21)}$$

$$J(t) = \frac{1 - \int_0^\infty \frac{S(\tau)}{1+S(\tau)}\,\exp[-t/(1+S(\tau)]\,d\tau}{1 - \int_0^\infty \frac{S(\tau)}{1+S(\tau)}\,d\tau} \qquad \text{(A-22)}$$

$$M(\omega) = \frac{1 + \int_0^\infty S(\tau)\frac{\omega\tau\,d\tau}{\omega\tau + \frac{1}{\omega\tau}} + i\int_0^\infty [S(\tau)/(\omega\tau + \frac{1}{\omega\tau})]\,d\tau}{1 + \int_0^\infty S(\tau)\,d\tau} \qquad \text{(A-23)}$$

DERIVATION OF THE COMPUTATION EQUATIONS (III-12 & III-13)

For a continuous relaxation spectrum

$$S(\tau) = C/\tau \qquad \tau_1 < \tau < \tau_2$$

$$= 0 \text{ elsewhere}$$

equations (A-21), (A-22) and (A-23) can be expressed as follows:

$$G(t) = [1 + \int_{\tau_1}^{\tau_2} \frac{C \exp(-t/\tau)}{\tau} d\tau]/[1 + \int_{\tau_1}^{\tau_2} \frac{C}{\tau} d\tau] \qquad (A-24)$$

$$J(t) = [1 - \int_{\tau_1}^{\tau_2} \frac{C}{C + \tau} \exp (\frac{-t}{C + \tau}) d\tau]/[1 - \int_{\tau_1}^{\tau_2} \frac{C}{C + \tau} d\tau] \qquad (A-25)$$

$$M(\omega) = \frac{[1 + \int_{\tau_1}^{\tau_2} \frac{C \omega \tau \, d(\omega\tau)}{1 + (\omega\tau)^2}] + i \int_{\tau_1}^{\tau_2} \frac{C \, d(\omega\tau)}{1 + (\omega\tau)^2}}{1 + \int_{\tau_1}^{\tau_2} \frac{C}{\tau} d\tau} \qquad (A-26)$$

let $z = t/\tau$

$$G(t) = [1 + \int_{t/\tau_2}^{t/\tau_1} \frac{C \exp(-Z)}{Z} dZ]/[1 + \int_{\tau_2}^{\tau_1} \frac{C}{\tau} d\tau] \qquad (A-27)$$

make use of the properties of an exponential integral

$$-E_i(-x) = \int_x^{\infty} \frac{\exp(-Z)}{Z} dZ \equiv E_1(x) \qquad (A-28)$$

equation (A-27) becomes

$$G(t) = \frac{1 + C\,[E_1\,(t/\tau_2) - E_2(t/\tau_1)]}{1 + C\ln\left(\frac{C + \tau_2}{C + \tau_1}\right)} \qquad \text{(A-29)}$$

similarly,

$$J(t) = \frac{1 - C\left[E_1\left(\frac{t}{C + \tau_2}\right) - E_1\left(\frac{t}{C + \tau_1}\right)\right]}{1 + C\ln\left(\frac{C + \tau_2}{C + \tau_1}\right)} \qquad \text{(A-30)}$$

$$M(\omega) = \frac{1 + C(.5)\,[\ln(1 + \omega^2\tau_2^2) - \ln(1 + \omega^2\tau_1^2)]}{[\,1 + C\ln(\tau_2/\tau_1)]} + \frac{i\,C\,[\tan^{-1}(\omega\tau_2) - \tan^{-1}(\omega\tau_1)]}{[\,1 + C\ln(\tau_2/\tau_1)]} \qquad \text{(A-31)}$$

The exponential integral in equations (A-29) to (A-31) can be evaluated by an approximation method [3].

For $0 \leq X \leq 1$ in equation (A-28)

$$E_1(x) = a_0 + a_1x + a_2x^2 + a_3x^3 + a_4x^4 + a_5x^5 - \ln x + \epsilon(x) \qquad \text{(A-32)}$$

where

$a_0 = -.05772$

$a_1 = .9999$

$a_2 = -.02499$

$a_3 = .05519$

$a_4 = -.00976$

$a_5 = .001078$

For $1 \leq x \leq \infty$

$$E_1(x) = [(\frac{x^4 + a_1x^3 + a_2x^2 + a_3x + a_4}{x^4 + b_1x^3 + b_2x^2 + b_3x + b_4}) + \epsilon(x)]/x \exp(x) \qquad \text{(A-33)}$$

where the error term $|\epsilon(x)| < 2 \times 10^{-8}$

and

$a_1 = 8.5733$	$b_1 = 9.5733$
$a_2 = 18.05901$	$b_2 = 25.6329$
$a_3 = 8.6347$	$b_3 = 21.09915$
$a_4 = .2677$	$b_4 = 3.9584$

For a large value of x

$$E_1(x) \simeq \frac{\exp(x)}{x}\left(1 - \frac{1}{x} + \frac{2!}{x^2} - \frac{3!}{x^3} + \ldots\right) \tag{A-34}$$

$$E_1(x) = O(\exp(-x)/x)$$

O = of the order of

For a small value of x

$$E_1(x) = -\gamma - \ln x + o(x) \tag{A-35}$$

where γ = Euler's constant $\gamma = .5772$

If τ_1 and τ_2 are sufficiently apart, then there is an interval (t_1, t_2)

$$\tau_1 << t_1 \leq t \leq t_2 << \tau_2$$

for which we obtain equations II-12 and II-13 as follows:

$$G(t) = \frac{1 - C\gamma - C\ln(t/\tau_2)}{1 + C\ln(\tau_2/\tau_1)} + o(C) \tag{A-36}$$

$$J(t) = \frac{1 + C\gamma + C\ln[t/(C + \tau_2)]}{1 - C\ln[(C + \tau_2)/(C + \tau_1)]} + o(C) \tag{A-37}$$

APPENDIX D

Conversion Factors for Some Often Used Units

Convert From	To	Multiply By
gm/denier	gm/Tex	9
gm/denier	dyne/cm^2	$8.83 \times 10^8 \rho$
gm/denier	psi	$1.28 \times 10^4 \rho$
psi	dynes/cm^2	6.895×10^4
dynes/sq cm	psi	1.450×10^{-5}
gm/sq cm	dynes/cm^2	980.665
gm/denier	MN/Tex	88.3
MN/Tex	dynes/cm^2	$10^8 \rho$
denier	cm^2	$1/(9 \times 10^5 \rho)$
denier	in^2	$1/(58 \times 10^5 \rho)$
poise	gm/cm sec	1

Denier = linear density = gm/9000 m

Tex = linear density = gm/1000 m

ρ = grams/cm^3 = density

BIBLIOGRAPHY

LITERATURE CITED

[1] Abbott, N. J., "Extension and Relaxation of Nylon Filaments," Textile Res. J., 21, 227 (1951).

[2] Abbott, N. J., J. G. Donovan, M. M. Schoppee, and J. Skelton, "Some Mechanical Properties of Kevelar® and Other Heat Resistant, Nonflammable Fibers, Yarns, and Fabrics", Technical report AFML-TR- 74 -65, Part III, March, 1975.

[3] Abramowitz, M., and I. A. Segun, Hand Book of Mathematical Functions, Dover, New York, 1968.

[4] Alfrey, T., Mechanical Behavior of High Polymers, Interscience, New York, 1948.

[5] Ballou, J. W. and S. Silverman, "Sound Velocity Measurements", Textile Research, 14, 282 (1944).

[6] Becker, R., Z. Phys. 33, 192 (1925).

[7] Black, W. B. and J. Preston, in Mark, H. F., S. M. Atlas, and E. Cernia, (editors), Man-Made Fibers, Vol. 2, pp. 297-400, Interscience, New York, 1968.

[8] Boltzmann, L., "Zur Theorie de elastischen Nachwirkung", Sitzber Kgl. Akad. Wiss. Wien, Math-Naturw, 70, 275(1874).

[9] Burleigh, E. G., and H. Wakeham, "Stress Relaxation of Cotton and Rayon Cords", Textile Res. J., 17, 245(1947).

[10] Burte, H., G. Halsey, and J. H. Dillon, "A New Concept of the Mechanical Behavior of Fibers", Textile Res. J., 18, 449(1948).

[11] Catsiff, E., T. Alfrey and M. T. O'Shaughnessy, "Generalized Creep Curves for Nylon", Textile Res. J., 23, 808(1953).

[12] Chapman, B. M., "Bending Stress Relaxation and Recovery of Nylon 66 and Terylene Fibers", J. Appl. Sci., 17, 1693(1973).

[13] Chen, Y-L. and Y. C. Fung, "Stress-Strain-History Relations of Rabbit Mesentery in Simple Elongation", Biomechanics Symposium, AMD-VOL.2, ASME, 9-10(1973).

[14] Chen, Y-L. H., F. K. Ko and J. L. Lundberg, "Nonlinear Viscoelasticity of Hard Elastic Polypropylene Fibers", Polymer Eng. and Sci., 16, 406(1976).

[15] Coleman, B. D. and W. Noll, "Foundations of Linear Viscoelasticity", Rev. Mod. Phys., 33, 239(1961).

[16] Comstock, J. H., The Spider Book, Comstock Publishing Co., Inc., Ithaca, N. Y., 1948.

[17] Conte, S. D. and C. de Boor, Elementary Numerical Analysis, 2nd edition, McGraw-Hill Book Company, New York, 1972.

[18] Daniel, I. M., "Theoretical Stress Analysis", in Brown, W. C., Testing of Polymers, Vol. 4, Interscience, New York, 1969.

[19] Dunell, B. A. and J. H. Dillon, "Measurement of Dynamic Modulus and Energy Losses in Single Textile Filaments Subjected to Forced Longitudinal Vibrations", Textile Res. J. , 21, 393 (1951).

[20] Dunell, B. A., A. A. Joanes, and R. T. B. Rye., "Viscoelastic Behavior of Nylon 66 Monofilaments Below Room Temperature", J. Colloid Sci., 15, 193(1960).

[21] Eyring, H., M. G. Alder, S. A. Rossmassler,and C. T. Christenson, "Force Vibrations of Polyamide Monofils", Textile Res. J., 22, 223 (1952).

[22] Ferry, J. D., Viscoelastic Behavior of Polymers, 2nd edition, Wiley, New York, 1970.

[23] Feughelman, M., "Creep of Wool Fibers in Water", J. Textile Inst., 45, T50(1954).

[24] Flugge, W., Viscoelasticity, Blasidell Publishing Co., Waltham, Mass.,1967.

[25] Friedrich, V. L. Jr., and R. M. Langer, "Fine Structure of Cribellate Spider Silk", Am. Zoologist, 9, 91 (1969).

[26] Fujino, K., H. Kawal, and T. Horino, "Experimental Study of the Viscoelastic Properties of Textile Fibers--Dynamic Measurements from Subsonic to Supersonic Frequencies", Textile Res. J., 25, 722 (1955).

[27] Fung, Y. C. B., "Elasticity of Soft Tissues in Simple Elongation", Am. J. of Physiology, 213, 1532(1967).

[28] Fung, Y. C. B., N. Perrone, and M. Anliker, (editors), Biomechanics - Its Foundations and Objectives, Chapter 7, Prentice-Hall, Englewood Cliffs, N. J., 1972.

[29] Gross, B. Mathematical Strecture of the Theories of Viscoelasticity, Hermann, Paris, 1953.

[30] Hadley, D. W. and I. M. Ward, "Nonlinear Creep and Recovery Behavior of Polypropylene Fibers", J. Mech. Phys. Solids, 13, 397(1965).

[31] Halsey, G., H. J. White and H. Eyring, "Mechanical Properties of Textiles, I", Textile Res. J., 15, 295(1945).

[32] Halsey, G., H. J. White and H. Eyring, "The Mechanical Properties of Textiles, II", Textile Res. J., 16, 451(1946).

[33] Haut, R. C. and R. W. Little, "A Constitutive Equation for Collagen Fibers", J. Biomechanic, 5, 423(1972).

[34] Holland, H. D., G. Halsey, and H. Eyring, "Mechanical Properties of Textiles, VI , A Study of Creep of Fibers", Textile Res. J., 16, 201 (1946).

[35] Hopkins, I. L. and R. W. Hamming, "On Creep and Relaxation", J. Appl. Phys., 28, 906(1957).

[36] Hopkins, I. L., "Iterative Calculation of Relaxation Spectra from Relaxation Data", Technical Memorandum, Bell Telephone Laboratories, Inc., (1961).

[37] Hopkins, I. L., "Iterative Calculation of Relaxation Spectrum from Free Vibration Data", J. Appl. Polymer Sci., 7, 971, (1963).

[38] Hopkinson, J., "On the Torsional Strain Which Remains in a Glass Fiber after Release from Twisting Stress", Proc. Roy. Soc. (London), 28, 148(1878).

[39] Howard, W. H. and M. L. Williams, "The Viscoelastic Properties of Oriented Nylon 66 Fibers, Part I. Creep at Low Loads and Anhydrous Conditions", Textile Res. J., 32, 689(1963).

[40] Jenkins, R. B., and R. W. Little, "A Constitutive Equation for Parallel-Fibered Elastic Tissue", J. Biomechanics, 7, 397(1974).

[41] Kaston, B. J., How to Know the Spiders, 2nd edition, Wm. C. Brown Company, Dubuque, Iowa, 1972.

[42] Katz, S. M., and A. W. Tobolsky, "The Relaxation of Stress in Wool Fibers", Textile Res. J., 20, 87(1950).

[43] Kirkwood, J. G. and R. M. Fuoss, "Anomalous Dispersion and Dielectric Loss in Polar Polymers", J. Chem. Phys., 9, 329(1941).

[44] Ko, F. K., Y. L. Chen, and J. L. Lundberg, "Nonlinear Viscoelasticity of Fibers", Bull. Am. Phys. Soc., Ser. II, 20 (No.3), 480(1975).

[45] Konopasek, L., M. S. Thesis, University of Manchester, 1975.

[46] Kubu, E. T., "The Stress Relaxation of Fibrous Materials", Textile Res. J., 22, 765 (1952).

[47] Kuhn, W. O., Kunzle and A. Preissman, "Relaxationszeitspektrum, Elastizitat und Viskositat von Kautschuk, I.", Helv. Chem. Acta, 30, 307(1947).

[48] Laible, R. C. and H. M. Morgan, "The Viscoelastic Behavior of Oriented Polyvinyle Alcohol Fibers at Large Strain", J. Polymer Sci., 54, 53(1961).

[49] Lasater, J. A., E. L. Nimer and H. Eyring, "Mechanical Properties of Cotton Fibers, Part I and II", Textile Res. J. , 23, 237, 481 (1953).

[50] Leaderman, H., Elastic and Creep Properties of Filamentous Materials and other High Polymers, The Textile Foundation, Washington, D. C., 1943.

[51] Lee, E. H., "Viscoelastic Stress Analysis in Structural Mechanics" in J. N. Goodier and J. J. Hoff (editors), Proceeding of the 1st Symposium on Naval Structural Mechanics, Pergamon Press, London, 1960.

[52] Lemiszka, T. and J. C. Whitwell, "Stress Relaxation of Fibers as a Means of Interpreting Physical and Chemical Structures", Textile Res. J., 25, 947(1955).

[53] Levi, H. W., L. R. Levi, and H. S. Zim, A Guide to Spiders, Golden Press, New York, 1968.

[54] Lincoln, B., "Flexural Fatigue and Viscoelastic Properties of Wool Fibers", J. Textile Inst., 43, T198 (1952).

[55] Lucas, F., J. T. B. Shaw, and S. G. Smith, "The Chemical Constitution of Some Silk Fibroins and Its Bearing on their Physical Properties", J. Textile Inst., 4, T440 (1955).

[56] Lucas, F., J. T. B. Shaw, and S. G. Smith, "Comparative Studies of Fibroins: I. The Amino Acid Composition of Various Fibroins and Its Significance in Relation to Their Crystal Structure and Taxonomy", J. of Molecular Biology, 2, 339(1960).

[57] Lunn, A. C., B. L. Lee, and I. V. Yannas, "Strain Recovery of Polyester and Nylon 66 Monofilaments Under Various Temperature Histories", Polymer Eng. and Sci., 14, 610(1974).

[58] Lyons, W. J. and I. B. Prettyman, "Method for Absolute Measurement of Dynamic Properties of Linear Structures at Sonic Frequencies", J. Appl. Phys., 19, 473(1948).

[59] Lyons, W. J., "Dynamic Properties of Filaments, Yarns, and Cord at Sonic Frequencies", Textile Res. J., 19, 123(1949).

[60] Lyons, W. J., "Some Theoretical Considerations of Dynamic-Property Data on Textile Specimens", J. Appl. Phys., 21, 520(1950).

[61] Mark, H. and J. J. Press, "Elasticity, Creep and Recovery of Acetate and Viscose Rayon Yarns", Rayon Textile Monthly, 24, 297, 339, 405 (1943).

[62] Marples, B. J., "The Spinnerets and Epiandrous Glands of Spiders", J. Linnean Soc. (Zoology), 46, 209(1967).

[63] Maxwell, J. C., "On the Dynamic Theory of Gas", Phil.. Trans. Royal Soc., 157, 49(1867).

[64] Meluch, W. C., "Calculation of Dynamic Spectra from Relaxation Data", Appl. Polymer Symposium, No. 24, 55(1974).

[65] Meredith, R., "The Tensile Behavior of Cotton and Other Textile Fibers", J. Textile Inst., 36, T107(1945).

[66] Meridith, R., (editor), The Mechanical Properties of Textile Fibers, Interscience, New York, 1956.

[67] Meridith, R. and B. S. Hsu, "Stress Relaxation in Nylon and Terylene: Influence of Strain, Temperature, and Humidity", J. Polymer Sci., 61, 253 (1962).

[68] Meridith, R. and B. S. Hsu, "Dynamic Bending Properties of Fibers: Effect of Temperature on Nylon 6.6, Terylene, Orlon, and Viscose Rayon", J. Polymer Sci., 61, 271(1962).

[69] Meyer, K. H., and W. Lotmar, "Sur l'elasticite de la Cellulose", Helv. Chim. Acta. 19, 68(1936).

[70] Nagamatsu, K., "On the Viscoelastic Properties of Crystalline High Polymers", Kolloid Zeitschrift, 172, 141(1960).

[71] Neubert, H. K. P., "A Simple Model Representing Internal Damping in Solid Materials", The Aeronautical Quarterly, 14, 187(1963).

[72] Nielsen, L. E., Mechanical Properties of Polymers, Reinhold Publishing Co., New York, 1962.

[73] Nolle, A. W., "Acoustic Determination of the Physical Conditions of Rubber-Like Materials", J. Acoustic Soc. Am., 19, 194(1947).

[74] Nolle, A. W., "Methods for Measuring Dynamic Mechanical Properties of Rubber-Like Materials", J. Appl. Phys., 19, 753(1948).

[75] Nolle, A. W., "Dynamic Mechanical Properties of Rubberlike Materials", J. Polymer Sci., 5, 1(1950).

[76] Peakall, D. B., "Synthesis of Silk, Mechanism and Location", Am. Zoologist, 9, 71(1969).

[77] Peirce, F. T., "Time Effects", J. Textile Inst., 18, T481(1927).

[78] Phoenix, S. L. and J. Skelton, "Transverse Compressive Moduli and Yield Behavior of Some Orthotropic, High Modulus Filaments", Textile Res. J., 44, 934(1974).

[79] Pipkin, A. C. and T. G. Rogers, "A Nonlinear Integral Representation for Viscoelastic Behavior", J. Mech. Phys. Solids, 16, 59(1968).

[80] Press, J. J.,"Flow and Recovery Properties of Viscose Rayon Yars", J. Appl. Phys., 14, 224(1943).

[81] Price, S. J. W., A. D. McIntyre, J. P. Pattison, and B. A. Dunell, "Stress-Relaxation and Vibrational Properties of Some Fibrous Polymers at Various Conditions of Temperature and Relative Humidity", Textile Res. J., 26, 276(1956).

[82] Ratcliffe, W. F. and S. Turner, "Engineering Design: Data Required for Plastic Materials", Trans. J. Plastics Inst., 34, 137(1966).

[83] Ree, T., M. C. Chen, and H. Eyring, "Molecular Theory of Damping in Fibers, Part I.", Textile Res. J., 21, 789(1951).

[84] Ree, T., M. C. Chen, and H. Eyring, "Part II: The Effect of Temperature and Heat Treatment on the Energy Loss in Saran", Textile Res. J., 21, 799(1951).

[85] Reese, C. E. and H. Eyring, "Mechanical Properties and the Structure of Hair", Textile Res. J., 20, 743(1950).

[86] Reiner, M., Deformation, Strain, and Flow, H. K. Lewis & Co., London, 1969.

[87] Rigby, B. J., N. Hirai, J. D. Spikes, and H. Eyring, "The Mechanical Properties of Rat Tail Tendon", J. Gen. Physiol., 43, 265(1959).

[88] Schapery, R. A., "On the Characterization of Nonlinear Viscoelastic Materials", Polymer Eng. and Sci., 9, 295(1969).

[89] Shorter, S. A., "An Investigation of the Nature of the Elasticity of Fibers", J. Textile Inst., 15, T207(1924).

[90] Smith, H. D. W. and R. Eisenschitz, "The Flow and Relaxation of Rayon Filaments", J. Textile Inst., 22, T170(1931).

[91] Smith, H. D. W. and R. Eisenschitz, "Apparatus for the Measurements of Flow and Relaxation of Textile Fibers", J. Textile Inst., 22, T158(1931).

[92] Speakman, J. B., "The Extension of Wool Fibers Under Constant Stress", J. Textile Inst., 17, T42(1926).

[93] Speakman, J. B., and A. K. Saville, "Some Physical Properties of Nylon", J. Textile Inst., 27, P271(1946).

[94] Steinberger, R. L., "The Stress-Strain Relation in Textile Fibers", Physics, 5, 53(1934).

[95] Steinberger, R. L., "The Elastic and Plastic Properties of Textile Fibers I", Textile Research, 4, 207(1934).

[96] Steinberger, R. L., "Elastic and Plastic Properties of Textile Fibers II", Textile Research, 4, 271(1934).

[97] Steinberger, R. L., "The Stress-Strain Relation in Celanese Single Fibers", Textile Research, 4, 543(1934).

[98] Steinberger, R. L., "Creep in Cellulose Acetate Filaments", Textile Research, 6, 191(1936).

[99] Steinberger, R. L., "Creep in Cuperammonium Filaments", Textile Research, 6, 267(1936).

[100] Steinberger, R. L., "Creep in Single Fibers of American Delta Cotton", Textile Research, 6, 325(1936).

[101] Steinberger, R. L., "Torque Relaxation and Torsional Energy in Crepe Yarn", Textile Research, 7, 83(1936).

[102] Thomson, W. (Lord Kelvin), "Elasticity", Math. and Phys. Paper, Vol. 3, Cambridge, 1890.

[103] Tipton, H., "The Dynamic Tensile Mechanical Properties of Textile Filaments and Yarns", J. Textile Inst., 46, T322(1955).

[104] Tobolsky, A. V., Properties and Structure of Polymers, Wiley, New York, 1960.

[105] Tokita, N., "Viscoelastic Properties of Fibers", J. Polymer Sci., 20, 515(1956).

[106] Treloar, L. R. G., The Physics of Rubber Elasticity, 2nd edition, Oxford University Press, 1958.

[107] Turner, S., "The Foundations of Possible Engineering Design Methods for Plastics", Trans. J. Plastics Inst., 34, 127(1966).

[108] Vidimsky, R. G., H. Keith, F. J. Padden, Jr.,"Electron Microscopic Study of Deformation in Polyethylene", J. Polymer Sci., 7, 1367(1969).

[109] Voigt, W., "Uber innere Reibung fester Korper, insbesondere de Metalle", Ann. d. Phys., 47, 671(1892).

[110] Volterra, V., Theory of Functionals, Dover, 1959.

[111] deVries, H., "The Dynamic Modulus of Elasticity of Regenerated Cellulose Fibers in Relation to Large Deformation", Appl. Sci. Res., A3, 111(1951).

[112] Wakelin, J. H., E. T. L. Voong, D. J. Montgomery, and J. H. Dusenbury, "Vibroscope Measurements of Nylon-66 and Dacron Filaments of Various Draw Ratios:, J. Appl. Phys., 26, 786(1955).

[113] Ward, I. M., Mechanical Properties of Solid Polymers, Wiley, New York, 1971.

[114] Ward, I. M. and E. T. Onat, "Nonlinear Mechanical Behavior of Oriented Polypropylene", J. Mech. Phys. Solids, 11, 217(1963).

[115] Ward, I. M. and J. M. Wolfe, "The Nonlinear Mechanical Behavior of Polypropylene Fibers Under Complex Loading Programs", J. Mech. Phys. Solids, 14, 131(1966).

[116] Warwicker, J. O., "Comparative Studies of Fibroins", J. Molecular Biology, 2, 350(1960).

[117] Weber, W., "Ueber die Elasticitat der Seidenfaden", Pogg. Ann. Physik., 4, 247(1835).

[118] Witt, P. N., C. F. Reed, and D. B. Peakall, A Spider's Web: Problems in Regulatory Biology, Springer-Verlag, New York, 1968.

[119] Wilson, R. S., "The Structure of the Dragline Control Valves in the Garden Spiders", Quart. J. Micr. Sci., 104, 549(1962).

[120] Wilson, R. S., "The Control of Drag Line Spinning in the Garden Spiders", Quart. J. Micr. Sci., 104, 557(1962).

[121] Wilson, R. S., "Control of Drag-line Spinning in Certain Spiders", Am. Zoologist, 9, 103(1969).

[122] Willett, P. R., "Viscoelastic Properties of Tire Cords", J. Appl. Polymer Sci., 19, 2005(1975).

[123] Woo, J. L. and R. Postle, "Measurement of the Dynamic Elastic Modulus of Short Staple Fibers", J. Appl. Polymer Sci., 18, 589(1974).

[124] Wood, G. C., "The Relaxation of Stretched Animal Fibers II. The Relaxation of Human Hair", J. Textile Inst., 45, (1954).

[125] Work, R. W., Personal communication.

[126] Zemlin, J. C., A Study of the Mechanical Behavior of Spider Silks, U. S. Army Natick Report AD684333, 1968.

[127] Zener, C., Elasticity and Anelasticity of Metals, University of Chicago Press, Chicago, 1948.

[128] Zimmerman, J., "Factors that Affect Wear Life of Textiles", Textile Mfgr., 101, 19(1974).

[129] Zimmerman, J., Unpublished report.

VITA

The author was born on August 5, 1947 and grew up in the rural village of Da Dao in the beautiful and fertile Pearl River Delta of the Kwantung province in China.

From 1960 to 1966, he attended the Baptist Middle School in Macao and the Lingnan Middle School in Hong Kong.

In February, 1967, the author came to the United States to start his college education at the Philadelphia College of Textiles and Science, where he received his Bachelor of Science degree in Textile Engineering in May 1970.

In September, 1970, the author started his graduate study at the School of Textile Engineering of the Georgia Institute of Technology. He was married to Catherine Lee from Philadelphia in December of the same year.

In September, 1971, the author received his Master of Science degree in Textile Engineering from the Georgia Institute of Technology.

From 1972 to 1973, the author was employed as an assistant research engineer by the Georgia Institute of Technology.

In 1973, he enrolled in the newly developed Ph.D. program in Textile and Fiber Science and Engineering.

During the period 1973 and 1975, he was selected to be a Tennessee Eastman Fellow and was elected graduate student senator.

In October, 1974, his daughter Kara was born.

In 1975, the author became the first Ph.D. candidate of the School of Textile Engineering.

In April, 1976, the author joined the staff members of the Philadelphia College of Textiles and Science to teach and do research on the biomedical application of fibrous structures.

PUBLICATIONS

1) "Viscoelastic Behavior of Strong Nylon Fibers", Bull. Am. Phys. Soc., Ser. II, 19(No. 3), 286(1974).(co-authors: W. D. Freeston, Jr. and J. L. Lundberg)

2) "Nonlinear Viscoelasticity of Fibers", Bull. Am. Phys. Soc., Ser.II, 20(No. 3) 480(1975). (co-authors: H. Y-L. Chen and J. L. Lundberg)

3) "Nonlinear Viscoelasticity of 'Hard Elastic' Polypropylene Fibers", J. Polymer Eng. & Sci., 16(No. 6), 406(1976). (co-authors: H. Y-L. Chen and J. L. Lundberg)

4) "Nonlinear Viscoelasticity of Polyamide Fibers", Bull. Am. Phys. Soc., Ser. II, 21, (No.3), 415(1976). (co-authors: H. Y-L. Chen and J. L. Lundberg)